Technische Universität München
TUM School of Engineering and Design

Automated Parameter Identification of High-Fidelity Structural Dynamic Machine Tool Models

Johannes Stefan Ellinger

Vollständiger Abdruck der von der TUM School of Engineering and Design der Technischen Universität München zur Erlangung eines

Doktors der Ingenieurwissenschaften (Dr.-Ing.)

genehmigten Dissertation.

Vorsitz: Prof. Dr. ir. Daniel Rixen

Prüfende der Dissertation:

1. Prof. Dr.-Ing. Michael F. Zäh
2. Prof. Dr.-Ing. Christian Brecher

Die Dissertation wurde am 14.03.2025 bei der Technischen Universität München eingereicht und durch die TUM School of Engineering and Design am 09.07.2025 angenommen.

Editors' Preface

In times of global challenges, such as climate change, the transformation of mobility, and an ongoing demographic change, production engineering is crucial for the sustainable advancement of our industrial society. The impact of manufacturing companies on the environment and society is highly dependent on the equipment and resources employed, the production processes applied, and the established manufacturing organization. The company's full potential for corporate success can only be taken advantage of by optimizing the interaction between humans, operational structures, and technologies. The greatest attention must be paid to becoming as resource-saving, efficient, and resilient as possible to operate flexibly in the volatile production environment.

Remaining competitive while balancing the varying and often conflicting priorities of sustainability, complexity, cost, time, and quality requires constant thought, adaptation, and the development of new manufacturing structures. Thus, there is an essential need to reduce the complexity of products, manufacturing processes, and systems. Yet, at the same time, it is also vital to gain a better understanding and command of these aspects.

The research activities at the Institute for Machine Tools and Industrial Management (*iwb*) aim to continuously improve product development and manufacturing planning systems, manufacturing processes, and production facilities. A company's organizational, manufacturing, and work structures, as well as the underlying systems for order processing, are developed under strict consideration of employee-related requirements and sustainability issues. However, the use of computer-aided and artificial intelligence-based methods and the necessary increasing degree of automation must not lead to inflexible and rigid work organization structures. Thus, questions concerning the optimal integration of

ecological and social aspects in all planning and development processes are of utmost importance.

The volumes published in this book series reflect and report the results from the research conducted at iwb. Research areas covered span from the design and development of manufacturing systems to the application of technologies in manufacturing and assembly. The management and operation of manufacturing systems, quality assurance, availability, and autonomy are overarching topics affecting all areas of our research. In this series, the latest results and insights from our application-oriented research are published, and it is intended to improve knowledge transfer between academia and a wide industrial sector.

Ruediger Daub Gunther Reinhart Michael Zaeh

Geleitwort der Herausgeber

Die Produktionstechnik ist in Zeiten globaler Herausforderungen, wie der Klimakrise, des Mobilitätswandels und der Überalterung der Gesellschaft in westlichen Ländern, für eine nachhaltige Weiterentwicklung unserer Industriegesellschaft von zentraler Bedeutung. Der Einfluss eines Industriebetriebs auf die Umwelt und die Gesellschaft hängt dabei entscheidend von den eingesetzten Produktionsmitteln, den angewandten Produktionsverfahren und der eingeführten Produktionsorganisation ab. Erst das optimale Zusammenspiel von Mensch, Organisation und Technik erlaubt es, alle Potenziale für den Unternehmenserfolg auszuschöpfen. Dabei muss größtes Augenmerk darauf gelegt werden, möglichst ressourcenschonend, effizient und resilient zu werden, um flexibel im volatilen Produktionsumfeld zu agieren.

Um in dem Spannungsfeld Nachhaltigkeit, Komplexität, Kosten, Zeit und Qualität bestehen zu können, müssen Produktionsstrukturen ständig neu überdacht und weiterentwickelt werden. Dabei ist es notwendig, die Komplexität von Produkten, Produktionsabläufen und -systemen einerseits zu verringern und andererseits besser zu beherrschen.

Ziel der Forschungsarbeiten des *iwb* ist die ständige Verbesserung von Produktentwicklungs- und Planungssystemen, von Herstellverfahren sowie von Produktionsanlagen. Betriebsorganisation, Produktions- und Arbeitsstrukturen sowie Systeme zur Auftragsabwicklung werden unter besonderer Berücksichtigung der Anforderungen des Personals sowie von Nachhaltigkeitsaspekten entwickelt. Die dabei eingesetzten rechnergestützten und Künstliche-Intelligenz-basierten Methoden und die notwendige Steigerung des Automatisierungsgrades dürfen jedoch nicht zu einer Verfestigung arbeitsteiliger Strukturen führen. Fragen der optimalen Einbindung ökologischer und sozialer Aspekte in alle Planungs- und Entwicklungsprozesse spielen deshalb eine sehr wichtige Rolle.

Die im Rahmen dieser Buchreihe erscheinenden Bände stammen thematisch aus den Forschungsbereichen des *iwb*. Diese reichen von der Entwicklung von Produktionssystemen über deren Planung bis hin zu den eingesetzten Technologien in den Bereichen Fertigung und Montage. Die Steuerung und der Betrieb von Produktionssystemen, die Qualitätssicherung, die Verfügbarkeit und die Autonomie sind Querschnittsthemen hierfür. In den *iwb*-Forschungsberichten werden neue Ergebnisse und Erkenntnisse aus der praxisnahen Forschung des Institutes veröffentlicht. Diese Buchreihe soll dazu beitragen, den Wissenstransfer zwischen dem Hochschulbereich und den Anwendenden zu verbessern.

Rüdiger Daub Gunther Reinhart Michael Zäh

Acknowledgements

This dissertation originated from my time as a research associate at the Institute for Machine Tools and Industrial Management (*iwb*) of the Technical University of Munich (TUM). I would like to express my sincere gratitude to Prof. Dr.-Ing. Michael F. Zäh for his support and guidance throughout my research. His mentorship has been instrumental in my academic and professional development, as well as in the successful completion of this dissertation. I would also like to thank Prof. Dr.-Ing. Christian Brecher for functioning as co-examiner and for his thorough review of my work and Prof. Dr. ir. Daniel Rixen for chairing the examination committee.

Additionally, I am deeply grateful to Robin, Thomas, and Max for their time and effort in reading my thesis. Their constructive feedback and thoughtful suggestions have played a crucial role in improving the overall quality of my dissertation. I would also like to thank the entire machine tool department of the *iwb* for the great collaboration, the time we spent together, and the lasting personal connections that continue well beyond my time at the institute.

My family has always supported me in all my endeavors. First, I would like to thank my sister, Elisabeth, for her love and her encouragement and for showing me that it is possible to catch up and even surpass others. Second, the time in which this thesis was written is inseparably linked to my life partner Ramona. I am very grateful to her for being there for me, for her love, and for the joy she brings into my life. In particular, I would like to thank her for giving me the freedom to work on this dissertation and for supporting me even in moments when she did not fully understand my motives. Lastly, I would like to express my deepest gratitude to my parents, Maria and Georg, for their unwavering support throughout my life. Without them, I would not have been able to achieve this milestone.

Contents

Nomenclature

Abbreviations

Symbol	Description
AA	anti-aliasing
AI	artificial intelligence
ANOVA	analysis of variance
BSD	ball screw drive
BT	Bachelor's thesis
CAD	computer-aided design
CNC	computerized numerical control
CMS	component mode synthesis
CPL	coupling
CSF	cross signature scale factor
DOF	degree of freedom
DOI	digital object identifier
EA	evolutionary algorithm
EMA	experimental modal analysis
ES	evolutionary strategy
FB	fixed bearing
FEA	finite element analysis
FFT	fast Fourier transform
FRAC	frequency response assurance criterion
FRF	frequency response function
GA	genetic algorithm

Symbol	Description
GSA	global sensitivity analysis
HDMR	high-dimensional model representation
IDP	interdisciplinary project
IoT	internet of things
iwb	Institute for Machine Tools and Industrial Management (in German: Institut für Werkzeugmaschinen und Betriebswissenschaften) of Technical University of Munich
LB	loose bearing
LGS	linear guiding system
LS	least squares
LSCE	least squares complex exponential
LSCF	least squares complex frequency domain
LSRF	least squares rational function
MAC	modal assurance criterion
MACXP	extended modal assurance criterion
MBS	multibody system
MDOF	multi-degree-of-freedom
ME	mounting element
MOR	model order reduction
MPC	multipoint constraint
MS	mean squares
MT	Master's thesis
NDD	natural damping difference
NFD	natural frequency difference
PSO	particle swarm optimization
PUB	publication
RG	research gap
RT	research target
SDOF	single-degree-of-freedom
SLSQP	sequential least squares programming
SSB	sum of squares between groups
SSI	stochastic subspace identification
ST	Semester's thesis
SVD	singular value decomposition

Symbol	Description
TF	transfer function
TSS	total sum of squares
TUM	Technical University of Munich (in German: Technische Universität München)
WPT	workpiece table

Notation

If not indicated otherwise, vector symbols are printed in bold type and in lower case, whereas matrices are written in bold type and upper case.

Symbol	Description
$\mathbf{0}$	zero vector or matrix
$\boldsymbol{I}$	identity matrix
a	scalar quantity
$\boldsymbol{a}$	vector
$\boldsymbol{A}$	matrix
$\dot{a}$	first derivative with respect to time
$\ddot{a}$	second derivative with respect to time
$\boldsymbol{a}^*$	complex conjugate
$\boldsymbol{a}^\mathsf{T}$	transpose
$\boldsymbol{a}_{-i}$	vector of model factors with fixed value for index i
$\boldsymbol{a}^\mathsf{H}$	conjugate transpose (Hermitian transpose)
j	imaginary unit
$\mathbb{E}(a)$	expected value of a random variable a
$\mathbb{R}\mathrm{e}(a)$	real part of a complex number a
$\mathbb{V}(a)$	variance of a random variable a

Latin Symbols

If not indicated otherwise, vector symbols are printed in bold type and in lower case, whereas matrices are written in bold type and upper case. Symbols that cannot be assigned a unique unit are marked with "–", and dimensionless quantities are shown with the unit 1.

Symbol	Description	Unit
A	modal constant	–
$\hat{A}$	estimated modal constant	–

Symbol	Description	Unit
b	viscous damping coefficient	$\mathrm{N\,s\,m^{-1}}$
$\bar{b}$	modal viscous damping coefficent	$\mathrm{N\,s\,m^{-1}}$
$\boldsymbol{B}$	viscous damping matrix	$\mathrm{N\,s\,m^{-1}}$
c	regressor	–
$\boldsymbol{c}$	regressor vector	–
$\boldsymbol{C}$	regressor matrix	–
d	hysteretic damping coefficient	$\mathrm{N\,m^{-1}}$
$\bar{d}$	modal hysteretic damping coefficent	$\mathrm{N\,m^{-1}}$
$\boldsymbol{D}$	hysteretic damping matrix	$\mathrm{N\,m^{-1}}$
E	loss function	–
ΔE	energy offset	J
$\boldsymbol{e}$	error vector	–
f	force	N
f_C	Coulomb friction force	N
f_N	normal force	N
f_S	sticking friction force	N
F	F-ratio	1
$\boldsymbol{f}$	nodal force vector	N
$\bar{\boldsymbol{f}}$	nodal force amplitude vector	N
g	function	–
$\hat{g}$	objective function observation	–
$\hat{\boldsymbol{g}}$	objective function observation vector	–
h	symbolic frequency response function	–
$\boldsymbol{h}$	numerical frequency response function vector	–
i	index variable or iteration number	1
j	index variable	1
k	stiffness	$\mathrm{N\,m^{-1}}$
k_B	Boltzmann constant	$\mathrm{kg\,m^2\,s^{-2}\,K^{-1}}$
$\bar{k}$	modal stiffness	$\mathrm{N\,m^{-1}}$
$\boldsymbol{K}$	stiffness matrix	$\mathrm{N\,m^{-1}}$
$\hat{\boldsymbol{K}}$	reformulated stiffness matrix	$\mathrm{N\,m^{-1}}$
l	index variable	1
L	number of reduced degrees of freedom	1
$\bar{m}$	modal mass	kg

Symbol	Description	Unit
$\boldsymbol{M}$	mass matrix	kg
$\hat{\boldsymbol{M}}$	reformulated mass matrix	kg
n	number of model parameters	1
$\tilde{n}$	number of constraints	1
N	number of degrees of freedom	1
N_{av}	number of frequency response function averages	1
$\hat{N}$	number of data points or observations	1
p	probability	1
P	frequency response function placeholder	–
q	eigenvector truncation number	1
Q	frequency response function placeholder	–
$\boldsymbol{q}$	modal degree of freedom vector	–
r	random number	1
S	Sobol' index	1
$\boldsymbol{s}$	power spectrum vector	–
t	time	s
T	temperature	K
$\boldsymbol{T}$	general transformation matrix	–
$\boldsymbol{T}_{CB}$	Craig-Bampton method transformation matrix	–
u	nodal displacement	m
$\boldsymbol{u}$	nodal displacement vector	m
$\bar{\boldsymbol{u}}$	nodal amplitude vector	m
$\boldsymbol{u}_b$	boundary nodal displacement vector	m
$\boldsymbol{u}_i$	inner nodal displacement vector	m
v_S	Stribeck velocity	$\mathrm{m\,s^{-1}}$
$\boldsymbol{v}$	velocity vector	$\mathrm{m\,s^{-1}}$
w	weight variable	1
x	model factor or model parameter	–
$\boldsymbol{x}$	model factor or model parameter vector	–
$\tilde{\boldsymbol{x}}$	temporary best model parameter vector	–
y	model output	–
$\bar{y}$	average model output	–
$\boldsymbol{y}$	model output vector	–

Symbol	Description	Unit
$\boldsymbol{z}$	reduced degree of freedom vector	–

Greek Symbols

If not indicated otherwise, vector symbols are printed in bold type and in lower case, whereas matrices are written in bold type and upper case. Symbols that cannot be assigned a unique unit are marked with "–", and dimensionless quantities are shown with the unit 1.

Symbol	Description	Unit
α	receptance frequency response function	–
$\mathbf{A}$	receptance frequency response function matrix	–
δ	Stribeck factor	1
ε	model error	–
η	loss factor	1
$\boldsymbol{\gamma}$	numerical coherence function vector	1
κ	constraint function	–
λ	number of children in evolutionary strategies	1
λ	eigenvalue	$(\mathrm{rad/s})^2$
$\mathbf{\Lambda}$	eigenvalue matrix	$(\mathrm{rad/s})^2$
μ	friction coefficient	1
μ	population size in evolutionary strategies	1
η	step length	1
ν	first Rayleigh damping coefficent	s^{-1}
ω	angular frequency	$\mathrm{rad\,s}^{-1}$
$\bar{\omega}$	angular eigenfrequency	$\mathrm{rad\,s}^{-1}$
$\tilde{\omega}$	damped angular eigenfrequency	$\mathrm{rad\,s}^{-1}$
$\hat{\omega}$	estimated angular eigenfrequency	$\mathrm{rad\,s}^{-1}$
Ω	function space	–
ϕ	model constant	–
Φ	mass-normalized mode shape matrix entry	$\mathrm{kg}^{-0.5}$

Symbol	Description	Unit
$\mathbf{\Phi}$	mass-normalized mode shape matrix	$\mathrm{kg}^{-0.5}$
ψ	mode shape	–
$\mathbf{\Psi}$	mode shape matrix	–
$\mathbf{\Psi}_{ib}$	static constraint mode matrix	–
$\mathbf{\Psi}_{iq}$	fixed-interface normal mode matrix	–
ρ	recombination parameter in evolutionary strategies	1
τ	input variable	–
$\boldsymbol{\tau}$	input variable vector	–
ϑ	second Rayleigh damping coefficent	s
ξ	modal damping ratio	1
$\hat{\xi}$	estimated modal damping ratio	1

Chapter 1

Introduction

Machine tools are mechanized and, to a varying degree, automated production devices which lead to a predefined shape or cause a desired form change on a workpiece via relative movements between the workpiece and a tool (DIN 69651-1 1981). In this way, all kinds of parts, ranging from simple forms to very complex shapes, can be manufactured. Even though the market size of the machine tool industry is small compared to other sectors with, in Germany, a sales volume of EUR 14.1 billion and 64,264 employees (VDW 2022), it plays an important role as an enabler for manufacturing capabilities of many other sectors. One might even go as far as to say that without machine tools as the so-called mothers of production (SCHULZ 2014), our current standard of living would not have been possible (WECK 2002). Nevertheless, the European machine tool industry faces several challenges such as, for example, the transformation in the automotive industry and the increasing pressure from Asian competitors (VDW 2022). As a result, the sector's demand for cost-efficiency, innovativeness, and flexibility is higher than it has ever been.

One of the key performance indicators for the economic success of machine tools is their dynamic behavior (WECK 2002). Cutting machine tools, in particular, are constantly exposed to periodic excitations caused by the intermittent tool-workpiece engagement. This potentially results in form errors and chatter. The latter is characterized by self-excited and exponentially growing vibrations and leads to increased wear, poor surface quality, and even damage to the tool, the workpiece, and the machine itself (ALTINTAS 2012; BRECHER and WECK 2006). These vibrations are limiting the productivity of machine tools (ALTINTAS 2012; MUNOA et al. 2016). To increase the productivity and robustness of machine

tools, their dynamic behavior must be properly designed. Nowadays, simulation methods are available which have replaced the time-intensive and costly testing of several physical prototypes (ALTINTAS et al. 2005). Dynamic machine tool models offer the opportunity to evaluate and implement possible improvements more quickly, resulting in a reduced number of physical prototypes and, in the end, a shorter time to market.

Apart from the machine tool design process, other applications of machine tool dynamic simulation models exist. For example, an integrated simulation of the machine tool including its control, the workpiece, and the cutting process offers the opportunity to assess and even improve the part quality before starting the manufacturing process (REBELEIN 2019; WIMMER 2020; WITT 2007). In this way, dynamic instabilities can be avoided, and geometrical errors can be reduced. During production, dynamic simulation models can also be used for monitoring the condition of critical components. These models correlate to the specific point in time at which they were set up. Wear processes, however, change the machine tool's dynamic behavior (BENKER et al. 2022), eventually leading to a mismatch between the model and the real-world machine tool. Monitoring these deviations and parameterizing the model again at specific intervals enables the detection and localization of wear. Furthermore, the gathered information can be even used for remaining useful life predictions (IMIELA 2005).

An absolute prerequisite for these applications to be successful is the availability of a high-fidelity machine tool dynamic simulation model that is able to accurately predict the real-world structure's dynamic behavior. Even though these models already exist (REBELEIN 2019; SEMM 2020), they are rarely sufficiently well-parameterized for a predictive simulation. Since this is a cumbersome and manual process (NIEHUES 2015; REBELEIN 2019), these models are currently only used for specialized research applications. No automated procedure for parameterizing these models exists, thus hindering their industrial application and the exploitation of the above-mentioned use cases.

This publication-based thesis aims at automating the parameterization process of high-fidelity dynamic machine tool models. Parameterization, in other words, means finding those values for the model parameters that lead to the best approximation of the real-world structure's behavior. This can be formulated as a complex optimization problem. Thus, the main objective of this work is to

provide a method for solving this problem as highly automated and effortlessly as possible. The parameterization requires information about the machine tool, typically in the form of modal parameter estimates. Automatically determining these estimates is another objective of this thesis. Furthermore, the benefits of well-parameterized high-fidelity machine tool dynamic simulation models are to be demonstrated by providing and exploiting a condition monitoring use case.

To reach these objectives, this thesis first gives an overview of the theoretical foundations in chapter 2. The basics of structural dynamics will be briefly covered, and sensitivity analysis methods for examining and understanding models will be presented. The remainder of the chapter is dedicated to numerical optimization methods, which are an elementary component of the developed automated parameter identification method. Chapter 3 contains a detailed review of the state of the art of machine tool simulation models and their identification methods. It will be shown that gaps exist in the state of the art, in particular regarding the parameterization of these models. To overcome these gaps, research targets will be formulated in chapter 4, and a research approach will be presented. This involves five publications, whose key results will be presented in detail in chapter 5. Chapter 6 critically discusses the papers' results as a whole and relates them to the research gaps and research targets defined in chapters 3 and 4. Finally, chapter 7 concludes this thesis with a short summary and an outlook.

Chapter 2

Fundamentals

The intention of this chapter is to briefly show the relevant theoretical foundations for understanding the remainder of this thesis, especially the publications summarized in chapter 5. The presented method for parameterizing high-fidelity machine tool dynamic simulation models strongly relies on both sensitivity analyses and numerical optimization methods, which are described in the sections 2.1 and 2.2, respectively. Finally, section 2.3 covers the basics of structural dynamics and shows how to calculate and measure the dynamic properties of real-world structures.

2.1 Sensitivity Analysis

Today's simulation models are becoming more and more complex, which is especially true in the modern field of machine learning for neuronal networks. For analyzing models, it can be helpful to understand the relation between the variance of the model's output and the variances of its input variables. This is the definition of sensitivity analyses (SALTELLI and RATTO 2008; SIEBERTZ et al. 2017), which will be covered in this section. First, sensitivity analysis for linear models will be presented, before the transition to analyzing nonlinear models will be made.

2.1.1 Linear Models

Linear models with two-way interaction effects only are often a good compromise between accuracy and simplicity (SIEBERTZ et al. 2017). They can be written as

$$y = \phi_0 + \sum_{i=1}^{n} \phi_i x_i + \sum_{i=1}^{n-1} \sum_{j=i+1}^{n} \phi_{ij} x_i x_j + \varepsilon. \tag{2.1}$$

Here, y denotes the model's output, n is the number of model factors, ϕ_i are model parameters, x_i are model factors (i.e., the model's input values), and ε accounts for the model's errors in describing a real-world effect or quantity. For this type of models, the so-called analysis of variance (ANOVA) approach is a very popular sensitivity analysis method (SIEBERTZ et al. 2017), and it will be explained in detail using an illustrative example. This is based on the work of SIEBERTZ et al. (2017), which also demonstrates other linear sensitivity analysis methods such as, for example, the partial correlation coefficient, the coefficient of partial determination, or the standardized regression coefficient.

The following explanations are based on the assumption that an experiment was conducted in which the participants have received a coffee and rated its taste on a scale from one to ten. In this experiment, one indicates a poor and ten an excellent coffee taste. Each participant was given coffee in different containers (disposable or reusable) with a different temperature level (low, medium, and high), and with or without sugar. In other words, an experiment with three factors, that is, the container type, the coffee temperature, and the sugar level, was conducted. The sugar and container factors take two different values (i.e., levels), meaning that these factors have one degree of freedom (DOF) each. The temperature level can take three values, thus having two so-called statistical DOFs. Table 2.1 contains exemplary results for this experiment with 24 participants. Under the assumption that rating the taste of coffee can be described with a linear model (see equation 2.1), it will be examined which of the three factors (i.e., adding sugar or not, the container type, and the coffee temperature) have a statistically significant influence on the taste.

Therefore, a so-called ANOVA table given in table 2.2 is constructed. The first column contains all factors of the model, including the interaction effects (e.g., "Sugar:Temperature"). Interaction effects indicate combined (i.e., second-order)

Table 2.1: Exemplary results of a coffee tasting experiment; the participants were offered coffee in different containers with and without sugar with different temperatures, and they were asked to rate their coffee on a scale from one to ten with one indicating a poor and ten an excellent coffee.

Sugar	Container	Temperature	Rating
yes	disposable	low	1
yes	disposable	low	3
yes	disposable	medium	1
yes	disposable	medium	4
yes	disposable	high	2
yes	disposable	high	2
yes	reusable	low	4
yes	reusable	low	2
yes	reusable	medium	4
yes	reusable	medium	7
yes	reusable	high	10
yes	reusable	high	10
no	disposable	low	1
no	disposable	low	2
no	disposable	medium	2
no	disposable	medium	2
no	disposable	high	3
no	disposable	high	3
no	reusable	low	3
no	reusable	low	3
no	reusable	medium	6
no	reusable	medium	5
no	reusable	high	7
no	reusable	high	8

impacts exceeding the sum of the direct (i.e., first-order) effects (SALTELLI 2004). The second column shows the sum of squares between groups (SSB), which is a measure for the contribution of each factor to the total variance. A group denotes all experiments which have a fixed value of a certain factor. The SSB is computed as

$$\mathrm{SSB}_i = \sum_{j=1}^{n_i+1} \hat{N}_{ij} \left(\bar{y}_{ij} - \bar{y}\right)^2 . \tag{2.2}$$

Here, the index i denotes the considered factor, n_i is the number of factor DOFs, $\hat{N}_{ij}$ is the number of data points with the considered factor in level j, $\bar{y}$ is the total mean value of all observations (see table 2.1), and $\bar{y}_{ij}$ is the mean value of the group j. The next and third column shows the factors' number of DOFs.

Table 2.2: ANOVA table for the coffee experiment (see table 2.1); "Sugar:Temperature," for example, denotes the interaction effect between the factors "Sugar" and "Temperature."

	SSB	n	F	p
Sugar	1.04	1	0.74	40.56 %
Temperature	42.33	2	14.94	0.03 %
Container	77.04	1	54.38	0 %
Sugar:Temperature	0.33	2	0.12	88.99 %
Sugar:Container	1.04	1	0.74	40.56 %
Temperature:Container	25.33	2	8.94	0.31 %
Residual	19.83	14		

Relating the SSB to the number of DOFs n_i gives the so-called mean squares (MS) value, which is defined as

$$\mathrm{MS}_i = \frac{\mathrm{SSB}_i}{n_i}. \tag{2.3}$$

In column four of table 2.2, the so-called F-ratio

$$F_i = \frac{\mathrm{MS}_i}{\mathrm{MS}_{Residual}} \tag{2.4}$$

is shown, which relates the strength of each factor's effect to the residual effect. Note that the residual sum of squares between groups $\mathrm{MS}_{Residual}$ is simply defined as the total sum of squares (TSS) minus all other sums of squares between groups divided by the number of residual DOFs, where

$$\mathrm{TSS} = \sum_{j=1}^{\hat{N}} \left(y_j - \bar{y}\right)^2, \tag{2.5}$$

$\hat{N}$ is the total number of data points, $\bar{y}$ is the total mean value, and y_j is the outcome of experiment j. The last column of table 2.2 contains the so-called p-values, that is, the probability of unfairly rejecting the null hypothesis, which states that the corresponding factor has no effect. This probability can be computed based on the F-ratio (using a precomputed F-distribution) under the assumptions that

1. the model errors (i.e., residuals) are independent,
2. the residuals follow a normal distribution, and

3. the data in the groups have the same variance.

These assumptions have to be validated on a case-by-case basis (SIEBERTZ et al. 2017).

A high p-value means that the null hypothesis cannot be rejected and that the factor has little to no effect, whereas, for a low p-value, the null hypothesis can be fairly rejected, meaning that there indeed is an effect of the factor on the model's outcome. In practice, a p-value threshold of 5 % has turned out to be reasonable for rejecting the null hypothesis (SIEBERTZ et al. 2017).

Considering the coffee tasting example in table 2.2, the coffee temperature, the container type, and the interaction effect between these two would be classified as statistically significant. Possible explanations therefore are that hot coffee might taste better than cold coffee and a reusable cup feels better than a disposable container. The combination of hot coffee and a reusable cup might even create a better taste than the mere combination of these two effects, as indicated by the interaction effect's significance. Adding sugar, in turn, seems to have no effect, which could be caused by the fact that some people like sweet coffee while others like coffee without sugar. Similarly, all sugar-related interaction effects are statistically not significant, as the null hypothesis cannot be proven to be untrue.

2.1.2 Nonlinear Models

For nonlinear models, linear sensitivity analysis methods such as the ANOVA approach cannot be used anymore (SIEBERTZ et al. 2017), and nonlinear methods must be used instead. A very common example of a nonlinear sensitivity analysis method is the use of partial derivatives, that is,

$$\frac{\partial y_i}{\partial x_j}. \tag{2.6}$$

Here, y_i represents a possible model output and x_j stands for one of the model's factors. However, the evaluation of partial derivatives is a so-called local sensitivity analysis method, meaning that it strongly depends on the location at which the derivatives are computed. In other words, the model output y_i can be very sensitive concerning an input variable x_j at a certain point but is

not affected by it at all at any other point (SALTELLI and RATTO 2008). If a global perspective is desired, a variance-based analysis, which is often called Sobol' method, is the first choice (SALTELLI and RATTO 2008). In the following, its basic principle will be described based on the explanations in the works of SALTELLI (2004) and SALTELLI and RATTO (2008).

The starting point of the Sobol' method is the so-called high-dimensional model representation (HDMR)

$$y := g = g_0 + \sum_{i=1}^{n} g_i + \sum_{i=1}^{n}\sum_{j>i}^{n} g_{ij} + \ldots + g_{12\ldots n}, \tag{2.7}$$

which can be applied to any square-integrable function g defined over the n-dimensional hypercube

$$\Omega^n = (\boldsymbol{x} \mid 0 \leq x_i \leq 1; i = 1, \ldots, n). \tag{2.8}$$

Here, $g_i = g_i(x_i)$ is only a function of the variable x_i, $g_{ij} = g_{ij}\left(x_i, x_j\right)$ is only a function of x_i and x_j, and so on. The variable y represents a model's output. Each term is, again, square-integrable over Ω^n. By exploiting this, the ANOVA-HDMR

$$\mathbb{V}(y) = \sum_{i=1}^{n} \mathbb{V}_i + \sum_{i=1}^{n}\sum_{j>i}^{n} \mathbb{V}_{ij} + \ldots + \mathbb{V}_{12\ldots n} \tag{2.9}$$

can be formulated. Here, $\mathbb{V}(y)$ is the total variance, $\mathbb{V}_i = \mathbb{V}_i(g_i)$ the (first-order) variance of the term g_i and thus the input factor x_i, and $\mathbb{V}_{ij} = \mathbb{V}_{ij}(g_{ij})$ is the variance caused by the interaction of the factors x_i and x_j, and so on. By dividing both sides of equation 2.9 by the total variance $\mathbb{V}(y)$,

$$\sum_{i=1}^{n} S_i + \sum_{i=1}^{n}\sum_{j>i}^{n} S_{ij} + \ldots + S_{12\ldots n} = 1 \tag{2.10}$$

follows with S denoting Sobol' indices, which are a measure of global sensitivity. For example, S_i denotes the first-order Sobol' index measuring the direct sensitivity of the model's output on the variable x_i. S_{ij}, in turn, is called second-order Sobol' index and describes the combined sensitivity of y to x_i and x_j exceeding their respective first-order effects. To measure the total sensitivity of a factor x_i,

the total effect

$$S_{Ti} = S_i + \sum_{j \neq i} S_{ij} + \ldots + S_{12\ldots n} \tag{2.11}$$

can be used, which is the sum of the first-order effect of x_i and all higher-order interaction effects with any other factor(s). It can be shown that

$$S_{Ti} = \frac{\mathbb{E}(\mathbb{V}(y \mid \boldsymbol{x}_{-i}))}{\mathbb{V}(y)}, \tag{2.12}$$

where $\mathbb{E}(\mathbb{V}(y \mid \boldsymbol{x}_{-i}))$ is the expected value of the variance of the model y when all factors (i.e., model variables) are fixed but x_i.

This formulation is useful for determining which model factors can be disregarded (by setting them to a fixed but arbitrary value) since they have little or no influence on the model output. Assuming that x_i has no influence, fixing all variables but x_i (i.e., $\boldsymbol{x}_{-i}$) leads to y being constant for any value of x_i. Thus, $\mathbb{V}(y \mid \boldsymbol{x}_{-i})$ will be zero. $\mathbb{E}(\mathbb{V}(y \mid \boldsymbol{x}_{-i}))$ is the average of $\mathbb{V}(y \mid \boldsymbol{x}_{-i})$ over the definition domain of $\boldsymbol{x}$ and, consequently, will also vanish. Thus, if x_i has no influence on the model, its total effect will be zero (see equation 2.12). If, however, the total effect S_{Ti} is zero, it follows that $\mathbb{E}(\mathbb{V}(y \mid \boldsymbol{x}_{-i}))$ is zero. $\mathbb{V}(y \mid \boldsymbol{x}_{-i})$ then also must be zero for all x_i since it cannot be negative. In other words, x_i cannot have any influence on y. To sum up, $S_{Ti} = 0$ is a necessary and sufficient condition for the variable x_i having no influence on the output of the model y. This is beneficial for models with many variables of which some have a small total effect, as the dimensionality of such models can be reduced by fixing these variables at an arbitrary value with only small impacts on the output of the model.

2.2 Numerical Optimization

In engineering, one almost always seeks the best solution to a given problem. The decision on the quality of a solution may, for example, be made in terms of its accuracy, its durability, or its performance. Most often, these criteria, in the end, determine the cost-effectiveness of a found solution, which may be the ultimate objective. For example, cutting processes are often designed for the lowest

manufacturing costs. Determining the best solution to a given problem may not always be straightforward, thus requiring the use of models and numerical optimization. If the design target to be optimized (i.e., the objective function) is linear in the design parameters (i.e., the model parameters), linear optimization algorithms, which are presented in section 2.2.1, can be used. Otherwise, nonlinear optimization strategies (see section 2.2.2) must be deployed. These can be further classified into global and local methods. The latter can be based either on gradients, which indicate the direction of the steepest increase of the objective function, or not. Figure 2.1 gives an overview of the classification of numerical optimization algorithms.

For numerical optimization to be applicable, the relationship between the design target and the design parameters must be described in the form of an objective function $g(\boldsymbol{x})$, which depends on model parameters $\boldsymbol{x}$ (i.e., the design parameters). Even though optimization can mean both minimization and maximization, the existing literature is often restricted to either one of them. However, a new objective function $g^*(\boldsymbol{x}) = -g(\boldsymbol{x})$ can always be constructed, which transforms a minimization into a maximization problem, and vice versa. Note that, depending on the used optimization algorithm, the objective function does not have to be known in detail. However, it must be possible to evaluate the objective function for an arbitrary set of model parameters.

In the most general form, an optimization problem can be mathematically formulated as

$$\min_{\boldsymbol{x}\in\mathbb{R}^n} g(\boldsymbol{x}) \tag{2.13}$$

subject to

$$\kappa_j(\boldsymbol{x}) = 0,\ j = 1,\ldots,\tilde{n}_e, \tag{2.14}$$

$$\kappa_j(\boldsymbol{x}) \geq 0,\ j = \tilde{n}_e + 1,\ldots,\tilde{n}, \tag{2.15}$$

$$\text{and } \boldsymbol{x}_l \leq \boldsymbol{x} \leq \boldsymbol{x}_u, \tag{2.16}$$

with $\boldsymbol{x}$ being a vector containing n model parameters with lower and upper bounds $\boldsymbol{x}_l$ and $\boldsymbol{x}_u$, g being the objective function, κ_j the constraint functions, $\tilde{n}_e$ the number of equality constraints, and $\tilde{n}$ the total number of constraints (KRAFT 1988).

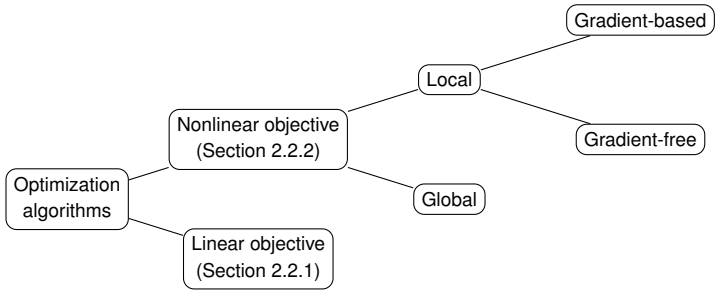

Figure 2.1: Classification of optimization algorithms based on the work of SCHRÖDER and BUSS (2017)

2.2.1 Linear Optimization

Linear optimization algorithms can be used whenever the objective function $g(\boldsymbol{x})$ depends linearly on the n model parameters $\boldsymbol{x} = [x_1, \ldots, x_n]^\intercal$ (NELLES 2020), that is,

$$g(\boldsymbol{x}, \boldsymbol{\tau}) = \sum_{i=1}^{n} c_i(\boldsymbol{\tau}) x_i = \boldsymbol{c}^\intercal(\boldsymbol{\tau})\boldsymbol{x}. \tag{2.17}$$

The entries of $\boldsymbol{c}^\intercal$ are called regressors and, optionally, depend on the model's input values $\boldsymbol{\tau}$. If there are at least as many observations of the objective function $\hat{\boldsymbol{g}} = \left[\hat{g}_1, \ldots, \hat{g}_{\hat{N}}\right]^\intercal$ as model parameters $\boldsymbol{x}$ (i.e., with different input state and thus different regressors $\boldsymbol{c}^\intercal$) and the error sum of squares is used as a loss function, the least squares (LS) method can be used to find the optimal model parameter values $\boldsymbol{x}^*$(NELLES 2020). In this case, the optimization problem reads

$$\min_{\boldsymbol{x}\in\mathbb{R}^n} E(\boldsymbol{x}) = \min_{\boldsymbol{x}\in\mathbb{R}^n} \frac{1}{2}\boldsymbol{e}^\intercal\boldsymbol{e} \tag{2.18}$$

with the vector $\boldsymbol{e} = \hat{\boldsymbol{g}} - \boldsymbol{C}\boldsymbol{x}$ containing the observation errors, and $\boldsymbol{C}$ grouping the different regressors for various model inputs. Setting the derivative of the loss function to zero yields the solution for the unknown model parameters:

$$\frac{\partial E(\boldsymbol{x})}{\partial \boldsymbol{x}} = -\boldsymbol{C}^\intercal(\hat{\boldsymbol{g}} - \boldsymbol{C}\boldsymbol{x}) \stackrel{!}{=} \boldsymbol{0} \tag{2.19}$$

$$\Rightarrow \boldsymbol{x} = (\boldsymbol{C}^\intercal\boldsymbol{C})^{-1}\boldsymbol{C}^\intercal\hat{\boldsymbol{g}}. \tag{2.20}$$

The matrix $(\boldsymbol{C}^\intercal \boldsymbol{C})^{-1} \boldsymbol{C}^\intercal$ is called the pseudoinverse of the matrix $\boldsymbol{C}$ and can be computed if $\boldsymbol{C}$ has full rank, which is the case if there are at least as many independent observations as unknown parameters (i.e., $\hat{N} \geq n$).

The presented LS algorithm is only applicable if no bounds for the model parameters exist. However, extensions of the algorithm are available which can, for example, solve the bounded-variable least squares problem

$$\min_{\boldsymbol{x} \in \mathbb{R}^n} E(\boldsymbol{x}) = \min_{\boldsymbol{x} \in \mathbb{R}^n} \frac{1}{2} \boldsymbol{e}^\intercal \boldsymbol{e} \tag{2.21}$$

subject to

$$\boldsymbol{x}_l < \boldsymbol{x} < \boldsymbol{x}_u \text{ with } \boldsymbol{x}_l, \boldsymbol{x}_u \in \mathbb{R}^n. \tag{2.22}$$

Here, $\boldsymbol{x}_l$ and $\boldsymbol{x}_u$ represent the lower and upper bounds of the n model parameters grouped in the vector $\boldsymbol{x}$. More information on the bounded-variable least squares algorithm can be found in the work of STARK and PARKER (1995). Note that these extensions are iterative solutions. Thus, they are computationally more expensive than the one-shot solution of the unconstrained LS problem in equation 2.20. For real-time applications, the so-called recursive least squares algorithm, which keeps the computational effort constant for a continuously increasing number of data points, can be used (NELLES 2020).

2.2.2 Nonlinear Optimization

In case the model parameters contribute to the model in a nonlinear way, nonlinear optimization algorithms have to be used. As shown in figure 2.1, two fundamental classes of nonlinear optimization exist. On the one hand, there are local algorithms that yield so-called local optima, which represent points that have smaller (or larger) objective function values than any other point in their vicinity. On the other hand, global algorithms seek the overall smallest value in the entire solution space (NOCEDAL and WRIGHT 2006). Global solutions are generally harder to find but may be needed for some applications (NOCEDAL and WRIGHT 2006). Local algorithms generally are deterministic, meaning that they always end up at the same optimum for a fixed starting point. In contrast, most global algorithms are not reproducible since they deliberately apply stochastic

elements to avoid ending up in local optima (SCHRÖDER and BUSS 2017). This section first covers and briefly describes local optimization methods. Second, it presents and explains global optimization algorithms.

Local Methods

Local optimization algorithms are iterative processes, which, in each step, examine the objective function at the current best solution and use the derived information to move on to the next best solution. These steps are repeated until the optimization is terminated, which can, for example, be the case if a sufficiently small value of the objective function has been reached or a maximum number of iterations has been performed. Again, several classes of local optimization methods exist depending on the order of derivates of the objective function needed for determining the next solution estimate (see figure 2.2).

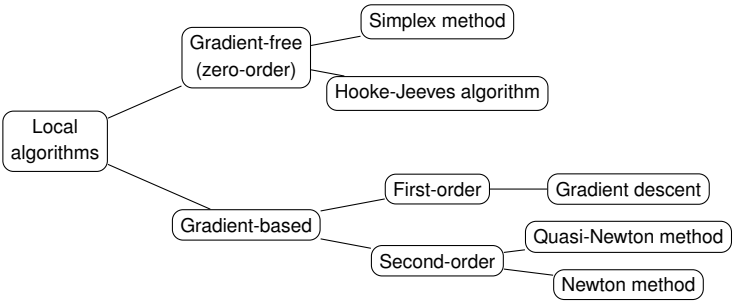

Figure 2.2: Classification of local optimization algorithms based on the work of SCHRÖDER and BUSS (2017)

The Hooke-Jeeves algorithm requires evaluations of the objective function itself but not of its derivates. Thus, it is an example for a zero-order local optimization algorithm (SCHRÖDER and BUSS 2017). In each step, information is gathered first by sequentially going a fixed-sized step in each coordinate direction. If the objective function value is lower than the starting point, the step is directly taken. If it is higher, the negative direction is tested. Whenever no improvement can be made in any direction, the step size is decreased and the procedure is repeated. From this routine, a new base point emerges. In most cases, the difference between the step's initial point and the new base point is a reasonable estimation of the objective function's gradient. If this direction leads to further

improvement (i.e., if a lower objective function value is found), it is directly executed. If not, the next step starts with gathering information by testing all coordinate directions again. Another example of zero-order algorithms is the Simplex method (SCHRÖDER and BUSS 2017). Using these algorithms, however, is only recommended if the objective function's derivatives cannot be computed, as their performance is inferior to higher-order algorithms (SCHRÖDER and BUSS 2017).

First-order algorithms evaluate the gradient of the objective function to determine more efficient search directions (SCHRÖDER and BUSS 2017). Note that the gradient does not need to be known analytically but can also be computed by finite difference techniques (NELLES 2020). It can be shown that the objective function's negative gradient

$$-\nabla g = \begin{bmatrix} -\frac{\partial g}{\partial x_1} \\ \vdots \\ -\frac{\partial g}{\partial x_n} \end{bmatrix} \tag{2.23}$$

with n being the number of model parameters is the direction of the steepest descent of the objective function (SCHRÖDER and BUSS 2017). Thus, a very simple form of a first-order optimization algorithm would be to choose an initial value of the model parameters, compute the gradient of the objective function with respect to these parameters, proceed to a new point by moving a fixed amount toward the negative gradient direction (i.e., $-\eta\nabla g$ with η being a fixed step length), and repeat this procedure until the value of the objective function is sufficiently small, a maximum number of iterations has been reached, or the objective function does not change significantly (SCHRÖDER and BUSS 2017). In practice, it is difficult to find good values for the step length η, and problems such as stagnation in shallow regions, oscillations, and missing good minima occur. Some of these problems can be mitigated by extending the algorithm with momentum terms and adaptive step size algorithms. However, second-order optimization algorithms with comparable computational efficiency exist, which generally outperform simple gradient descent algorithms (NELLES 2020; SCHRÖDER and BUSS 2017).

On top of the gradient, second-order algorithms directly or indirectly use second-order derivatives of the objective function. The basic idea of these so-called

Newton methods is to approximate the objective function in the current iteration by a quadratic function and to directly proceed to its stationary point. For this, the inverse Hessian matrix has to be computed. Only if it is positive definite at the new model parameter estimate, an actual minimum has been found. Thus, additional measures have to be taken to ensure that the algorithms do not converge in maxima or saddle points. However, the computation of the inverse Hessian matrix is numerically expensive. Thus, so-called quasi-Newton methods have emerged, overcoming these problems by approximating the (inverse) Hessian matrix instead of calculating it via finite difference techniques (NELLES 2020; SCHRÖDER and BUSS 2017). One of those techniques is the sequential least squares programming (SLSQP) method, which solves the general nonlinear optimization problem with equality and inequality constraints as defined in equation 2.13. Figure 2.3 shows an example of finding the minimum of a two-dimensional function. It can be seen that the global optimum was found with high accuracy in just five iterations, demonstrating the efficiency of second-order local optimization algorithms. More details on the SLSQP algorithm can be found in the works of KRAFT (1988) and NOCEDAL and WRIGHT (2006).

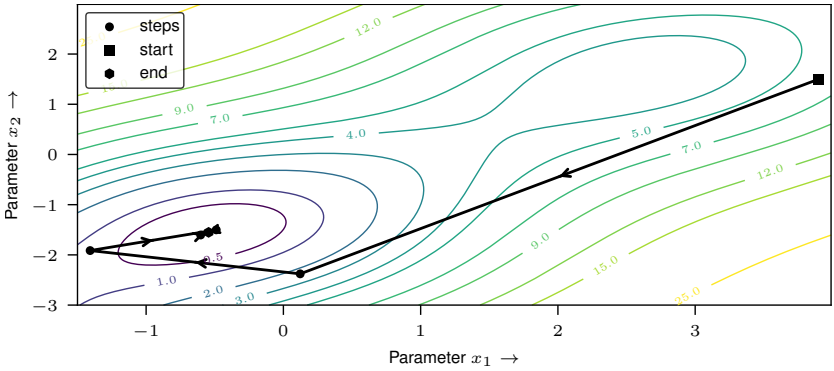

Figure 2.3: Illustration of the SLSQP second-order optimization algorithm

All presented methods have in common that they start from just one point in the solution space and iteratively generate a series of parameter vectors where, ideally, each vector has a lower objective function value than its predecessor. The optimization is only stopped when at least one of possibly several exit conditions is met. The key difference between local optimization methods is the level of information obtained from the objective function. While zero-order

algorithms only evaluate the objective function itself, first-order algorithms also exploit the objective function's gradient, and second-order algorithms further exploit its Hessian matrix to achieve faster convergence. However, they all tend to stall in local minima. In the design process of neural networks, for example, this drawback may be acceptable (SCHRÖDER and BUSS 2017). If it is not, global optimization methods have to be used, of which an overview is given in the next section.

Global Methods

Global optimization methods aim, in contrast to local methods, at finding an objective function's global optimum in the defined solution space. The most common are stochastic global optimization algorithms, which deliberately apply random elements for overcoming local minima (SCHRÖDER and BUSS 2017). In this section, these algorithms will be presented first. Afterward, Bayesian optimization, which relies on a statistical representation of the objective function (GARNETT 2023), will be described in detail. Figure 2.4 extends figure 2.1 and shows a classification of global optimization algorithms.

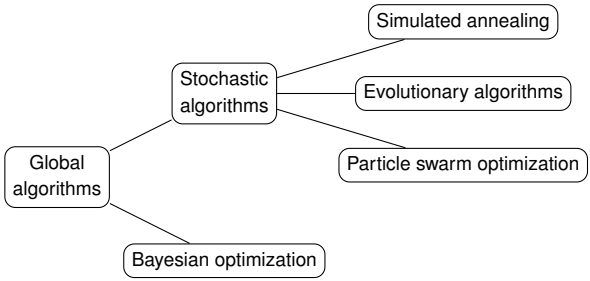

Figure 2.4: Classification of global optimization algorithms

Simulated annealing is a global optimization algorithm that is based on the cooling process of materials. Depending on a material's temperature, a particle state with minimal energy exists. However, particles have, based on the material's temperature T, a certain probability p to be found in a state with an energy that is ΔE higher than the minimal energy:

$$p(T, \Delta E) = w \exp\left(-\frac{\Delta E}{k_B T}\right). \tag{2.24}$$

Here, w is the so-called statistical weight of a certain energy level, and k_B is the Boltzmann constant. Equation 2.24 is called Boltzmann distribution. The lower the temperature is, the more unlikely are states different from the minimal energy level. Simulated annealing is an iterative algorithm. In each step, a random motion is proposed, which is directly executed if it leads to an improvement of the objective function. If it does not, it is only executed with a probability based on the original Boltzmann distribution in equation 2.24, in which w and k_B are eliminated by setting them to 1. Representing a cooling process, the virtual temperature T is decreased in each step, making a deterioration more and more unlikely in the course of the optimization process. The algorithm is stopped when one or several termination conditions are met. Examples are exceeding a maximum number of iterations or falling short of a minimum relative change of the objective function between two steps. In conclusion, the algorithm at the beginning almost randomly scans the solution space but tends to converge to an optimum in its later stages. More information on simulated annealing can be found in the work of SCHRÖDER and BUSS (2017).

Similarly to simulated annealing, evolutionary algorithms (EAs) are also based on a natural phenomenon. The search for the global optimum is mimicked by the evolution of a so-called population, which consists of several individuals. Each individual represents a point in the solution space of the objective function and thus a possible solution to the optimization problem. The population evolves in discrete steps, so-called generations. In other words, a generation represents a population at a fixed point in time. The members of the old population are called parents, while the new generation consists of so-called children. In the most general case, each generation evolves from the previous one by three principles also found in nature:

Recombination: Children are created by merging the properties of at least two parents.

Mutation: The properties of children are randomly disturbed. Similar to simulated annealing, this is the statistical element of EAs which tries to ensure that local minima can be overcome.

Selection: Only some but not all members of a new generation survive. This can, for example, be only the fittest children (i.e., the ones with the best objective function value).

While recombination and mutation increase the (genetic) diversity of the population, selection deliberately reduces it to steer the population toward the global minimum. EA is the generic term for a variety of specific algorithms, which include, among others, the genetic algorithm and evolutionary strategies (ESs). Both variants have been developed independently from each other (SCHRÖDER and BUSS 2017), and they originally differ in the importance and design of the number coding, the selection rule, and the mutation and recombination principles (NELLES 2020). One particular class of ESs are so-called $(\mu + \lambda)$-ESs. Here, μ parents are cloned and mutated (i.e., there is no recombination), resulting in λ children. The next generation then is formed by letting the best μ members survive. Since the individuals are immortal, only improvements can occur. However, it is possible that these algorithms converge to only a local optimum. In contrast, (μ, λ)-ESs dictate that each individual only lives for one generation. If, additionally, the recombination principle is exploited, one speaks of an $(\mu/\rho\#\lambda)$-ES. Here, each child is created by merging the properties of ρ parents (SCHRÖDER and BUSS 2017). ESs start from an initial population and, for example, are terminated after a fixed number of generations or when the improvement between the best individuals of two consecutive generations is smaller than a previously set bound.

Another example of nature-inspired global optimization algorithms is the particle swarm optimization (PSO) approach. Similar to a flock of birds, a swarm of particles explores the parameter space via movements in it. Again, each particle represents a possible solution to the optimization problem. The particles can exchange information, eventually leading to a coordinated movement toward the objective function's (global) optimum (SCHRÖDER and BUSS 2017). The movement of a single particle l in each iteration i can be described by

$$\boldsymbol{x}_{l,i+1} = \boldsymbol{x}_{l,i} + \boldsymbol{v}_{l,i} \tag{2.25}$$

$$\boldsymbol{v}_{l,i+1} = w_1 \boldsymbol{v}_{l,i} + w_2 r_2 (\tilde{\boldsymbol{x}}_{l,i} - \boldsymbol{x}_{l,i}) + w_3 r_3 (\tilde{\boldsymbol{x}}_i^s - \boldsymbol{x}_{l,i}), \tag{2.26}$$

where $\boldsymbol{v}_{l,i}$ is the particle's velocity, $\tilde{\boldsymbol{x}}_{l,i}$ is the location (i.e., the parameter vector) with the particle's best value of the objective function, $\tilde{\boldsymbol{x}}_i^s$ is the location with the swarm's best objective function value, $\boldsymbol{x}_{l,i}$ is the particle's current position in the parameter space, r_2 and r_3 are uniformly distributed random numbers in the interval $[0, 1]$, and w_1, w_2, and w_3 are user-defined weights controlling the

particle's inertial, nostalgic, and social behavior (POLI et al. 2007; SCHRÖDER and BUSS 2017). In other words, each particle is guided by a random mix of individual and common knowledge. The inertial term controlled by w_1 prevents premature convergence and encourages the exploration of the parameter space. Figure 2.5 illustrates an exemplary PSO process with 30 particles. It can be seen in figure 2.5a that, in the initial state, the particles are distributed randomly in the search domain and possess random velocities. After only six iterations they form a flock with a single target (see figure 2.5b), which represents the global optimum at $(-0.54, -1.55)$. As can be seen in figure 2.5d, the swarm has closely approximated the global optimum after 20 iterations. In fact, the best particle has approached it up to the third decimal place. Another example of an optimization based on swarm intelligence, which is better suited for combinatorial problems, is the so-called ant colony optimization algorithm. It is based on individuals exploring routes through the search domain and leaving odor trails (SCHRÖDER and BUSS 2017).

To sum up, the presented global optimization algorithms, unlike the local techniques presented above, can overcome local optima and converge to the global optimum. This is achieved by deliberately introducing random elements in the optimization routines. However, it is not guaranteed that the global optimum is found, in particular for objective function surfaces with symmetric or almost equally good minima. Furthermore, these algorithms often need a lot more function evaluations than local second-order algorithms (SCHRÖDER and BUSS 2017). For example, the optimization processes presented in figures 2.3 and 2.5 are based on the same objective function. The second-order SLSQP algorithm, however, has approximated the global optimum with even higher precision with only 26 objective function evaluations than did the global PSO routine with, in total, 600 evaluations.

In contrast to the presented algorithm, Bayesian optimization is a model-based approach which models the unknown objective function as a stochastic process (GARNETT 2023). The basis of the optimization is a prior (process), which ideally reflects as much information known about the objective function as possible. Figure 2.6 illustrates the overall Bayesian optimization process and figure 2.6a, in particular, the design of the prior. It shows a one-dimensional objective function, which serves as ground truth reference for the optimization to be conducted, and a prior approximating the true function, which contains only

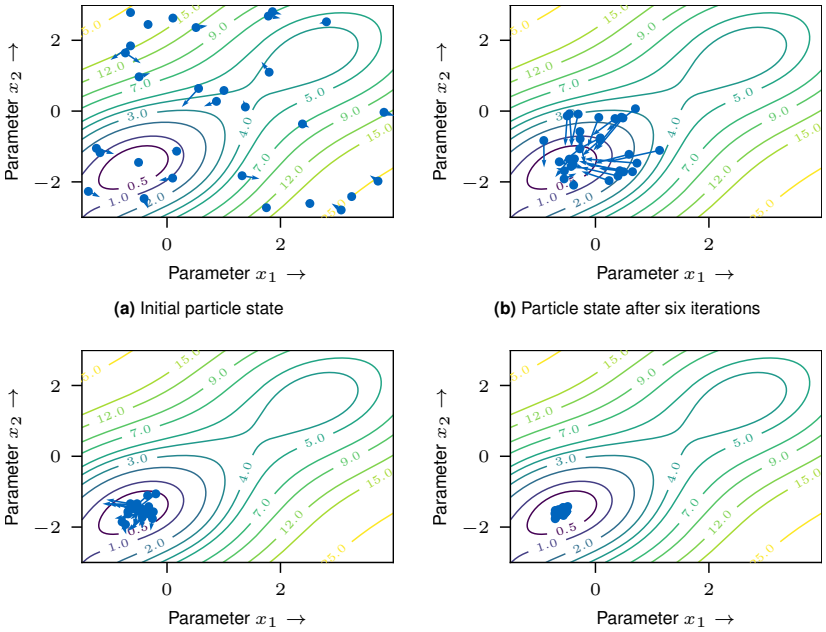

(a) Initial particle state

(b) Particle state after six iterations

(c) Particle state after ten iterations

(d) Particle state after 20 iterations

Figure 2.5: Illustration of the PSO algorithm with 30 particles

very basic assumptions such as being smooth. The statistical nature of the prior is visualized by showing the estimated mean value and the corresponding 95 % confidence interval. New information in the form of new observations of the objective function is gradually merged with the prior, resulting in new posterior processes (see figures 2.6b to 2.6d). Since, in this case, the observations are assumed to be certain, the estimated mean of the posterior at the observation points exactly goes through the observation points with no uncertainty. In proximity to the observations, the uncertainty only decreases. When more observations are added (see figures 2.6c and 2.6d), the overall uncertainty is reduced, and the posterior approaches the ground truth reference function. The key idea of Bayesian optimization is to use the statistical information contained in the posterior process to propose and evaluate new observation points. This is done by optimizing an acquisition function. A common example is the so-called probability of improvement acquisition function, which proposes

the location with the highest chance of an improvement regardless of its size. Similarly, the expected improvement acquisition function targets the point with the highest improvement value, also quantifying the size of the improvement. Many more observation policies and acquisition functions exist (GARNETT 2023). However, all of them have in common that they must balance the so-called exploration-exploitation trade-off. As can be seen in figure 2.6d, regions with already known high values can be exploited to find even better values nearby, while regions with high uncertainty may not offer a direct improvement but the opportunity to explore new regions in the optimization domain with the overall global optimum. Like other optimization algorithms, Bayesian optimization is, for example, terminated when a certain number of observations has been made and the budget is consumed, or when the improvement stagnates.

For Bayesian optimization, knowledge about the objective function can be incorporated in the prior. However, this is only optional, meaning that Bayesian optimization can be applied to black-box models as well. The only requirement for the objective function is to be observable. This is allowed even under the presence of observation noise. Furthermore, Bayesian optimization is very cost-efficient and thus applicable to models that cannot be frequently evaluated. For Bayesian optimization, the existence of a gradient is not required, meaning that it can also handle discrete (i.e., non-continuous) parameters. All these properties make Bayesian optimization an ideal choice for hyperparameter tuning of complex machine learning models (GARNETT 2023). For more information about Bayesian optimization, the reader is kindly referred to the work of GARNETT (2023).

2.3 Structural Dynamics

First, the fundamentals of calculating the dynamic behavior of mechanical structures and modeling their damping properties are presented. Second, it is shown how these structures' properties can be measured. The last subsection deals with methods for comparing different dynamic behavior information.

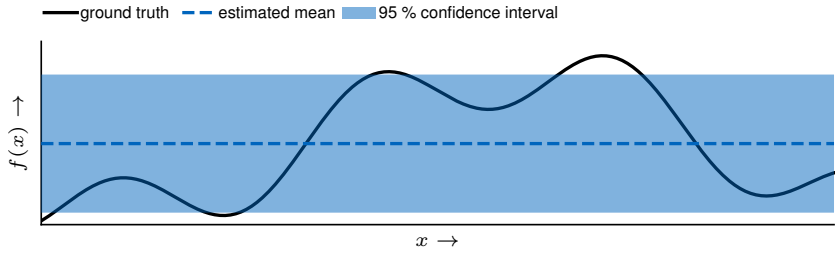

(a) Initial state: prior without any observations

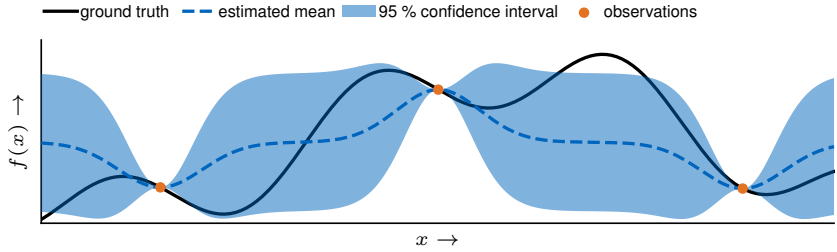

(b) Posterior after step 1 with three observations

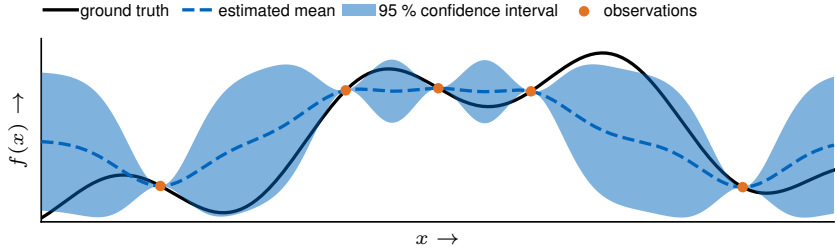

(c) Posterior after step 2 with five observations

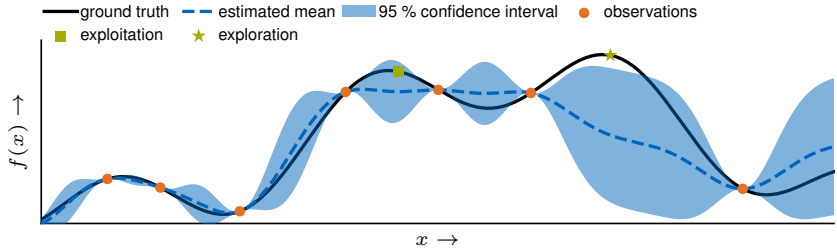

(d) Posterior after step 3 with seven observations and proposals for further explorative and exploitive steps

Figure 2.6: Illustration of the Bayesian optimization process based on the work of GARNETT (2023)

2.3.1 Modeling Fundamentals

This section aims at giving an overview of the dynamics of mechanical structures. It is based on the explanations in the works of EWINS (2000) and MAIA (1997), in which further information and a more detailed discussion of the topic can be found.

One way to model the behavior of mechanical structures is using theoretical bottom-up models, which, in contrast to black-box or data-driven models, generally offer more insights into the occurring physical phenomena. These models relate the system's mass, stiffness, and damping properties with its motion (NATKE 1992) and can be formulated as

$$\boldsymbol{M}\ddot{\boldsymbol{u}}(t)+\boldsymbol{B}\dot{\boldsymbol{u}}(t)+(\boldsymbol{K}+\mathrm{j}\boldsymbol{D})\,\boldsymbol{u}(t)=\boldsymbol{f}(t). \tag{2.27}$$

Here, the system's N displacement DOFs are grouped in the vector $\boldsymbol{u}$ and the forces acting on the system in the vector $\boldsymbol{f}$. Both depend on the time t. $\boldsymbol{M}$, $\boldsymbol{B}$, $\boldsymbol{D}$, and $\boldsymbol{K}$ are mass, viscous damping, hysteretic damping, and stiffness matrices of size $N \times N$. The variable j represents the imaginary unit.

Undamped Dynamics

The solution of equation 2.27 has two parts (MAIA 1997): the homogeneous part, representing the so-called free vibration system, and the particular solution for forced vibrations. The former can be obtained by setting $\boldsymbol{f}(t) = \boldsymbol{0}$ and, initially, disregarding the damping terms, resulting in

$$\boldsymbol{M}\ddot{\boldsymbol{u}}(t)+\boldsymbol{K}\boldsymbol{u}(t)=\boldsymbol{0}. \tag{2.28}$$

Substituting

$$\boldsymbol{u}(t)=\bar{\boldsymbol{u}}e^{\mathrm{j}\omega t} \tag{2.29}$$

with $\bar{\boldsymbol{u}}$ being a constant amplitude vector of size $N \times 1$ and ω denoting an angular frequency into equation 2.28 yields

$$\left(\boldsymbol{K}-\omega^2\boldsymbol{M}\right)\bar{\boldsymbol{u}}\,e^{\mathrm{j}\omega t}=\boldsymbol{0}. \tag{2.30}$$

Since $e^{j\omega t} \neq 0$ for any time t and $\bar{\boldsymbol{u}}$ is also generally unequal to the null vector for non-trivial solutions, the matrix term in equation 2.30 needs to be singular for a solution or, in other words,

$$\det\left(\boldsymbol{K} - \omega^2 \boldsymbol{M}\right) = 0. \tag{2.31}$$

Equation 2.30 is an eigenvalue problem and is called the characteristic equation of the multi-degree-of-freedom (MDOF) system modeled in equation 2.27. It yields N real-valued eigenvalues $\lambda_i := \bar{\omega}_i^2$. Their square roots $\bar{\omega}_i$ are the undamped eigenfrequencies of the MDOF system. If these are substituted into equation 2.30, N eigenvectors $\boldsymbol{\psi}_i$ of size $N \times 1$ can be obtained. These are also called the mode shapes of the system. With the help of the eigenvectors in matrix form, that is,

$$\boldsymbol{\Psi} = [\boldsymbol{\psi}_1, \boldsymbol{\psi}_2, \ldots, \boldsymbol{\psi}_N], \tag{2.32}$$

the coordinate transform

$$\boldsymbol{u}(t) = \boldsymbol{\Psi}\boldsymbol{q}(t) \tag{2.33}$$

can be defined, where $\boldsymbol{q}$ are the so-called modal DOFs. Substituting equation 2.33 into equation 2.28 and pre-multiplying with the transpose of the eigenvector matrix $\boldsymbol{\Psi}$ yields

$$\boldsymbol{\Psi}^\mathsf{T}\boldsymbol{M}\boldsymbol{\Psi}\ddot{\boldsymbol{q}}(t) + \boldsymbol{\Psi}^\mathsf{T}\boldsymbol{K}\boldsymbol{\Psi}\boldsymbol{q}(t) = \boldsymbol{0}. \tag{2.34}$$

It can be shown that pre- and post-multiplying the stiffness and mass matrices with $\boldsymbol{\Psi}^\mathsf{T}$ and $\boldsymbol{\Psi}$, respectively, leads to diagonal matrices (MAIA 1997). The eigenvectors can be arbitrarily scaled. It is common to mass-normalize them, yielding the mass-normalized eigenvector matrix $\boldsymbol{\Phi}$ and resulting in

$$\boldsymbol{\Phi}^\mathsf{T}\boldsymbol{M}\boldsymbol{\Phi} = \operatorname{diag}(1, \ldots, 1) = \boldsymbol{I} \text{ and} \tag{2.35}$$

$$\boldsymbol{\Phi}^\mathsf{T}\boldsymbol{K}\boldsymbol{\Phi} = \operatorname{diag}\left(\bar{\omega}_1^2, \ldots, \bar{\omega}_N^2\right) = \boldsymbol{\Lambda}. \tag{2.36}$$

Here, $\boldsymbol{I}$ is the identity matrix, $\boldsymbol{\Lambda}$ is a matrix containing the system's eigenvalues, and $\bar{\omega}_1, \ldots, \bar{\omega}_N$ are the system's eigenfrequencies. In other words, the coupled MDOF problem from equation 2.27 has been uncoupled to N independent

single-degree-of-freedom (SDOF) systems, which can be efficiently solved.

The second part of the solution of equation 2.27 is the particular solution for forced vibrations. For the special case of harmonic excitation forces

$$\boldsymbol{f}(t) = \bar{\boldsymbol{f}} e^{\mathrm{j}\omega t}, \tag{2.37}$$

the assumption from equation 2.29 transforms the undamped equation 2.27 into

$$\left(\boldsymbol{K} - \omega^2 \boldsymbol{M}\right) \bar{\boldsymbol{u}} = \bar{\boldsymbol{f}}. \tag{2.38}$$

With the help of the receptance matrix $\mathbf{A}(\omega)$, which contains all receptance frequency response functions (FRFs) $\alpha_{ij}(\omega)$ of the MDOF system between each possible input DOF $i = 1,\ldots,N$ and output DOF $j = 1,\ldots,N$, this can be rewritten as

$$\mathbf{A}(\omega) := \frac{\bar{\boldsymbol{u}}}{\bar{\boldsymbol{f}}} = \left(\boldsymbol{K} - \omega^2 \boldsymbol{M}\right)^{-1}. \tag{2.39}$$

To avoid the computationally costly inversion of the non-diagonal matrix, equation 2.39 can be reformulated using the modal properties of the system (EWINS 2000) as

$$\mathbf{A}(\omega) = \boldsymbol{\Phi}^{\mathsf{T}} \operatorname{diag}\left(\bar{\omega}_1^2 - \omega^2, \ldots, \bar{\omega}_N^2 - \omega^2\right)^{-1} \boldsymbol{\Phi}, \tag{2.40}$$

or, for individual FRFs from input DOF i to output DOF j, as

$$\alpha_{ij}(\omega) = \sum_{l=1}^{N} \frac{\Phi_{il}\Phi_{jl}}{\bar{\omega}_l^2 - \omega^2}. \tag{2.41}$$

Here, Φ_{il} denotes entries of the mass-normalized eigenvector matrix. For example, Φ_{32} corresponds to the third entry of the second (mass-normalized) mode shape.

Proportionally Damped Dynamics

For real-world systems, damping can seldom be disregarded. However, before the transition to the generally damped case is made, a special case is to be

considered first, in which the system's undamped eigenvectors also diagonalize the damping matrices in a way analogous to the stiffness and mass matrices (see equations 2.35 and 2.36). This is called proportional damping and, among others, includes the so-called Rayleigh damping approach, in which the viscous damping matrix can be expressed by a linear combination of the mass and stiffness matrices (see section 2.3.2). The main advantage of proportionally damped systems is that the modal transformation derived above still decouples the MDOF system to N independent SDOF systems, strongly simplifying the simulation and the evaluation of these systems.

In the proportionally damped case, the undamped forced vibration solution (see equation 2.41) can be extended to the hysteretically damped solution as

$$\alpha_{ij}(\mathrm{j}\omega) = \sum_{l=1}^{N} \frac{\Phi_{il}\Phi_{jl}}{\bar{\omega}_l^2 - \omega^2 + \mathrm{j}\eta_l\bar{\omega}_l^2} = \sum_{l=1}^{N} \frac{A_{ij,l}}{\bar{\omega}_l^2 - \omega^2 + \mathrm{j}\eta_l\bar{\omega}_l^2}, \tag{2.42}$$

where

$$\eta_l = \frac{\bar{d}_l}{\bar{\omega}_l^2\bar{m}_l} \tag{2.43}$$

is the loss factor of mode l, $A_{ij,l}$ are so-called modal constants, $\bar{m}_l$ are the modal masses resulting from the diagonalization of the mass matrix (see equation 2.35), $\bar{\omega}_l$ are the system's (angular) eigenfrequencies, and $\bar{d}_l$ are the modal hysteretic damping values which result from the diagonalization of the hysteretic damping matrix

$$\boldsymbol{\Psi}^{\mathsf{T}}\boldsymbol{D}\boldsymbol{\Psi} = \mathrm{diag}\left(\bar{d}_1, \ldots, \bar{d}_N\right). \tag{2.44}$$

Note that the definition of $\mathrm{j}\omega$ as function input highlights the generally complex-valued nature of FRFs (ALTINTAS 2012).

Similarly, the solution for proportional viscous damping reads

$$\alpha_{ij}(\mathrm{j}\omega) = \sum_{l=1}^{N} \frac{\Phi_{il}\Phi_{jl}}{\bar{\omega}_l^2 - \omega^2 + 2\mathrm{j}\xi_l\omega\bar{\omega}_l} = \sum_{l=1}^{N} \frac{A_{ij,l}}{\bar{\omega}_l^2 - \omega^2 + 2\mathrm{j}\xi_l\omega\bar{\omega}_l}, \tag{2.45}$$

with

$$\xi_l = \frac{\bar{b}_l}{2\sqrt{\bar{m}_l \bar{k}_l}} \tag{2.46}$$

being the modal damping ratio of mode l, $\bar{m}_l$ the modal masses resulting from the diagonalization of the mass matrix (see equation 2.35), $\bar{k}_l$ the modal stiffnesses resulting from the diagonalization of the stiffness matrix (see equation 2.36), and $\bar{b}_l$ the modal viscous damping values which result from the diagonalization of the viscous damping matrix

$$\boldsymbol{\Psi}^{\mathsf{T}} \boldsymbol{B} \boldsymbol{\Psi} = \operatorname{diag}\left(\bar{b}_1, \ldots, \bar{b}_N\right). \tag{2.47}$$

In contrast to the undamped (see equation 2.28) and the hysteretically damped system, a structure with proportional viscous damping will vibrate in the damped eigenfrequencies $\tilde{\omega}_l = \bar{\omega}_l \sqrt{1 - \xi_l^2}$.

Generally Damped Dynamics

The special case of proportional damping will hardly be present in models of real-world systems. There are two ways to deal with this: First, in contrast to the real-valued eigenvalue problem of equation 2.30, a complex eigenvalue problem can be formulated and solved (EWINS 2000). For both cases of viscous and hysteretic damping, this results in receptance FRFs in the form

$$\alpha(\mathrm{j}\omega) = \sum_{l=1}^{N} \frac{P}{\bar{\omega}_l^2 - \omega^2 + \mathrm{j}Q}. \tag{2.48}$$

Here, P and Q are placeholders whose value depends on the damping model as described in table 2.3.

Second, the diagonality of the damping matrices and thus the modal uncoupling are commonly enforced by simply neglecting any off-diagonal terms (SHAHRUZ 1990). This was extensively studied in the work of HASSELMAN (1976) and was found to be justified when there is either a sufficiently high eigenfrequency separation or the modal damping ratios are low. These results were confirmed by the work of NIEHUES (2015), who generally assumed machine tools to be lightly damped and also studied the effect of neglecting off-diagonal damping terms.

Table 2.3: Properties of the FRF placeholders defined in equation 2.48 based on the work of EWINS (2000); the placeholders are either constant or a function of the angular frequency ($g(\omega)$).

Damping model		Placeholder P	Placeholder Q
Undamped		Real, constant	0
Proportional	**hysteretic**	Real, constant	Real, constant
	viscous	Real, constant	Real, $g(\omega)$
General	**hysteretic**	Complex, constant	Real, constant
	viscous	Complex, $g(\omega)$	Real, $g(\omega)$

Furthermore, the work of SHAHRUZ (1990) proved that simply disregarding the off-diagonal terms is more accurate than any other diagonal approximation.

2.3.2 Damping Models

In all dynamic processes, mechanical energy is irreversibly converted into other forms of energy, most often into thermal energy. This dissipative conversion process is called damping, and it can be caused by many physical effects including, among others, friction, fluid flow effects, or electromagnetic processes (VDI 2004). To achieve reliable results in machine tool simulation, damping effects must be modeled correctly. However, this is a difficult task since damping is influenced by many factors, which are usually not well known (ALTINTAS et al. 2005). For these systems, energy dissipation originates mainly from three sources (see figure 2.7). First, there is structural damping, which denotes damping caused by the structural parts of the machine tool and can be further classified into material, joint, and motion damping (GROSSMANN et al. 2012). When energy is dissipated due to inner deformations within materials, one speaks of material damping. Joint damping occurs between two rigidly connected surfaces due to micro-movements. In contrast, motion damping denotes energy dissipation between moving surfaces due to rigid-body or fluid friction, as it, for example, can be found in linear guides, bearings, and ball screw drives. Second, drive damping means that machine tool vibrations are counteracted by the machine tool's (feed) drives. For this, appropriate control algorithms and laws must be designed. Finally, there is process damping, which describes

energy dissipation in machining by friction between, for example, the cutting tool and the workpiece (AHMADI and ISMAIL 2010; GROSSMANN et al. 2012). In the following, different approaches are presented for modeling these damping effects, which, based on their level of detail, can be either classified as global or local damping models.

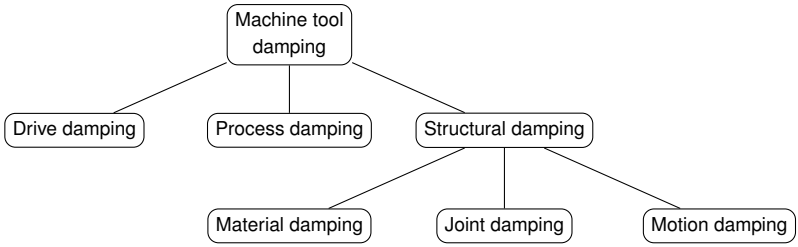

Figure 2.7: Damping sources found in machine tools based on the work of GROSSMANN et al. (2012)

Global Damping Models

Global damping models disregard both the location and mechanism of the energy dissipation, thus working on a higher abstraction level. In other words, these models aim at finding an estimate for the viscous and hysteretic damping matrices $\boldsymbol{B}$ and $\boldsymbol{D}$ from equation 2.27.

One example of global damping modeling is the so-called Rayleigh damping approach (RAYLEIGH 1945)

$$\boldsymbol{B} = \nu \boldsymbol{M} + \vartheta \boldsymbol{K}, \tag{2.49}$$

which expresses the viscous damping matrix $\boldsymbol{B}$ as a linear combination of the mass matrix $\boldsymbol{M}$ and the stiffness matrix $\boldsymbol{K}$ by means of the Rayleigh damping coefficients ν and ϑ. This is, to some extent, physically justified since the actual damping mechanisms of a system are usually geometrically parallel either to its stiffness or its mass elements (EWINS 2000). The Rayleigh damping approach is popular because of its simplicity but, more importantly, also because it leads to a proportionally damped system and all its benefits coming along with it. However, the Rayleigh damping factors have no physical meaning (OERTLI 2008), and they must be determined from experimental data. If just two modes

exist or only two modal damping values are known, the two factors can be uniquely determined. If more information is present, averaging techniques can be applied (OERTLI 2008). Note that the Rayleigh damping approach is just a special case of the more general Caughey series (CAUGHEY 1960).

Another possibility for global damping modeling is to directly determine the modal damping matrix, that is, the modal damping ratios in equation 2.45. According to the work of ALBERTZ (1995), this method is preferred over the Rayleigh damping approach since it, on the one hand, is physically more interpretable. On the other hand, in contrast to the Rayleigh damping factors ν and ϑ, empirical data for choosing modal damping values exist. For example, the linear guiding system of machine tools mostly leads to modes with a modal damping of 1 % to 3 % depending on the specific vibrational form and the linear guiding system type (ALBERTZ 1995). Furthermore, the modal damping values can easily be estimated from experimental data, as briefly demonstrated in section 2.3.3. Per definition, directly setting modal damping also leads to a proportionally damped system.

The Rayleigh damping and modal damping approaches operate on a restricted set of possibilities. Only two Rayleigh damping factors or N modal damping values are set instead of the N^2 entries of the full viscous or hysteretic damping matrices. An alternative approach would be to directly set fully occupied damping matrices. However, this so-called direct updating approach is complex and difficult as, in contrast to the modal damping approach, no empirical guidelines exist and, in contrast to the Rayleigh damping method, more than just two parameters need to be determined. The direct updating approach is capable of exactly representing the reference measurement data, making it a so-called representational method. However, the identified damping matrices have no physical meaning anymore, and spurious modes may be introduced (FRISWELL and MOTTERSHEAD 1996). Furthermore, this approach generally leads to non-proportional damping, complicating the system's simulation and its further analyses. More information on this can be found in the works of FRISWELL and MOTTERSHEAD (1996) and FRISWELL et al. (1998).

Local Damping Models

The basic idea of local damping models is to directly model the damping at the source of origin considering the respective energy dissipation mechanism. This can be done either via linear or nonlinear local damping models. The former class shows a linear relationship between the model's displacement or velocity and its damping force (BALASUBRAMANIAN 2019). The corresponding hysteresis curve, which describes the cyclic relationship between the displacement and the damping force, is elliptic (NIEHUES 2015). Nonlinear damping models allow any shape of the corresponding hysteresis curve and arbitrary correlations of displacements, velocities, and damping forces.

For modeling linear damping of mechanical systems, the viscous and hysteretic damping models are particularly suitable (MAIA 1997; SCHWARZ 2015). Viscous damping

$$f_{visc}(\mathrm{j}\omega) = b\dot{u}(\mathrm{j}\omega) = \mathrm{j}\omega b u(\mathrm{j}\omega) \tag{2.50}$$

leads to a damping force f_{visc}, which is proportional to the velocity by the viscous damping coefficient b. In this equation, ω denotes the angular frequency of the vibration. Hysteretic damping, in turn, models the damping force to be proportional to the displacement by a hysteretic damping coefficient d:

$$f_{hyst}(\mathrm{j}\omega) = \mathrm{j}d u(\mathrm{j}\omega). \tag{2.51}$$

Figures 2.8b and 2.8c illustrate these two linear (local) damping models in their most used variant, that is, in combination with a linear spring element. Furthermore, figure 2.8a visualizes the properties of the equations 2.50 and 2.51 showing that viscous damping is frequency-dependent, while hysteretic damping is not. Even though the viscous damping element is the simplest linear damping model, which can be solved for any type of input, this is the reason for the existence of the hysteretic damping model since most materials' damping properties depend only little or not at all on the excitation frequency (MAIA 1997). However, the hysteretic damping model is limited to steady-state vibrations only. Hence, analyses can only be conducted in the frequency domain (MAIA 1997). To overcome this limitation, an equivalent viscous damping can be defined by setting equal the viscous and hysteretic damping forces from the equations 2.50

and 2.51 as

$$b_{eq} = \frac{d}{\omega}. \tag{2.52}$$

Here, b_{eq} is the equivalent viscous damping coefficient for the hysteretic damping coefficient d at the angular frequency ω. According to equation 2.52, both models can only be equivalent at one fixed frequency. However, it can be shown that, using the respective eigenfrequencies of the system $\bar{\omega}_l$ as a fixpoint, an overall good approximation can be obtained (GENTA 2009). Local damping modeling will hardly follow the restrictions necessary for proportional damping, thus generally leading to non-proportional damping. As mentioned before in section 2.3.1, it is common to simply neglect off-diagonal terms in the modal transformation process, again resulting in a decoupled system.

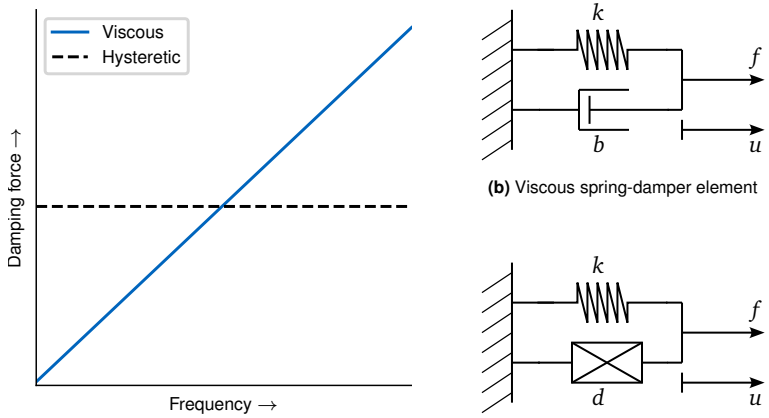

(a) Frequency dependence of linear damping models

(b) Viscous spring-damper element

(c) Hysteretic spring-damper element

Figure 2.8: Visualization of hysteretic and viscous damping models and their properties based on the works of SCHWARZ (2015), NIEHUES (2015), and SEMM (2020)

While linear damping models can accurately describe the inner energy dissipation of most materials (MAIA 1997), energy dissipation between surfaces is best described using nonlinear models (RUDERMAN 2012). In this context, the energy dissipation is often called friction. The simplest variant is the Coulomb friction model

$$f = -\operatorname{sgn}(\dot{u}) f_C = -\operatorname{sgn}(\dot{u}) \mu f_N, \tag{2.53}$$

which expresses the tangential friction force f as a product of the normal force between two surfaces f_N and the Coulomb friction coefficient μ. f_C is called the Coulomb friction force. The direction of the friction force is opposed to the relative velocity $\dot{u}$ between the two surfaces. A more complex model is the so-called Stribeck friction model, which extends the Coulomb friction model by a viscous term and, additionally, adds a more detailed model for the transition between sticking and sliding:

$$f = -\operatorname{sgn}(\dot{u}) \left[f_C + (f_S - f_C) \exp\left(- \left| \frac{\dot{u}}{v_S} \right|^{\delta} \right) \right]. \tag{2.54}$$

Here, $\dot{u}$ is the relative velocity between the two surfaces, f_C is the Coulomb friction force, f_S is the sticking force, v_S is the so-called Stribeck velocity, and δ is called Stribeck factor (RUDERMAN 2012). Figure 2.9 shows the shape of the Stribeck friction force representing, for example, the friction between two metallic surfaces with lubricant in between.

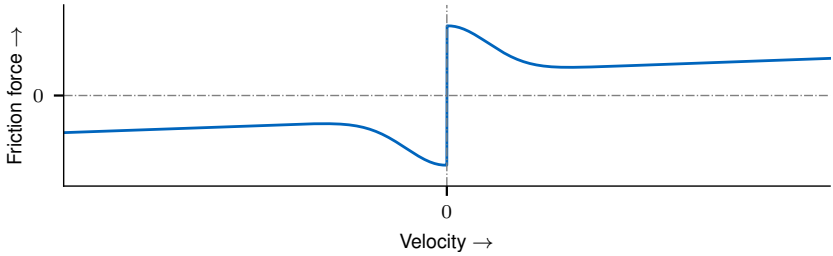

Figure 2.9: Exemplary Stribeck friction force model

It can be seen that the friction force decreases after overcoming the sticking region, which is characterized by velocities which are very small but unequal to zero. The reason for this is a gradually emerging lubricant film, which reduces the friction between the two surfaces. This so-called Stribeck friction effect marks the transition from pure solid body friction to hydrodynamic friction. With higher velocity, the friction force approximates the viscous friction model force, which linearly increases with the relative velocity between the two surfaces.

The Coulomb friction and the Stribeck friction models are so-called static friction models, and they can accurately simulate quasi-static movements, that is, movements with constant or only slowly changing velocity (RUDERMAN

2012). However, in reality, this assumption is rarely valid. Furthermore, the discontinuity of both models at zero velocity (see figure 2.9) causes numerical problems, which can be mitigated by choosing an appropriate solver but cannot be completely overcome (RUDERMAN 2012). Dynamic friction models enable a more detailed simulation of the transition between sticking and sliding. They define a so-called pre-sliding regime, where, in contrast to the already known sliding regime for high velocities, the friction force is a function of the relative displacement instead of the relative velocity. Popular dynamic friction models are the Lund-Grenoble model (CANUDAS DE WIT et al. 1995) and an improved version of it, the so-called Leuven model (SWEVERS et al. 2000).

Note that the presented friction models are both nonlinear and only defined in the time domain. This excludes frequency domain analyses and leads to computationally expensive time domain simulations. However, linearization approaches exist which can approximate the nonlinear friction behavior of these models with linear spring-damper elements. More information on this can be found in the work of SEMM et al. (2020b).

2.3.3 Experimental Characterization

In section 2.3.1, it was shown how frequency response functions (FRFs) can be calculated from a structural dynamics model. In this section, the process of measuring them will be described. Similarly, in section 2.3.1, modal parameters were derived from a system's fundamental equations of motions, and it will be shown how to derive them from measurement data. This section is largely based on the works of ALTINTAS (2012) and AVITABILE (2017), in which further information can be found.

In general, an FRF relates a system's output response to an input excitation in the frequency domain, such as, for example, visible in equation 2.39. Thus, the most straightforward way would be to simply measure input and output signals, transform them into the frequency domain using the fast Fourier transform (FFT), and divide them by each other. Even though this is, in theory, a viable way, calculating high-quality FRFs requires more effort than this simple approach, as hinted by the many steps visible in figure 2.10. Before the actual measurements, choices have to be made on how to generate the excitation input and how to measure the resulting structural vibrations. The former is

typically done either with impact hammers or shakers, while the latter can be done using accelerometers or contactless laser sensors. These devices differ in terms of automation capability, setup time, cost, accuracy, repeatability, and many other criteria (ALTINTAS 2012; AVITABILE 2017; IGLESIAS et al. 2022), and an individual choice has to be made. However, they all have in common that they result in analogous signals, which need to be further processed.

Figure 2.10 illustrates the FRF measurement process as described in the works of AVITABILE (2017) and ALTINTAS (2012). First, the measurement signals have to pass an analogous anti-aliasing (AA) filter to avoid spurious aliasing effects, which occur when a signal is sampled with less than twice its maximum frequency content. Second, the signals need to be digitalized, leading to a discretization in time and quantity. Afterward, window functions are commonly applied to enforce the periodicity of the signals and to prevent signal leakage. With the help of the FFT, the time-domain signals can then be transformed into the frequency domain. When performing analogous measurements, the presence of measurement noise is inevitable. However, noise is generally a random process. Thus, FRF measurements are typically repeated several times and averaged to attenuate measurement noise. Furthermore, the direct division of the system's response vibrations by the corresponding excitation input is also avoided, as it is prone to measurement noise (ALTINTAS 2012). Instead, the FRF $\boldsymbol{h}(\mathrm{j}\omega)$ in numerical vector representation is estimated either as

$$\boldsymbol{h}(\mathrm{j}\omega) \approx \boldsymbol{h}_1(\mathrm{j}\omega) = \frac{\frac{1}{N_{av}} \sum_{i=1}^{N_{av}} \boldsymbol{s}_{y\tau,i}(\mathrm{j}\omega)}{\frac{1}{N_{av}} \sum_{i=1}^{N_{av}} \boldsymbol{s}_{\tau\tau,i}(\mathrm{j}\omega)} \tag{2.55}$$

or

$$\boldsymbol{h}(\mathrm{j}\omega) \approx \boldsymbol{h}_2(\mathrm{j}\omega) = \frac{\frac{1}{N_{av}} \sum_{i=1}^{N_{av}} \boldsymbol{s}_{yy,i}(\mathrm{j}\omega)}{\frac{1}{N_{av}} \sum_{i=1}^{N_{av}} \boldsymbol{s}_{y\tau,i}(\mathrm{j}\omega)}, \tag{2.56}$$

where $\boldsymbol{s}_{\tau\tau,i}(\mathrm{j}\omega)$, $\boldsymbol{s}_{yy,i}(\mathrm{j}\omega)$, and $\boldsymbol{s}_{y\tau,i}(\mathrm{j}\omega)$ are the average input, output, and cross-power spectra in numerical vector representation of the conducted and repeated measurements. For example, the cross-power spectrum of repetition

number i is defined as

$$\boldsymbol{s}_{y\tau,i}(\mathrm{j}\omega) = \boldsymbol{y}_i(\mathrm{j}\omega)\boldsymbol{\tau}_i^*(\mathrm{j}\omega), \tag{2.57}$$

with $\boldsymbol{y}_i(\mathrm{j}\omega)$ and $\boldsymbol{\tau}_i(\mathrm{j}\omega)$ being the measured response and input spectra and $\boldsymbol{a}^*$ denoting the complex conjugate. The expression $\boldsymbol{h}_1(\mathrm{j}\omega)$ attenuates response measurement noise while $\boldsymbol{h}_2(\mathrm{j}\omega)$ mitigates excitation measurement noise. If there is no noise, $\boldsymbol{h}_1(\mathrm{j}\omega) = \boldsymbol{h}_2(\mathrm{j}\omega) = \boldsymbol{h}(\mathrm{j}\omega)$ holds. A similar assessment can be achieved with the so-called coherence function

$$\boldsymbol{\gamma}(\omega) = \sqrt{\frac{\left|\frac{1}{N_{av}}\sum_{i=1}^{N_{av}} \boldsymbol{s}_{y\tau,i}(\mathrm{j}\omega)\right|^2}{\left(\frac{1}{N_{av}}\sum_{i=1}^{N_{av}} \boldsymbol{s}_{yy,i}(\mathrm{j}\omega)\right)\left(\frac{1}{N_{av}}\sum_{i=1}^{N_{av}} \boldsymbol{s}_{\tau\tau,i}(\mathrm{j}\omega)\right)}} \cdot 100\,\%, \tag{2.58}$$

which is real-valued and indicates 100 % if all response vibrations are caused by the excitation input, and 0 % if the response and the input are totally unrelated.

In the state of the art, various methods for experimental modal analysis, that is, deriving modal parameters from experimental data, exist (see section 3.2.1). To illustrate their way of working and their output, the peak-picking method is exemplarily described here. This algorithm operates on frequency-domain data (i.e., FRFs) and is a so-called SDOF method, meaning that the underlying system only has one (vibrational) DOF or, at least, well-separated modes. All following explanations are based on the work of EWINS (2000).

Figure 2.11 shows a magnitude plot of the symbolic FRF h of a SDOF system with viscous damping only, which, according to equation 2.45, can be modeled by

$$h(\mathrm{j}\omega) = \frac{A}{\bar{\omega}^2 - \omega^2 + 2\mathrm{j}\xi\omega\bar{\omega}}, \tag{2.59}$$

with A being the modal constant, $\bar{\omega}$ the angular eigenfrequency, and ξ the modal damping ratio. The first step of the peak-picking method is to find the largest magnitude of the FRF, which is denoted $\hat{h}$ (see figure 2.11). The corresponding angular frequency $\hat{\omega}$ is a close estimate of the system's eigenfrequency $\bar{\omega}$. In a second step, the frequencies ω_1 and ω_2 are determined, which denote the points where the magnitude drops to a fraction of $1/\sqrt{2}$ of the peak value. These are

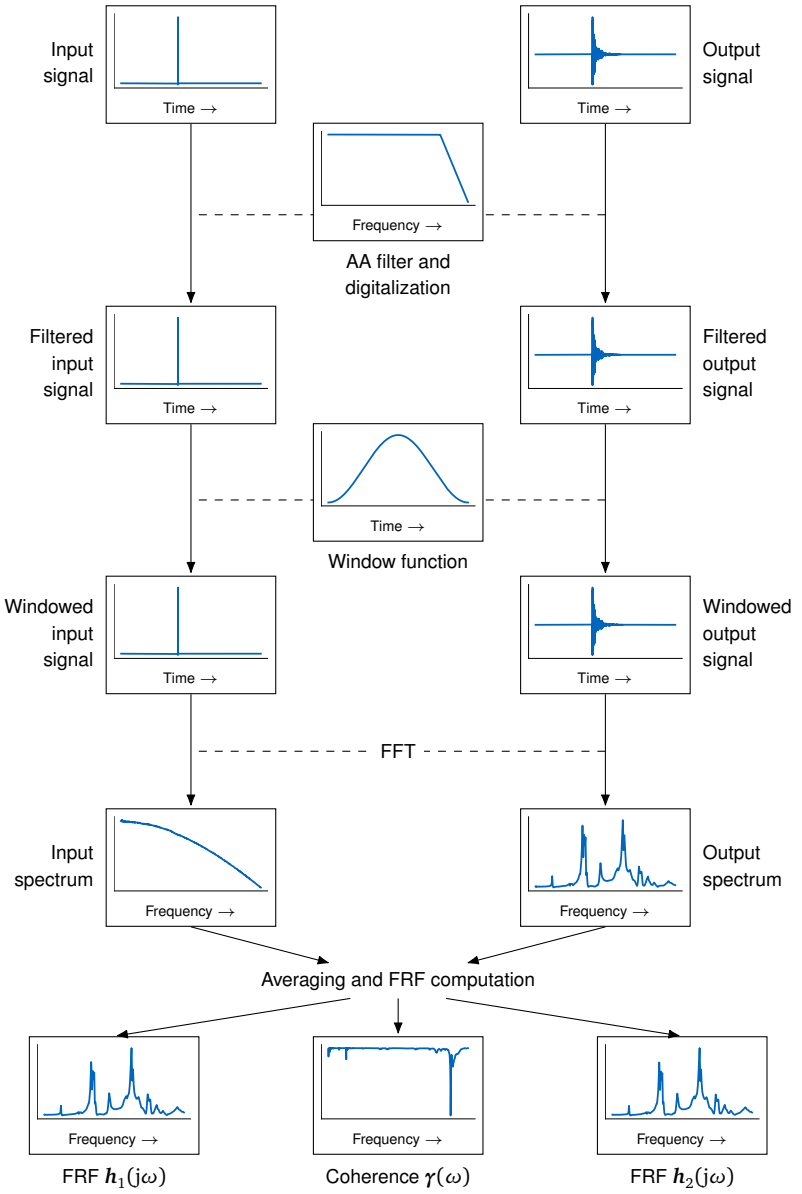

Figure 2.10: Illustration of the FRF measurement process based on AVITABILE (2017); for reasons of clarity, the y-axis was omitted. Note that the anti-aliasing (AA) filter is an analogous element, whose effect can be better illustrated in the frequency domain.

called half-power points. In this way, an estimate for the modal damping ratio

$$\hat{\xi} = \frac{\omega_2^2 - \omega_1^2}{4\hat{\omega}^2} \approx \xi \tag{2.60}$$

can be calculated. Finally, an estimate for the modal constant A can be determined by

$$\hat{A} = 2\xi\hat{\omega}^2 \left|\hat{h}\right| \approx A. \tag{2.61}$$

Note that, even though the shown example only has one DOF, this method can be applied to any FRF with well-separated modes locally exhibiting SDOF properties. More information on modal parameter estimation methods can be found in the works of EWINS (2000) and MAIA (1997), and a more comprehensive classification is given in section 3.2.1.

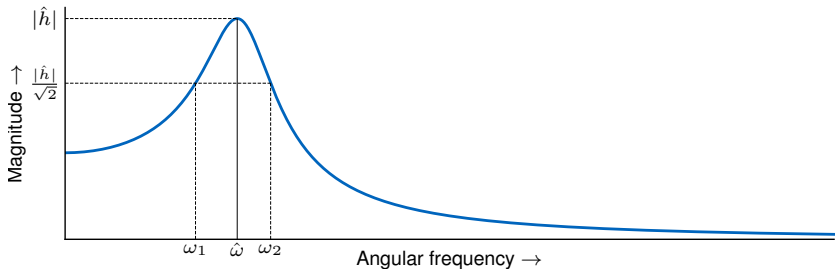

Figure 2.11: Illustration of the peak-picking method on the magnitude plot of an SDOF oscillator

2.3.4 Model Evaluation Criteria

Dynamic systems are often described with modal models due to their intuitive interpretability (VERBOVEN 2019). To assess these models in terms of their capability to replicate their real-world counterpart's behavior, or to compare different models with each other, criteria are needed indicating the match between a model and the data upon which it was built. This section presents several model evaluation criteria serving this purpose.

One way of comparing models and real-world structures is in the modal domain, which is described by the modal parameters eigenfrequencies, modal damping

values, and mode shapes. For real-world structures, these parameters must be determined by an experimental modal analysis (see section 2.3.3). The model is either already a modal model, or modal parameters must be calculated first (see section 2.3.1). Then, the modal assurance criterion (MAC), which is defined as

$$\mathrm{MAC}(\boldsymbol{\psi}_1, \boldsymbol{\psi}_2) = \frac{|\boldsymbol{\psi}_1{}^{\mathsf{T}} \boldsymbol{\psi}_2{}^{*}|^2}{(\boldsymbol{\psi}_1{}^{\mathsf{T}} \boldsymbol{\psi}_1{}^{*})(\boldsymbol{\psi}_2{}^{\mathsf{T}} \boldsymbol{\psi}_2{}^{*})} \cdot 100\,\%, \tag{2.62}$$

can be used for comparing mode shapes (Allemang and Brown 1982). Here, $\boldsymbol{\psi}_1$ and $\boldsymbol{\psi}_2$ are the mode shapes being compared, $\boldsymbol{a}^*$ denotes the complex conjugate, and $\boldsymbol{a}^{\mathsf{T}}$ is the transpose operator. A MAC value of 100 % indicates perfect conformity, and a value of 0 % no match at all. A more complex variant of the MAC is the extended modal assurance criterion (MACXP), which, in the presence of a limited number of DOFs, leads to an improved discriminability of neighboring modes by also considering the model's and reference modes' eigenvalues λ_1 and λ_2, that is, in other words, the combined damping and eigenfrequency information (Vacher et al. 2010). The MACXP is defined as

$$\mathrm{MACXP}(\boldsymbol{\psi}_1, \boldsymbol{\psi}_2, \lambda_1, \lambda_2) = \frac{\left(\frac{|\boldsymbol{\psi}_1^{\mathsf{H}} \boldsymbol{\psi}_2|}{|\lambda_1^* + \lambda_2|} + \frac{|\boldsymbol{\psi}_1^{\mathsf{T}} \boldsymbol{\psi}_2|}{|\lambda_1 + \lambda_2|} \right)^2}{\left(\frac{\boldsymbol{\psi}_1^{\mathsf{H}} \boldsymbol{\psi}_1}{2|\,\mathbb{R}\mathrm{e}(\lambda_1)|} + \frac{|\boldsymbol{\psi}_1^{\mathsf{T}} \boldsymbol{\psi}_1|}{2|\lambda_1|} \right) \left(\frac{\boldsymbol{\psi}_2^{\mathsf{H}} \boldsymbol{\psi}_2}{2|\,\mathbb{R}\mathrm{e}(\lambda_2)|} + \frac{|\boldsymbol{\psi}_2^{\mathsf{T}} \boldsymbol{\psi}_2|}{2|\lambda_2|} \right)} \cdot 100\,\%. \tag{2.63}$$

Here, $\mathbb{R}\mathrm{e}(a)$ denotes the real part of a complex variable, and $\boldsymbol{a}^{\mathsf{H}}$ the conjugate transpose operator.

For comparing (angular) eigenfrequencies, the natural frequency difference (NFD) criterion (Imamovic 1998)

$$\mathrm{NFD}(\bar{\omega}_1, \bar{\omega}_2) = \frac{|\bar{\omega}_1 - \bar{\omega}_2|}{\min(\bar{\omega}_1, \bar{\omega}_2)} \cdot 100\,\% \tag{2.64}$$

can be used. Similar to equation 2.62, $\bar{\omega}_1$ and $\bar{\omega}_2$ are the eigenfrequencies being compared. The larger the NFD is, the higher is the deviation between the two eigenfrequencies and thus also between the model and the reference data. An NFD of 0 % indicates a perfect match. Finally, modal damping ratios can be compared with the reference modal damping ratios by means of the natural

damping difference (NDD)

$$\mathrm{NDD}(\xi_1, \xi_2) = \frac{|\xi_1 - \xi_2|}{\min(\xi_1, \xi_2)} \cdot 100\,\%, \tag{2.65}$$

where ξ_1 and ξ_2 are the compared damping ratios. Again, a perfect match is indicated by an NDD of 0 %, while larger NDDs imply higher deviations.

Another possibility for comparing models and real-world structures is available in the frequency domain. Here, measured FRF data is usually directly available, while it has to be computed for modal models first. A very common criterion is the frequency response assurance criterion (FRAC), which, following the work of HEYLEN and LAMMENS (1996), is defined as

$$\mathrm{FRAC}(\boldsymbol{h}_1(\mathrm{j}\omega), \boldsymbol{h}_2(\mathrm{j}\omega)) = \frac{\left|\boldsymbol{h}_1^{\mathsf{T}}(\mathrm{j}\omega)\boldsymbol{h}_2^{*}(\mathrm{j}\omega)\right|^2}{\left(\boldsymbol{h}_1^{\mathsf{T}}(\mathrm{j}\omega)\boldsymbol{h}_1^{*}(\mathrm{j}\omega)\right)\left(\boldsymbol{h}_2^{\mathsf{T}}(\mathrm{j}\omega)\boldsymbol{h}_2^{*}(\mathrm{j}\omega)\right)} \cdot 100\,\%. \tag{2.66}$$

In this equation, $\boldsymbol{h}_1$ and $\boldsymbol{h}_2$ denote FRFs being compared. Note that $\boldsymbol{h}(\mathrm{j}\omega)$ represents a numerical FRF vector with one entry per frequency sample instead of a symbolic FRF h. The FRAC ranges from 0 % to 100 % for totally uncorrelated to perfectly matching FRFs. Very similar, but more sensitive to damping differences is the cross signature scale factor (CSF) defined in the work of HAAPANIEMI et al. (2003) as

$$CSF(\boldsymbol{h}_1(\mathrm{j}\omega), \boldsymbol{h}_2(\mathrm{j}\omega)) = \frac{2\left|\boldsymbol{h}_1^{\mathsf{H}}(\mathrm{j}\omega)\boldsymbol{h}_2(\mathrm{j}\omega)\right|}{\left(\boldsymbol{h}_1^{\mathsf{H}}(\mathrm{j}\omega)\boldsymbol{h}_1(\mathrm{j}\omega)\right) + \left(\boldsymbol{h}_2^{\mathsf{H}}(\mathrm{j}\omega)\boldsymbol{h}_2(\mathrm{j}\omega)\right)} \cdot 100\,\%. \tag{2.67}$$

Here, $\boldsymbol{a}^{\mathsf{H}}$ again denotes the conjugate transpose operator. The CSF has the same range as the FRAC, and its implications are also identical.

2.4 Summary

In this chapter, the theoretical foundation for the remainder of this thesis has been laid. Section 2.1 provided an introduction to sensitivity analysis, which, in its linear form, is an important tool for distinguishing true, systematic effects from random, spurious ones. This instrument will, for example, be used in section 5.1 and was used for publication PUB1 to demonstrate the effect of

wear on the modal parameters of a dynamic system. Sensitivity analysis in its nonlinear form will be used in section 5.2.1 and was used for publication PUB2 to simplify high-fidelity dynamic models. This simplification aids in the search for optimal model parameters, a process known as *parameter identification*, which ultimately constitutes a complex optimization problem. Methods to solve this type of problem were presented in section 2.2. Some of these algorithms will be applied in section 5.2 and were used in the embedded publications PUB3 and PUB5. In section 2.3, it was shown how complex dynamic systems can be modeled and how the resulting models can be assessed with respect to their ability to replicate their real-world counterparts. This knowledge is important for understanding the state of the art, which will be presented next in chapter 3.

Chapter 3

State of the Art

This chapter first gives an overview of the state of the art of simulating the dynamic behavior of machine tools (see section 3.1), leading to the conclusion that a variety of methods exists for accurately predicting the behavior of real-world structures. Section 3.2 shows that parameterizing these models, however, is a challenging problem, which has not been solved yet. Thus, concise research gaps (RGs) are formulated in section 3.3, which this thesis addresses in the following chapters.

3.1 Simulation of Machine Tool Structural Dynamics

In the current state of the art, several ways exist for setting up the basic dynamic equation of motion (see equation 2.27) for machine tools, which can subsequently be used to predict their behavior (see section 2.3.1). This section gives an overview of these approaches and is divided into finite element analysis (FEA) and multibody system (MBS) methods.

3.1.1 Finite Element Analysis

The basic idea of FEA is to discretize a structure into small but finite elements and to approximate its behavior within these elements (ZIENKIEWICZ et al. 2005). In this way, the partial differential equations describing structural deformations

in continuum mechanics, which are generally not solvable in closed form,[1] can be transformed to the linear multi-degree-of-freedom (MDOF) second-order differential equation system formulated in equation 2.27 (SCHWERTASSEK and WALLRAPP 1999).

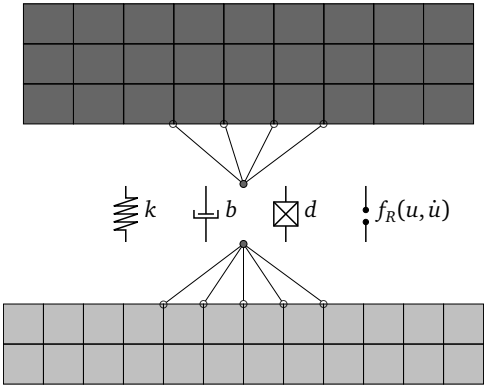

Figure 3.1: General joint model for machine tool components

For machine tools, computer-aided design (CAD) models describing their geometry form the basis of finite element modeling (ALTINTAS et al. 2005). The CAD model is simplified by removing details such as small holes and radii, which have only local influence, and split up into partitions representing independently moving components. To avoid direct contact modeling, surrogate models are used to connect these components. These models typically consist of spring and damping elements (ALTINTAS et al. 2005), but may also contain elaborate nonlinear friction functions (REBELEIN 2019). Figure 3.1 illustrates such a joint model. It can be seen that the two component meshes are connected via spring elements (k), viscous and hysteretic damping elements (b, d), and, optionally, nonlinear friction models ($f_R(u,\dot{u})$). The combination of one viscous or hysteretic damper and one spring per degree of freedom (DOF) is also called scalar connection (SCHWARZ 2015). To avoid numerical problems (OERTLI 2008) and to mimic the real-world joint behavior, the meshes are not connected directly but by means of multipoint constraints (MPCs). These constraints relate the kinematics of a primary node to those of one or several secondary nodes and

[1] Solvable in closed form means that a solution can be found by an exact expression with only a finite number of operations, as it is, for example, the case for linear equation systems.

thus distribute the joint forces over a larger number of mesh nodes. More details on the commonly used types of MPCs and their implementation can be found in the works of SEMM et al. (2019a) and OERTLI (2008). As an alternative to MPCs, in the works of SIEDL (2008) and SPESCHA (2018) forced fields were used to distribute the joint loads.

Depending on the machine tool element intended to be represented and user-specific preferences, each surrogate model is built from several scalar connections. Whereas constraining DOFs by springs is largely straightforward, the distribution and the selection of the type of damping are more complicated. For example, REBELEIN (2019) modeled the linear guiding system (LGS) shoes with springs and viscous dampers in the lateral directions (i.e., perpendicular to the intended movement) and applied a nonlinear friction model in the moving direction. To improve the computational efficiency of these nonlinear models, SEMM et al. (2020b) presented a linearization approach for replacing the nonlinear friction law by a spring and a viscous damper. Table 3.1 gives an overview of the surrogate models used in the work of REBELEIN (2019). Other examples of machine tool element modeling can be found in the works of SCHWARZ (2015), NIEHUES (2015), LAW (2013), and OERTLI (2008). The ball screw drive (BSD) represents a more complicated case for surrogate modeling of machine tool elements since it relates translational with rotational DOFs. OERTLI (2008) modeled the screw, the ball, and the nut kinematics in detail and ended up with a so-called ten-springs model, one for each DOF and four more to actually enable the conversion between rotation and translation. This model was extended by OKWUDIRE and ALTINTAS (2009) and SCHWARZ (2015), who generalized it and made it more accurate.

Even with these non-contact surrogate models, machine tool FEA models tend to have a high number of DOFs, often even in the range of millions or at least hundreds of thousands (LAW 2013; REBELEIN 2019). This leads to considerably high hardware requirements and slows down the corresponding simulations. To circumvent these problems, HERNANDEZ-VAZQUEZ et al. (2018) conducted an analysis of variance to find the most influential factors on the FEA of a machine tool and built a quadratic response surface meta-model using this information. In this way, the identification of crucial machine tool model parameters, which requires numerous model evaluations, was accelerated. Since building the meta-model involves many time-consuming function evaluations and signifi-

Table 3.1: Overview of machine tool component modeling with scalar connections based on the works of REBELEIN (2019) and OERTLI (2008)

Component	Number of springs	Number of dampers	Constrained DOFs Stiffness	Constrained DOFs Damping
Loose bearing (LB)	2	3	Lateral translations	All translations
Fixed bearing (FB)	3	3	All translations	All translations
Elastic coupling (CPL)	6	6	All	All
Linear guiding system (LGS) shoe	2	2	Lateral translations	Lateral translations
Mounting element (ME)	3	3	All translations	All translations
Energy chain	0	1	–	Axial translation
Ball screw drive (BSD)*	10	3	All but screw DOF	All translations

*with the stiffness model from OERTLI (2008) and the damping model from REBELEIN (2019)

cantly restricts the universality of the model, this approach for computation time reduction is not very common in the literature. More common is the use of (projection-based) model order reduction (MOR) techniques (BESSELINK et al. 2013; REBELEIN 2019; SEMM et al. 2019a; SPESCHA 2018), which leads to a lower-order approximation of the original model (BESSELINK et al. 2013). The basic idea of these methods is to project the original DOFs $\boldsymbol{u}$ (with size $N \times 1$) by means of a transformation (or projection) matrix $\boldsymbol{T}$ into a lower-dimensional subspace represented by a reduced set of DOFs $\boldsymbol{z}$ (with size $L \times 1$), that is,

$$\boldsymbol{u} = \boldsymbol{T}\boldsymbol{z}. \tag{3.1}$$

The transformation matrix has the dimensions $N \times L$, which, for $L < N$, leads to a DOFs reduction from N to L. Similar to equation 2.34, substituting equation 3.1 into equation 2.27 and pre-multiplying with $\boldsymbol{T}$ leads to a system of equations with the same structure but a lower number of DOFs. There are many techniques to find transformation matrices $\boldsymbol{T}$. For reasons of simplicity, these are not further discussed here. More information on the general design of transformation matrices can be found in the works of BESSELINK et al. (2013) and GASCH et al. (2021), and the work of BONIN (2015) specifically deals with transformation matrices for machine tools. However, as it is very common in structural dynamics (KLERK et al. 2008), the Craig-Bampton method (CRAIG and BAMPTON 1968) shall be briefly explained here based on the work of SEMM (2020). The first

step is partitioning and rearranging the system's[2] DOFs into boundary DOFs $\boldsymbol{u}_b$ and inner DOFs $\boldsymbol{u}_i$:

$$\begin{bmatrix} \boldsymbol{M}_{bb} & \boldsymbol{M}_{bi} \\ \boldsymbol{M}_{ib} & \boldsymbol{M}_{ii} \end{bmatrix} \begin{bmatrix} \ddot{\boldsymbol{u}}_b \\ \ddot{\boldsymbol{u}}_i \end{bmatrix} + \begin{bmatrix} \boldsymbol{K}_{bb} & \boldsymbol{K}_{bi} \\ \boldsymbol{K}_{ib} & \boldsymbol{K}_{ii} \end{bmatrix} \begin{bmatrix} \boldsymbol{u}_b \\ \boldsymbol{u}_i \end{bmatrix} = \begin{bmatrix} \boldsymbol{f}_b \\ \boldsymbol{f}_i \end{bmatrix}. \tag{3.2}$$

The boundary DOFs are preserved during the MOR and can be, for example, used to couple other machine tool structural parts, whereas the inner DOFs are transformed in the projection process. This also becomes visible when looking at the Craig-Bampton method reduction matrix $\boldsymbol{T}_{CB}$, which can be written as

$$\boldsymbol{T}_{CB} = \begin{bmatrix} \boldsymbol{I}_{bb} & \boldsymbol{0} \\ \boldsymbol{\Psi}_{ib} & \boldsymbol{\Psi}_{iq} \end{bmatrix}. \tag{3.3}$$

Here, $\boldsymbol{I}_{bb}$ is the identity matrix, $\boldsymbol{0}$ is the null matrix, and $\boldsymbol{\Psi}_{ib}$ is called the static constraint mode matrix. It can be calculated from the system's stiffness matrix, and it is sometimes used for MOR alone as it perfectly preserves the stiffness properties of the original system (GASCH et al. 2021; GUYAN 1965). The matrix $\boldsymbol{\Psi}_{iq}$ can be denoted as fixed-interface normal mode matrix and is obtained by setting all boundary DOFs $\boldsymbol{u}_b$ to zero and solving the resulting eigenvalue problem from equation 2.27. Note that the Craig-Bampton method only leads to a DOF reduction when a strict subset of the full eigenvector matrix, most commonly the q first eigenvectors in ascending order with respect to the corresponding eigenfrequency, is used. This is also called modal truncation (GAWRONSKI 2004). Inserting the transformation law from equation 3.1 with respect to the reduction matrix $\boldsymbol{T}_{CB}$ to the rearranged system from equation 3.2 yields

$$\begin{bmatrix} \hat{\boldsymbol{M}}_{bb} & \hat{\boldsymbol{M}}_{bq} \\ \hat{\boldsymbol{M}}_{qb} & \boldsymbol{I}_{qq} \end{bmatrix} \begin{bmatrix} \ddot{\boldsymbol{u}}_b \\ \ddot{\boldsymbol{z}}_q \end{bmatrix} + \begin{bmatrix} \hat{\boldsymbol{K}}_{bb} & \boldsymbol{0} \\ \boldsymbol{0} & \boldsymbol{\Lambda}_{qq} \end{bmatrix} \begin{bmatrix} \boldsymbol{u}_b \\ \boldsymbol{z}_q \end{bmatrix} = \begin{bmatrix} \boldsymbol{f}_b \\ \boldsymbol{f}_q \end{bmatrix}. \tag{3.4}$$

Here, the submatrices $\hat{\boldsymbol{M}}_{bb}$, $\hat{\boldsymbol{M}}_{bq}$, $\hat{\boldsymbol{M}}_{qb}$, and $\hat{\boldsymbol{K}}_{bb}$ and the vector $\boldsymbol{f}_q$ can be calculated from the rearranged equation 3.2 and the reduction matrix $\boldsymbol{T}_{CB}$ (SEMM 2020). The matrix $\boldsymbol{\Lambda}_{qq}$ contains the eigenvalues of the system when all boundary DOFs are fixed, and $\boldsymbol{I}_{qq}$ is the identity matrix. $\boldsymbol{z}_q$ is a vector containing a reduced

[2] For simplicity, the undamped system is considered here.

set of DOFs.

In conclusion, it can be stated that machine tool simulation via FEA is well-established in the research community. Methods for creating these models starting from CAD data exist, the modeling of machine tool components has been well described, and measures have been developed to handle the increasing size and computational effort of these models. However, the accuracy of these models, which has been validated in several works (LAW 2013; OERTLI 2008; REBELEIN 2019; SEMM 2020), crucially depends on a variety of model parameters such as, for example, the stiffness and damping parameters involved in the surrogate component models (see table 3.1). Furthermore, FEA models are limited to a fixed axes position configuration of the machine tool.

3.1.2 Multibody Systems

Originally, MBS models consisted of rigid bodies connected by massless joints and were used to calculate the behavior under large-scale movements of these bodies over time (RILL et al. 2020). In contrast, FEAs focussed on small deformations within a body (RUST 2015). However, there is some overlap between both methods since flexible MBS models can also deal with inner deformations of bodies (SCHWERTASSEK and WALLRAPP 1999), and nonlinear FEAs can also compute large-scale deformations and movements and, depending on the system border definition, also calculate the movements of several bodies. First, this section introduces the basics of MBS models for machine tools. Second, the transition to more powerful flexible MBS simulations will be made. Finally, component mode synthesis (CMS) will be introduced as an alternative method for simulating machine tool systems.

Classic MBSs are typically used in the early design stages of machine tools to estimate the kinematic behavior, calculate loads, predict (necessary) actuator forces, and evaluate their static properties over the entire workspaces (ALTINTAS et al. 2005). In this way, actuators and components can be dimensioned, and a first estimate of the machine tool's performance can be generated. Furthermore, MBS models offer the opportunity for early-stage parameter variations. Each body is reduced to its mass and inertia properties, often based on CAD data (ALTINTAS et al. 2005). In their most general form, MBSs can be described by a differential-algebraic system of equations (SCHWERTASSEK and WALLRAPP 1999).

These equations can be derived using various mechanical principles, for example, the Euler-Lagrange equations, d'Alembert's principle, the Jourdain principle, or Hamilton's principle (RILL et al. 2020; SCHWERTASSEK and WALLRAPP 1999), and solved iteratively using appropriate solvers. Rigid-body MBSs typically constitute computationally efficient problems with only a few DOFs, as there are less than or equal to six DOFs per body (RILL et al. 2020). However, deformations of the bodies are typically disregarded.

As an extension of rigid-body MBSs, flexible MBSs have evolved. Here, it is most common to use the floating-frame-of-reference formulation, which defines the motion of a body as a superposition of a large-scale movement of a reference coordinate system and small deformations within this coordinate system. In this way, the governing dynamic differential equations can be linearized, thus enabling simpler and more efficient calculation algorithms (SCHWERTASSEK and WALLRAPP 1999). However, this comes at the cost of being restricted to only small deformations.

As an alternative to flexible MBSs, dynamic substructuring techniques can be used. Even though the general concept also works for nonlinear and time-variant systems, it is most common to assume linear and time-invariant dynamics (KLERK et al. 2008) and thus only small deformations, too. However, it is possible to represent large-scale movements of systems in this way (SEMM et al. 2019b; SPESCHA 2018). Existing works in dynamic substructuring can be classified in three groups: coupling in the physical domain, the modal domain, and CMS (KLERK et al. 2008). Figure 3.2 gives an overview of these three different domains and the corresponding substructuring techniques. Note that the same information is contained in all these domains, meaning that ways to switch between these domains exist (KLERK et al. 2008).

When a system is described by its mass, stiffness, and damping properties such as, for example, in equation 2.27, one speaks of the physical domain and direct coupling applies. In this case, substructures can be coupled using the primal or dual formulation. In the former, a new system is derived from the substructures to be coupled by keeping only the interface DOFs, which is similar to the way FEA models are constructed from basic element matrices (KLERK et al. 2008). As an alternative better suited for parallel computing, the dual formulation retains all substructures' DOFs and enforces the coupling via Lagrange multipliers (KLERK

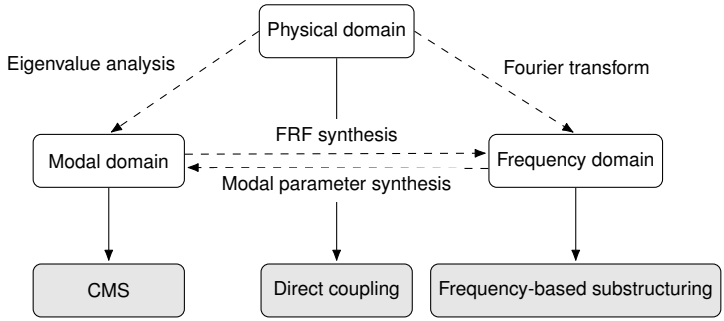

Figure 3.2: Overview of modeling domains and corresponding substructuring techniques based on the work of KLERK et al. (2008)

et al. 2008). Both methods satisfy the compatibility condition (i.e., synchronous displacements of coupled DOFs from all substructures' perspectives) and the force equilibrium. The physical approach is based on a precise description of the mass, stiffness, and damping properties of the involved bodies, which is impossible to obtain purely based on experimental data. Thus, it has hardly found applications in the experimental community (KLERK et al. 2008).

If the substructure models are, in contrast to the theoretical physical models mentioned above, available in the frequency domain in the form of frequency response function (FRF) measurement results, frequency-based substructuring techniques can be applied. In a way very similar to the physical domain and direct coupling, this can be done in a primal or dual way, either using a reduced set of interface DOFs or making use of Lagrange multipliers. Again, both approaches are in line with both the compatibility condition and the force equilibrium (KLERK et al. 2008). Many specific techniques for frequency-based substructuring exist, which are discussed in detail in the work of KLERK et al. (2008).

For substructure models which are available in the modal domain, CMS leads to a coupled overall model. Although it is possible to couple full-order substructure models, CMS usually refers to the coupling of reduced-order component models (KLERK et al. 2008). The most common CMS strategy in the structural dynamics community, which is also most relevant for this work, is the Craig-Bampton method, which has already been introduced as an MOR technique at the end of section 3.1.1. It was used extensively in the works of SEMM et al. (2018), SEMM

et al. (2019a), SEMM et al. (2019b), and SEMM et al. (2020b) to model modular and position-flexible machine tool components. The inherent preservation of the physical coupling DOFs enabled the combination with linear and nonlinear local damping models, which resulted in a high-fidelity overall machine tool model. QUEINS (2005) also used the Craig-Bampton method for modeling machine tools. Instead of damping and flexible axes positions, his work focussed on mechatronic simulations comprising not only the machine tool model but also additional control loops. LAW et al. (2013) used a slightly modified version to assemble an overall machine tool model from substructures and to validate the reduced model by comparing reduced and unreduced FRFs and stability lobes. More CMS strategies are discussed in the work of KLERK et al. (2008), which also gives a brief overview of the history of CMS.

Note that different substructuring approaches can be combined in one model since transformation rules exist between the physical, the frequency, and the modal domain (see figure 3.2). For example, LAW (2013) first used an extended Craig-Bampton method for building a machine tool model in the modal domain, which was then coupled with measured tool dynamics in the frequency domain by inverse receptance coupling.

In summary, MBSs have extended the possibilities of FEA models by increasing their flexibility, especially with regard to axes position changes of machine tool models. However, as for FEA models, MBSs can only deliver accurate results when parameterized correctly.

3.1.3 Uncertainty Modeling

Both the machine tool modeling process and the determination of the underlying model parameters are subject to uncertainties, which lead to inaccurate simulation results. Thus, to make robust predictions, additional uncertainty handling methods are needed. This section gives a short overview of these methods available as the state of the art prior to this thesis and the embedded publications.

According to OBERKAMPF and ROY (2013), there are two substantially different types of uncertainties. The first type is called aleatory uncertainties. It is caused by inherently random processes and cannot be reduced. An example in the

context of machine tool modeling are machining tolerances, which influence the dynamic behavior of machine tool components such as BSDs and the corresponding model parameters (REBELEIN 2019). However, these types of uncertainties can be dealt with by considering probabilistic modeling approaches (REBELEIN 2019). Second, there are epistemic uncertainties, which express a lack of knowledge and can be decreased up to a certain extent. For example, they can occur when CAD models are geometrically simplified for a more efficient modeling process (REBELEIN 2019), and they are either deliberately disregarded or, in the worst case, not known at all (SCHWARZ 2015).

In the literature, several ways of dealing with uncertainties in dynamic machine tool models exist. SCHWARZ (2015) developed a computationally efficient, non-probabilistic approach for simulating machine tool FRFs based on modal superposition (see equation 2.41). In this way, he was able to compute interval FRFs from uncertain stiffness and damping model parameters, which enclose the real FRFs with upper and lower bounds. REBELEIN (2019) extended the approach to nonlinear damping models but, for the sake of simplicity, assumed fixed values for his model's stiffness parameters. In contrast, there are also probabilistic modeling approaches, which are computationally expensive but have emerged in recent years due to the increasing availability of computational power. BUSCH et al. (2022) were able to quantify the uncertainty of four dominant eigenfrequencies of a milling robot model based on uncertain joint parameters. Similarly, BUSCH and ZAEH (2022) estimated probabilistic FRFs from uncertain modal parameter measurements.

It can be concluded that various sources of uncertainties negatively affect the design of machine tool models. However, methods exist in the literature that can model these effects and deal with them, noticeably extending the possibilities of existing FEA and MBS simulation models presented in sections 3.1.1 and 3.1.2.

3.2 Machine Tool Model Identification and Updating

For modeling dynamic systems in general and machine tools in particular, two fundamentally different modeling approaches exist (ISERMANN 1992). First, there is the experimental approach, which is based on measurements only. It

results in a black-box or gray-box model of the system, only replicating its input-output behavior. Experimental models are generally fast and accurate, but, due to their black-box or gray-box nature, offer only limited insights into the underlying system's physical properties. Examples for this type of models are FRFs (see section 2.3.3), more general transfer function (TF) models (TSENG et al. 2019), or modal models (REYNDERS et al. 2012). The identification of these models is often denoted as *system identification* (KEHNE et al. 2018), or, when no special measurement setup but already existing computerized numerical control (CNC) data is used, as *rapid identification* (TSENG et al. 2019; WONG and ERKORKMAZ 2010). The corresponding state of the art is presented in section 3.2.1.

Second, there is the class of theoretical modeling approaches, in which physical laws are used to generate a bottom-up overall model. This, in contrast to the experimental models, leads to a white-box model offering broad insights into the system. However, models belonging to this class are generally not as accurate since this approach is prone to modeling errors and relies on model parameters, which are typically unknown and thus have to be estimated. For machine tools, simple theoretical models can be derived analytically (ALTINTAS 2012; APPRICH et al. 2016; SATO 2012; SCHRÖDER and BUSS 2017), or finite element analyses (FEAs) and multibody system (MBS) simulations can be performed (see section 3.1). Section 3.2.2 deals with the existing literature for identifying the unknown model parameters, a process, which is denoted as *(parameter) identification*, *parametrization*, or *model updating*.

3.2.1 System Identification

This section gives an overview of the state of the art of determining the unknown parameters of experimental models. First, works in the field of rapid identification are presented, which quickly identify FRF or TF models using already available CNC data. Second, existing works for identifying modal parameters of dynamic systems are presented, summarized, and categorized.

Rapid Identification

Rapid identification is the determination of the unknown parameters of experimental models using already existing CNC data, which can be acquired without interfering with the machining process. A very common example of these models are TFs, which can be represented as fractions between nominator and denominator polynomials in the Laplace domain. Their behavior is governed by the roots of these polynomials. The roots of the nominator polynomials are called zeros, whereas the roots of the denominator polynomials are called poles of the TF (AVITABILE 2017). In the work of TSENG et al. (2019), a method was developed for identifying a multiple-input and multiple-output TF model. It is based on user inputs regarding the number of poles, pole search bounds, and the structure of the TF nominator polynomial. The presented approach exploits the common denominator property of the involved TFs and, in a first step, computes so-called multiple-input and multiple-output regressors based on candidate poles, which are, in a second step, used to estimate the nominator coefficients by solving a least squares problem. In a third step, the fitness of the found TF model is evaluated. Based on the result, either the pole locations are updated by solving a global optimization problem, or the identification is stopped, resulting in the final model. Only 2.45 s of time-domain CNC data were needed to identify a model of a five-axis machining center.

For identifying linear time-invariant machine tool dynamics, WANG et al. (2020) used the same algorithm. However, they extended the approach by first decoupling possible nonlinear dynamics of the examined system. Based on in-process measurements, an iterative identification routine was designed, which first solves a nonlinear optimization problem to obtain the nonlinear dynamics and, second, computes the linear time-invariant dynamics of the system using the approach presented by TSENG et al. (2019). Finally, the routine decides by evaluating the model's fitness to either repeat the identification or to stop and arrive at the final model. For identifying a model of a five-axis drilling machine, only three blocks of CNC data with a length of 12 s to 20 s each were needed.

Identification of Modal Models

Modal models are system descriptions using the parameters eigenfrequencies, mode shapes, and modal damping values. They are easily and intuitively

interpretable and thus very common in the field of structural dynamics. Modal models can be established either experimentally or computationally. The latter is, for example, a direct result of FEAs (see section 3.1.1). The process of building experimental modal models is often called experimental modal analysis (EMA), and it is typically performed under laboratory or stationary conditions. Operational modal analysis, in contrast, requires operating conditions, typically more accurately representing nonlinear systems in a specific state.

Many approaches exist for estimating the modal parameters of a system. In principle, they can be classified as single-degree-of-freedom (SDOF) or MDOF methods. The former calculate only one mode or, under certain conditions, sequentially one mode at a time, while the latter compute serveral modes simultaneously, which is generally more accurate in the presence of closely spaced modes. SDOF approaches are, for example, the line-fit method, the peak-picking method (see section 2.3.3), and the circle-fit method (EWINS 2000). Solving a global optimization problem (ALTINTAS 2012), the least squares rational function (LSRF) method (OZDEMIR and GUMUSSOY 2017), the global singular value decomposition (SVD) approach (EWINS 2000), the least squares complex exponential (LSCE) method, the least squares complex frequency domain (LSCF) method including its polyreference version PolyMAX (PEETERS et al. 2004), or the stochastic subspace identification (SSI) method (VAN OVERSCHEE and MOOR 1996) are popular examples for MDOF approaches. These methods operate either in the time domain or in the frequency domain. Table 3.2 shows a classification of the mentioned system identification algorithms into SDOF and MDOF and time and frequency domain methods.

Table 3.2: Classification of exemplarily modal parameter estimation algorithms

	SDOF	**MDOF**
Time domain	–*	SSI LSCE method
Frequency domain	circle-fit method line-fit method peak-picking method	global optimization LSRF method SVD method LSCF method PolyMAX algorithm

*No SDOF method in the time domain is known to the author of this thesis.

For building a modal model, all these algorithms require the number of modes

as an input parameter. Typically, this information is provided in form of a model order value, which equals twice the number of modes (REYNDERS 2012). Since this input can only be determined with profound system knowledge, which is not generally available, it is common in the literature to estimate modal parameters for several model orders which are higher than the assumed number of modes. Based on the results, an appropriate number of modes is set manually, reducing possible biases in the identified modes (EWINS 2000; REYNDERS 2012). For this strategy, it is essential to differentiate spurious modes that occur due to the overestimated model order from the true, physical modes. This can be done by visualizing the identified modes in a model order or number of modes over frequency plot, which is also called stabilization diagram. Figure 3.3 shows an example for an oscillator with three DOFs. It is easy to see that selecting modes from the stabilization diagram requires user input and a high level of knowledge (REYNDERS et al. 2012; SCIONTI and LANSLOTS 2005). The first approaches tackling this problem implemented a set of rules mimicking the decisions of an expert user (LAU et al. 2007; SCIONTI et al. 2003; VAN DER AUWERAER and PEETERS 2004). It was shown that modal analysis novices could produce results almost as good as those of experts with increased productivity (LAU et al. 2007). Instead of a set of rules, SCIONTI and LANSLOTS (2005) used Fuzzy clustering techniques together with a genetic algorithm (GA) as an initialization routine for overcoming the manual evaluation of stabilization diagrams. Again, their results were positively evaluated with respect to the outcomes produced by experts.

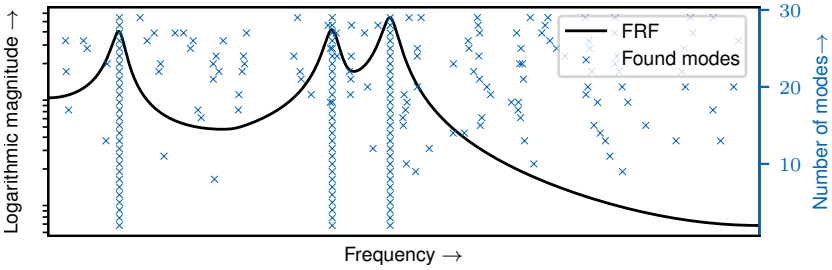

Figure 3.3: Exemplarily stabilization diagram for an oscillator with three DOFs

The first fully automated approach, which does not rely on user-defined parameters, was presented in the work of REYNDERS et al. (2012). By using

non-parametric rules, the modes were first classified as spurious or potentially stable. In a second step, the latter were clustered to find groups of similar modes. Finally, one mode per cluster was selected based on its proximity to the cluster center. Similar approaches were used in the works of NEU et al. (2017) and MUGNAINI et al. (2022), and further examinations were performed. However, the resulting modal model was not validated against the original input measurement data set.

It can be seen from the review above that a common ground has been formed in the literature regarding automated modal parameter identification by replacing originally user-defined inputs with corresponding rules (LAU et al. 2007; MUGNAINI et al. 2022; NEU et al. 2017; REYNDERS et al. 2012; SCIONTI and LANSLOTS 2005; SCIONTI et al. 2003; VAN DER AUWERAER and PEETERS 2004). However, no examinations have been made ruling out that this approach unnecessarily restricts the solution space of the underlying modal model identification problems. For example, the approach presented in the work of REYNDERS et al. (2012) selects the modes being closest to their respective cluster center, disregarding that another mode or another combination of modes may perform better. Additionally, the presented approaches have not evaluated the match between the final modal model and the original input data, which can, for example, be quantified by means of the frequency response assurance criterion (FRAC).

3.2.2 Parameter Identification

Theoretical bottom-up models are based on physical input parameter values. For example, the stiffness matrix $\boldsymbol{K}$ in equation 2.27 contains the structure's inner stiffness resulting from the applied material law and, depending on the modeling approach, may also involve lumped external stiffnesses. In terms of machine tool models, the matrix may, for example, be influenced by the structure's geometry, the material's Young's modulus, and spring stiffnesses modeling the physical contact between different structural parts such as the one between the shoes and the guideway of the LGS. Similarly, the mass ($\boldsymbol{M}$) and damping matrices ($\boldsymbol{B}$ and $\boldsymbol{D}$) depend on the physical properties of the corresponding continuum and, possibly, also external model parameters such as lumped masses or local damping sources. On the one hand, only some of

these values can be extracted from data sheets (SEMM et al. 2020a), and data sheet parameters seldom reflect the specific operating conditions in which the corresponding machine tool component is used. On the other hand, the final simulation results crucially depend on these parameter values. Thus, the models have to be parameterized before their first use. This process is called *parameter identification*. Note that this often involves already identified experimental models, in particular, when modal data is used to update theoretical models (ISERMANN 1992).

Direct Methods

There is a variety of existing methods in the literature, which can be classified as either direct or indirect (FRISWELL and MOTTERSHEAD 1996). Direct methods aim at solving for the unknown stiffness and damping matrices (see equation 2.27) directly (FRISWELL and MOTTERSHEAD 1996). This approach was demonstrated by FRISWELL et al. (1998) who identified the stiffness and damping matrices of a cantilever beam from measured modal data. Similarly, CARVALHO et al. (2007) presented a method to cope with incomplete modal data and also demonstrated its effectiveness using a beam model. In contrast to the two studies, WANG et al. (2018) used frequency-based input data for updating a nonlinear beam model. More works using direct model updating exist, which all lead to models exactly representing the measured input data (FRISWELL and MOTTERSHEAD 1996). However, the identified matrices are typically neither sparse nor symmetric, potentially causing numerical issues. Additionally, the identified parameter values lose their physical meaning in the updating process and thus are not related to specific properties of the original model anymore (FRISWELL and MOTTERSHEAD 1996). For example, it cannot be predicted how an increased damping of the LGS affects the overall dynamic performance of the machine tool using directly identified models. Thus, this type of parameter identification is not further considered in this thesis.

Indirect Methods

In contrast to direct methods, indirect methods solve for the unknown model parameters iteratively, considering their sensitivity with respect to a chosen

simulation outcome (FRISWELL and MOTTERSHEAD 1996; SCHWARZ 2015). In this way, the physical meaning of the identified parameters can be preserved (FRISWELL and MOTTERSHEAD 1996), potentially resulting in models that are both accurate and physically interpretable and can be used for multiple purposes. In the literature, three fundamental classes of indirect model updating exist, which differ in the complexity of the underlying real-world system.

First, parameters can be identified on distinct test benches and then transferred to an overall machine tool model. FEY (2014) developed an approach to identify viscous and hysteretic damping and stiffness parameters of machine tool components using simple test rigs. Parts of this approach have also been published in the work of BRECHER et al. (2013). Its key idea is to build a simple two-mass test rig for each component and parameterize a corresponding model via dynamic measurements using a dummy component with, compared to the component to be measured, negligible damping and similar stiffness. When the dummy is then replaced by the actual component, all additional damping can be attributed to it. By measuring modes in all six DOFs, replacement stiffness and damping parameters can be identified. Detuning the test rig and the model by altering it with additional masses helps to decide on a specific damping model to be used (see section 2.3.2) and to validate the identified parameters. By using this approach, FEY (2014) identified and validated parameters for the BSD, the feed drive bearings, and the LGS. REBELEIN (2019) applied the idea and determined the parameters of the coupling connecting the motors and the BSD shafts in his model. Similarly, SEMM et al. (2020a) identified bearing, BSD, coupling, and LGS parameters for their machine tool simulation model.

Second, the idea of isolating model parameters to be updated can be taken one step further using intermediate assembly states of the overall machine tool instead of separate test rigs. This approach is called *sequential assembly*. Its key idea is to assemble the overall system step by step. Additionally, a corresponding simulation model is also built incrementally so that it can be compared to the real-world system in any step. Similarly to parameter identification on test rigs, in each step only a few parameters, which correspond to the component that has been added last, have to be identified. This method was successfully applied by SCHWARZ (2015) to identify the Young's modulus, the Poisson's ratio, and the volumetric mass density of structural machine tool components. Furthermore, the author also determined some LGS and mounting element (ME)

parameters. Similarly, NIEHUES (2015) also identified ME, gap model, LGS, and BSD parameters but particularly focussed on damping values. Building upon the work of NIEHUES (2015), REBELEIN (2019) found values for motor and energy chain model parameters using the method of sequential assembly. When parameterizing their machine tool model, SEMM et al. (2020a) combined test rig parameters with the sequential assembly process. The latter method was used to update ME parameters and a tooth belt model. Applying the sequential assembly method, parameters are determined in-situ. Thus, it has, in particular, been demonstrated to be beneficial for components whose parameters depend on their operating conditions and therefore cannot be transferred from one system to another such as, for example, the MEs (NIEHUES 2015; SEMM et al. 2020a).

Finally, indirect parameter identification can be performed globally on the overall machine tool directly. NEBELING (1999) used a GA to identify the density, the Young's modulus, and three stiffness and two geometric parameters of a two-component test rig, and he also identified parameters of a three-component machine tool structure. In both cases, modal data from an EMA was used as input. The parameter identification process was guided by expert knowledge. Also using a GA and modal data as a reference, WITT (2007) updated 41 stiffness and damping parameters of an FEA machine tool simulation model. He also implemented a method for deploying expert knowledge within the model updating process, meaning that each parameter was identified by evaluating a specifically selected machine tool mode. In contrast, GARITAONANDIA et al. (2008) used a Bayesian optimization updating approach instead of a GA for parameter identification of a centerless grinding machine. Since a sensitivity analysis has found the stiffnesses of the MEs and of one of the BSD to be most influential, their analysis was focussed on these parameters. Again, expert knowledge was included by manually selecting three eigenfrequencies as optimization targets. So far, all presented works evaluated a model in one fixed state during the updating process. In contrast, HERNANDEZ-VAZQUEZ et al. (2014) examined the effect of including a second model state with a different position of the machine tool's axes. They found that the identified Young's modulus, the stiffness parameters, and the lumped masses from the model updating with one position better represented the corresponding reference data but were hardly transferable to the second axes position state. The parameters gained

from considering two axes positions simultaneously led to a model sufficiently well representing both positions but showed higher deviations in each position compared to the one-at-a-time approach. Instead of using the model directly in the updating process, HERNANDEZ-VAZQUEZ et al. (2018) first built a quadratic response surface surrogate model. After the model had been created, the computational effort of further model evaluations could be drastically reduced. By using EMA input data, values for nine joint stiffness parameters were found. However, their evaluations showed that two parameter values for the axial replacement stiffness between their model's ram and machine bed were possible, each better representing another eigenmode. To be able to account for such effects, which may be caused by nonlinear friction governing the axes' movements (REBELEIN 2019), SEMM et al. (2020a) used a nonlinear flexible MBS simulation model. However, before they applied and compared model updating with a GA, a particle swarm optimization, and a sequential least squares programming approach, they first linearized their model. Data from an EMA was used as input. They found that particle swarm optimization led to the most reliable results and applied it to identify ME parameters. Similarly to the work of WITT (2007), five modes were manually selected as optimization targets, and symmetry properties were enforced. In a later step, also the parameters of the LGS were updated this way.

In conclusion, it can be stated that a variety of methods exist for updating the parameters of machine tool models. However, they either require expert knowledge and manual tuning (GARITAONANDIA et al. 2008; NEBELING 1999; SEMM et al. 2020a; WITT 2007), they can only be applied to small or moderately complex systems (HERNANDEZ-VAZQUEZ et al. 2014, 2018; NEBELING 1999), or they are not applicable to fully assembled machine tool systems (BRECHER et al. 2013; FEY 2014; NIEHUES 2015; REBELEIN 2019; SCHWARZ 2015).

3.3 Summary and Need for Action

The review of the state of the art in section 3.1 has shown that approaches for creating complex simulation models are available, which can be used to simulate the dynamic behavior of machine tools with high fidelity and in a computationally efficient way. Furthermore, section 3.2 has demonstrated

that methods exist for identifying the input parameters which these models' accuracy crucially depends upon and that the modal reference data, which the parametrization relies upon, can be identified. However, at the time of writing this thesis, there were still some research gaps (RGs) which had to be addressed before the potential of high-fidelity machine tool models could be fully exploited. These were:

RG1 As shown in section 3.1, existing high-fidelity machine tool models were predominantly created and used for specialized applications in the field of machining only. It was still unclear, if these models were suitable for supporting and enhancing other, more widespread applications, justifying the effort of creating and parameterizing them.

RG2 Existing models had been parameterized using specialized test rigs, the method of sequential assembly, or a high level of expert knowledge (see section 3.2). While these test rigs were not always available and the resulting machine tool model parameters may have even been not transferable to the fully assembled machine tool model, the method of sequential assembly was only viable in research environments. New and commercially available machine tools could, even if they were not used in a productive industrial environment, only be disassembled and assembled again with unreasonable effort. The required temporal and financial resources were too high for industrial application, and there was a significant risk of damaging the machine tool and losing the manufacturer's warranty when doing so. The need for expert knowledge, in turn, strongly restricted the user group for these models. To sum up, no appropriate method existed for parameterizing high-fidelity machine tool models for the fully assembled system.

While the first two RGs addressed the cost-benefit ratio of advanced theoretical machine tool models, there was also an open point regarding experimental models.

RG3 Even though they are generally not as flexible and versatile as their theoretical counterparts, modal models are still very important. On the one hand, they are easily interpretable and offer valuable insights into many dynamic systems. On the other hand, they are often used as input for updating theoretical machine tool models, as shown in section 3.2.

Automated approaches for modal parameter estimation existed at the time of writing this thesis. However, these had largely replaced user input with metrics performed on the input data set, unnecessarily restricting the solution space. For example, humans traditionally recognize that physical modes occur at almost any model order in stabilization diagrams (see figure 3.3), which had been replaced by clustering algorithms. Additionally, the final modal model was, most often, not validated against the original input data set. Thus, there was still a lack of automated and high-fidelity modal parameter estimation methods. This especially held for complex machine tool systems.

In the following, a research approach will be presented that has addressed the outlined shortcomings (i.e., the RGs) of the state of the art at the time of writing this thesis and has paved the way for automated parameter identification of high-fidelity machine tool models. In this way, the potential of these models can now be fully exploited.

Chapter 4

Objectives and Research Approach

This chapter first presents research targets (RTs), which were derived based on the research gaps outlined in section 3.3. Second, section 4.2 relates the publications (PUBs) which this thesis consists of to these RTs and categorizes them in the context of the overall objective of this thesis.

4.1 Objectives

The overall objective of this thesis is to demonstrate how to automate the parameter identification process of high-fidelity structural dynamic machine tool models. At the time of writing this thesis, this was broken down into five RTs:

RT1 In research gap RG1, it was pointed out that widespread applications for complex machine tool models, which justify the effort of creating and parameterizing them, were missing. Thus, an exemplary use case in the field of condition monitoring was to be presented and highlighted, demonstrating the benefit of high-fidelity machine tool simulation models.

After addressing the motivation for this thesis, research targets RT2 to RT4 directly dealt with the parameter identification problem highlighted in research gap RG2.

RT2 High-fidelity machine tool simulation models are based on many unknown input parameters (SEMM 2020). On the one hand, the complexity

of the model updating process increases with a rising number of parameters to be identified. On the other hand, some parameters contribute more than others to the final accuracy of the simulation model. Thus, the overall parameterization problem had to be simplified as far as possible without affecting the fidelity of the simulation model.

RT3 After simplifying the overall identification problem, a method had to be presented to parameterize high-fidelity dynamic machine tool models for the fully assembled system. The method had to be designed to be as highly automated as possible to lower the effort of creating these types of models, paving the way for their widespread industrial application.

RT4 Finally, the developed parameter identification approach had to be validated by applying it on a real-world system. In this way, the accuracy of the final model could be evaluated, and the costs of updating the model could be estimated.

After the completion of these three RTs, the parameter identification problem described in research gap RG2 could be solved on the condition that a sufficient amount of high-quality input data was available. This data has to be acquired by performing measurements on real-world structures. Typically, modal data is used as a reference for machine tool parameter identification.

RT5 However, research gap RG3 pointed out that collecting this kind of information was either a cumbersome manual process or automated methods had to be used that unnecessarily restricted the solution space by mimicking a human user. Thus, a method needed to be developed for automatically extracting high-quality modal parameters from dynamic response measurements. This has avoided modal parameter estimation being a bottleneck of the entire model updating process.

The research approach pursued by this thesis is illustrated in figure 4.1. Research target RT1 aimed at demonstrating the benefits of high-fidelity machine tool simulation models, addressing research gap RG1. The research targets RT2 to RT4 dealt with the parameter identification methodology, which constitutes the main contribution of this thesis to the state of the art, and addressed research gap RG2. In research gap RG3, extracting modal parameters was described as a bottleneck. Research target RT5 aimed at solving this by automating the procedure. This has also contributed to finally closing research gap RG2.

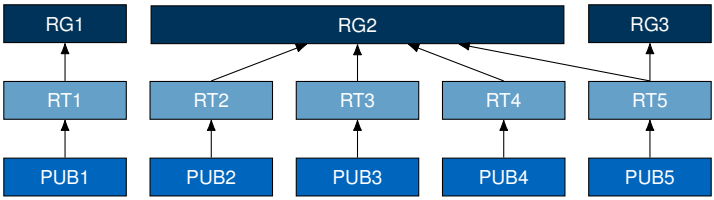

Figure 4.1: Research approach of this thesis

4.2 Research Approach

The present thesis is publication-based, meaning that it consists of five publications (PUBs)[3]:

PUB1 ELLINGER, J., SEMM, T., BENKER, M., KAPFINGER, P., KLEINWORT, R., and ZAEH, M. F. (2019). "Feed Drive Condition Monitoring Using Modal Parameters". In: *MM Science Journal*, pp. 3206–3213. DOI: 10.17973/MMSJ.2019_11_2019072

PUB2 ELLINGER, J., SEMM, T., and ZAEH, M. F. (2022b). "Dimensionality Reduction of High-Fidelity Machine Tool Models by Using Global Sensitivity Analysis". In: *Journal of Manufacturing Science and Engineering* 144.5, pp. 051010:1–051010:8. DOI: 10.1115/1.4052710

PUB3 ELLINGER, J. and ZAEH, M. F. (2022). "Automated Identification of Linear Machine Tool Model Parameters Using Global Sensitivity Analysis". In: *Machines* 10.7, pp. 1–18. DOI: 10.3390/machines10070535

PUB4 ELLINGER, J., PIENDL, D., and ZAEH, M. F. (2023). "Comparison of Sensitivity-Guided and Black-Box Machine Tool Parameter Identification". In: *Journal of Manufacturing and Materials Processing* 7.4, pp. 1–16. DOI: 10.3390/jmmp7040120

PUB5 ELLINGER, J., BECK, L., BENKER, M., HARTL, R., and ZAEH, M. F. (2022a). "Automation of Experimental Modal Analysis Using Bayesian Optimization". In: *Applied Sciences* 13.2, pp. 1–16. DOI: 10.3390/app13020949

Each PUB has addressed a distinct RT from section 4.1, as can be seen in figure 4.1. First, publication PUB1, which is summarized in section 5.1, presented a use case for high-fidelity dynamic machine tool models, motivating the auto-

[3]Volume and issue numbers are only indicated for journals using these.

mated parameter identification methodology provided by this thesis. By using a position-flexible multibody system dynamic machine tool model, which was assumed to be already sufficiently accurately parameterized, it was shown how the stiffnesses of the ball screw drive and the linear guiding system influenced the modal parameters of the machine tool system. By considering that abrasive wear in the roller elements of these two machine tool components manifests itself in decreasing component stiffnesses, this information could be used for condition monitoring. This was validated by equipping a machine tool with ball screw drives and linear guiding systems in various wear states, experimentally measuring the system's dynamic response, and extracting modal parameters from the measurement data.

Second, publication PUB2 (see section 5.2.1) presented a method showing how the dimensionality of the parameter identification problem can be significantly reduced. The method uses global sensitivity analyses to rank the model parameters based on their sensitivity concerning selected simulation outcomes. It was shown that a significant portion of the model parameters could be chosen randomly instead of being identified, simplifying the overall model updating process (see research target RT2). Publication PUB5 delivered the result defined in research target RT5, that is, an automated method for extracting high-quality modal parameters from dynamic response measurement data. The automation was achieved by combining existing but manual modal parameter estimation techniques with Bayesian optimization. Instead of deriving a set of rules from the input data set, which mimics the behavior of an experienced user, the presented approach keeps the solution space wide open by applying a global optimization method. A summary of publication PUB5 can be found in section 5.2.2. Publication PUB3 (see section 5.2.3) is based on both the results of publications PUB2 and PUB5 and has shown how global sensitivity analysis can be used to partition the overall parameter identification problem into many smaller subproblems with only a few parameters to be identified. In this way, the stiffness parameters of a dynamic model can be estimated by solving simple sequential least squares programming problems, while the damping parameters can be calculated afterward by means of a least squares algorithm. With this sensitivity-guided parameter identification approach, research target RT3 could be achieved.

Finally, the presented parameter identification methodology was validated

in publication PUB4 by applying it to a real-world machine tool structure. Additionally, a conventional black-box identification method was applied to the same system. It was shown that both the sensitivity-guided and the black-box approach led to model parameters significantly increasing the conformity of the model with measured reference data. However, the parameter identification method presented in section 5.2.3 was demonstrated to be more economical, offering the opportunity to update complex machine tool simulation models within a few minutes instead of hours. A summary of publication PUB4 can be found in section 5.3.

Table 4.1 illustrates the key ideas of the publications, which this thesis consists of, and relates them to the sections 5.1 to 5.3.

Table 4.1: Overview and categorization of the publications

Section 5.1	**Motivation**	**PUB1** Feed Drive Condition Monitoring Using Modal Parameters
Section 5.2	**Parameter Identification Framework**	**PUB2** Dimensionality Reduction of High-Fidelity Machine Tool Models by Using Global Sensitivity Analysis
		PUB5 Automation of Experimental Modal Analysis Using Bayesian Optimization
		PUB3 Automated Identification of Linear Machine Tool Model Parameters Using Global Sensitivity Analysis
Section 5.3	**Validation**	**PUB4** Comparison of Sensitivity-Guided and Black-Box Machine Tool Parameter Identification

Chapter 5

Research Results

This chapter presents the publications addressing the research targets defined in section 4.1. Each publication will be summarized, and the publications's key findings will be clearly stated. Section 5.1 will first present a condition monitoring use case of high-fidelity complex machine tool models, demonstrating the benefits of these models. Second, section 5.2 describes the developed parameter identification framework consisting of methods for dimensionality reduction (see section 5.2.1), automated modal parameter extraction (see section 5.2.2), and parameter identification (see section 5.2.3). Finally, section 5.3 validates the presented framework by showing the results of applying it to a real-world machine tool structure.

5.1 Feed Drive Condition Monitoring as Motivation for High-Fidelity Structural Dynamic Machine Tool Models (Publication PUB1)

In publication PUB1, feed drive condition monitoring is presented as a use case for high-fidelity machine tool simulation models. The preloads of the ball screw drive (BSD) and the linear guiding system (LGS) are declared decisive factors for the manufacturing accuracy, as they directly correspond to the overall stiffness of machine tools. Furthermore, it is explained that abrasive wear in these components leads to a preload loss and thus to a decreasing machining performance over time.

By using an existing model of a four-axis DMG DMC duo Block 55H machine tool and by assuming it to be sufficiently accurately parameterized, it was demonstrated how a decreasing stiffness of the BSD and the LGS affects the modal parameters of the machine tool. The presented evaluations showed that the stiffness of the BSD and the LGS had a different effect on individual modes, meaning that some modes were mainly affected by wear in the BSD and others by wear in the LGS. It was concluded that, by monitoring the modal parameters, wear can be detected and even attributed to distinct components of the machine tool. Illustrations of the respective mode shapes were used to support this conclusion.

Building upon these findings, a test cycle was developed to reproducibly measure the machine tool dynamics. Experiments showed that the measured dynamic response depends on the excitation source and the position and movement history of the machine tool axes. To ensure that these factors do not influence the modal parameter estimation, the test cycle was given a fixed starting position, a superimposed linear axis velocity, and a fixed excitation source.

The considered machine tool was easily accessible, thus enabling fast BSD and LGS changes. A set of three BSD and LGS each was available with three different preload levels each, ranging from the new to the worn state. These components were used to conduct a fully factorial screening for the effect of the BSD and LGS preloads on the modal parameters of the machine tool system. The peak-picking and the PolyMAX algorithm were used to estimate the modal parameters. Again, it was shown by using an analysis of variance that BSD and LGS preload loss differently affected the modal parameters of the system, confirming the conclusion that wear cannot only be detected globally but also localized. This result was independent of the used modal parameter estimation method.

Figure 5.1 shows the individual contributions[4] of the authors of publication PUB1. In conclusion, publication PUB1 introduced the following key findings which, in total, led to the accomplishment of research target RT1:

[4]The contributions are categorized using a simplified version of the CRediT contributor roles taxonomy (National Information Standards Organization 2022) with “idea” summarizing “conceptualization” and “methodology,” “execution” containing “data curation,” “formal analysis,” “investigation,” “software,” and “validation,” “administration” consisting of “funding acquisition,” “project administration,” “resources,” and “supervision,” and “publication” summarizing “writing of the original draft,” “review and editing,” and “visualization.”

- The dynamic response of machine tools can be reliably measured using a distinct test cycle.
- Modal parameters are suitable for detecting wear in the form of preload loss.
- High-fidelity machine tool models can be used to attribute the detected wear to specific feed drive components, which helps to avoid extensive and cumbersome experimental factor screening with worn components.

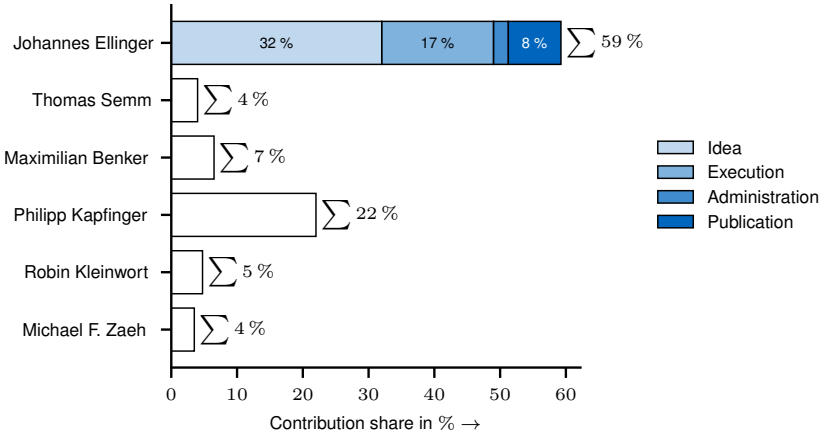

Figure 5.1: Author contributions to publication PUB1; detailed contributions are only labeled for the lead author and only if they are greater than or equal to 8 %.

5.2 Automated Parameter Identification Methodology for Structural Dynamic Machine Tool Models

This section presents the main contribution of this thesis to the state of the art, that is, the parameter identification methodology. Section 5.2.1 summarizes publication PUB2 and shows how the dimensionality of complex models can be reduced with only minor impacts on the fidelity of the model. This strongly simplifies the actual parameter identification. Section 5.2.2 summarizes publication PUB5 and demonstrates how the high-quality modal parameters, which are needed for parameter identification, can be estimated in an automated

way. Building upon these two sections, an approach for automated parameter identification is described in publication PUB3 and section 5.2.3.

5.2.1 Dimensionality Reduction of High-Fidelity Machine Tool Models (Publication PUB2)

Publication PUB2 presents a method for reducing the dimensionality of dynamic simulation models. In this case, the term dimension refers to the number of model input parameters that need to be known for running simulations. One step further, this also reduces the number of parameters that need to be identified, thus simplifying the overall model updating problem. At the same time, the presented approach aims at keeping the accuracy of the model as high as possible.

To demonstrate the proposed approach, a high-fidelity dynamic machine tool model of a four-axis test bench from earlier research (REBELEIN 2019; SEMM 2020) was selected. For this system, a set of updated parameters, which was chosen as a reference for all evaluations in publication PUB2, already existed. To increase the interpretability of the results, the model was simulated in a uniaxial configuration, that is, a machine bed on three mounting elements with a column and a workpiece table (WPT), which had one motion degree of freedom in the global z-direction. Based on nine important nodes across the system, nine frequency response functions (FRFs) were defined, which were considered essential for the usability of the model. In this configuration, 71 model input parameters representing the lumped stiffness and damping properties of the machine tool's mounting elements, fixed bearing, loose bearing, LGS, coupling, and the BSD had to be defined for running the simulation.

For each parameter, large bounds were set, which were assumed to contain the true parameter value to be identified. By using these bounds, two model evaluation criteria (see section 2.3.4), three selected WPT positions, and ten frequency intervals in the range from 0 Hz to 500 Hz, in total, 540 global sensitivity analyses (GSAs) were conducted. For each GSA, the 71 model input parameters were ranked according to their importance for the corresponding model outcome (i.e., the combination of frequency range, model evaluation criterion, WPT position, and input-output nodes). It could be observed, that

for each simulation outcome, only a few parameters were significant. By combining all conducted GSAs in a weighted sense and introducing a sensitivity threshold, the model input parameters could be split up into 22 significant and 49 non-significant parameters. It was highlighted that this implies that only 22 parameters actually have to be identified, and 49 parameters can be chosen randomly with only a very limited impact on the accuracy of the model.

To validate this conclusion, a Monte Carlo simulation experiment was conducted with, in total, 10,000 samples of model parameter sets. The 22 significant parameters were set to their true value known from earlier research, while the 49 non-significant parameters were sampled randomly. For all these combinations, the simulation results were compared to the reference model with all 71 parameters set to their true value. It was shown that the model conformity does not drop below 89 %, with a mean conformity value across all 540 simulation outcomes of 98.9 %. This was repeated for a second, disturbed set of reference parameters, confirming that the presented approach can be used to significantly reduce the complexity of the machine tool dynamic model parameter identification process. At the end of publication PUB2, a short outlook was given on how the results of the GSA can be used to also support the actual parameter identification process by partitioning the overall problem into several, smaller subproblems.

Figure 5.2 shows the individual contributions[5] of the authors of publication PUB2. With publication PUB2, research target RT2 was achieved. In summary, the following key findings were reached:

- GSA can significantly reduce the dimension of dynamic simulation models and thus simplify the model updating process.
- The overall parameter identification problem can be broken down into several smaller subproblems by means of GSAs.

5.2.2 Automated Modal Parameter Identification Using Bayesian Optimization (Publication PUB5)

As an alternative to existing methods from the state of the art, publication PUB5 presents a method for automatically extracting modal parameters from FRF

[5] see footnote 4 on page 74

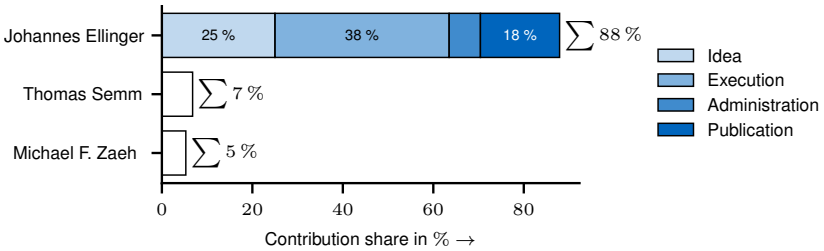

Figure 5.2: Author contributions to publication PUB2; detailed contributions are only labeled for the lead author and only if they are greater than or equal to 8 %.

measurement data, the so-called AutoEMA method. Instead of deriving a set of rules from the input data set and potentially restricting the solution space with regard to the modal parameters, the presented approach combines traditional modal parameter estimation methods with a Bayesian optimization algorithm. This, on the one hand, keeps the solution space as open as possible and, on the other hand, ensures a high conformity of the modal model with the input reference data.

The modal parameter estimation approach of publication PUB5 is based on the PolyMAX method, which was used to calculate pole candidates for all model orders up to and including the maximum selected order. Representing a point in the complex plane, these poles contain both eigenfrequency and damping information. Four additional hyperparameters were used to classify the found poles into spurious and potential poles. After that, a hierarchical clustering algorithm was used to group the potential poles into modes and to further eliminate spurious poles. This step involved three more hyperparameters. Finally, the pole closest to the median pole location of each cluster was selected as a final pole and used to calculate the mode shapes as remaining modal parameters.

In total, eight hyperparameters are needed for the modal parameter estimation. Instead of using predefined values or deriving them from the input data set, the described approach and procedure were embedded into a Bayesian optimization loop. As an objective function, the mean frequency response assurance criterion (FRAC) value between the input FRFs and the FRFs resulting from the modal model was used. Optionally, a small regularization parameter was introduced, preventing excessively high model orders. The choice for Bayesian optimization

was made because of the complexity of the objective function and the limited insight into it, the potentially high costs of evaluating it, and the absence of analytic gradient formulations.

The AutoEMA approach was applied to a small synthetic test data set and a larger experimental modal analysis (EMA) data set acquired on a machine tool structure, and it was benchmarked against the function `modalfit` from the well-established numerical computation application MATLAB®. For the synthetic test data set, ground truth values were known per definition. Assessed by the natural frequency difference and natural damping difference (NDD) values and the modal assurance criterion (MAC), both the `modalfit` and the AutoEMA approach replicated the reference modal parameters equally well. The EMA data set comprised 612 FRFs measured in four different positions of the machine's WPT, 17 nodes across the machine tool, three spatial directions, and three different excitation directions. The AutoEMA approach significantly outperformed the MATLAB® routine quantitatively in terms of FRAC conformity, qualitatively via visual FRF assessments, and also concerning the required computation time, which was reduced by more than 99 %.

Figure 5.3 shows the individual contributions[6] of the authors of publication PUB5. In conclusion, research target RT5 was achieved with publication PUB5, and the following key findings were obtained:

- With the AutoEMA approach, modal parameters can be automatically estimated.
- The AutoEMA approach does not restrict the solution space by predefined rules or rules derived from the input data set.
- The performance of the AutoEMA approach in terms of computation time and FRAC conformity outperforms the function `modalfit` from the application MATLAB®.

5.2.3 Automated Parameter Identification of Machine Tool Models (Publication PUB3)

Publication PUB3 presents an approach for automated parameter identification of high-fidelity machine tool models, which, in contrast to the previous state of

[6] see footnote 4 on page 74

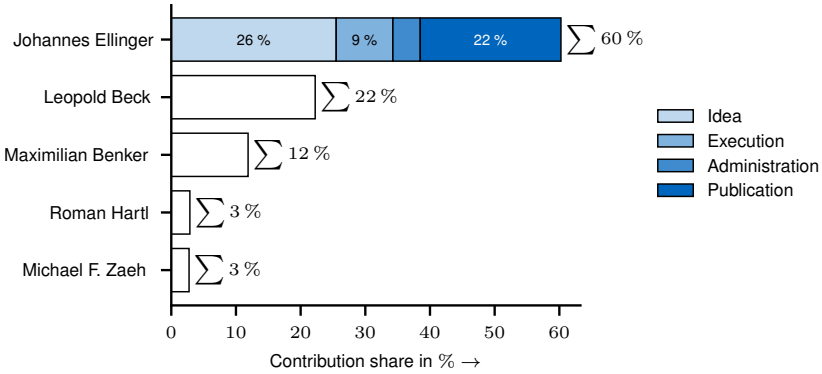

Figure 5.3: Author contributions to publication PUB5; detailed contributions are only labeled for the lead author and only if they are greater than or equal to 8 %.

the art, neither relies on expert knowledge nor is limited to moderately complex models with only a limited number of unknown parameters. Thus, the model updating process can be performed for fully assembled machine tool systems. As an input, modal reference data (see publication PUB5 and section 5.2.2) and, ideally, a dimensionality-reduced (see publication PUB2 and section 5.2.1) dynamic simulation model need to be provided.

The presented approach's key idea is to break down the overall parameter identification problem into smaller, more easily solvable subproblems. As a first step, GSAs were performed for each model output for which reference data has been provided. This can, for example, be the MAC conformity of a mode shape of a distinct mode at a certain position of the machine tool's axes with its corresponding reference mode shape. Similar to publication PUB2 (see section 5.2.1), it was observed that not all but only a few model input parameters influence one particular model output. For another model output (e.g., another mode shape's conformity at a different axis position), another limited number of parameters were significant. In other words, based on the results of the GSAs, smaller parameter identification problems could be derived, which only search for the significant parameters and assume random values for the non-significant parameters. This avoids local minima and significantly simplifies the parameter identification process.

Second, the model's stiffness input parameters were identified by solving those

subproblems that correspond to mode shape references. As lightly damped structures were assumed, these were independent of the model's damping parameters. For this, a gradient-based sequential least squares programming algorithm was used. To further avoid local minima, each subproblem was repeatedly solved, and the finally identified value of each stiffness parameter was determined from the subproblem with the least variation with respect to this parameter. After all stiffness parameters had been identified, the required linearity of the model was exploited by solving a least squares problem for the yet unknown damping parameters, resulting in the updated model.

The capability of the proposed approach was demonstrated using a model of a four-axis machine tool in uniaxial configuration. The dimensionality reduction approach proposed in publication PUB2 (see section 5.2.1) had already been applied, resulting in 27 model input parameters to be identified. Modal reference data was simulated using the model and a set of known model input parameters, which served as ground truth for all following evaluations. In a first validation scenario, this data was used to update another instance of the model, that is, a copy of the same model which, initially, had another set of input parameters and thus behaved differently. It was shown that the presented approach almost perfectly reproduced the set of stiffness parameters that were used to generate the reference data, and that deviations of the identified damping parameters from their ground truth values could be attributed to minor errors in the stiffness parameter identification. FRAC, cross signature scale factor, extended modal assurance criterion, and NDD value statistics and FRF plots were used to confirm the successful model updating process. Second, the same reference data was used to parameterize a disturbed instance of the model, which could not perfectly replicate the reference data anymore. This was done to simulate modeling errors. The resulting deviations of the finally found model parameters were slightly higher than in the first case but found to be still acceptable. The same evaluations (model conformity measures and plots) were conducted, also confirming the validity of the found model parameters in scenario two.

Figure 5.4 shows the individual contributions[7] of the authors of publication PUB3. In conclusion, publication PUB3 led to the following key findings which, in total, led to the accomplishment of research target RT3:

[7] see footnote 4 on page 74

- GSA can be used to partition parameter identification problems into smaller, more easily solvable subproblems.
- The damping parameters to be identified are very sensitive to stiffness parameter identification errors.
- The presented sensitivity-guided parameter identification approach can reliably identify the parameters of complex dynamic machine tool simulation models in an automated way.

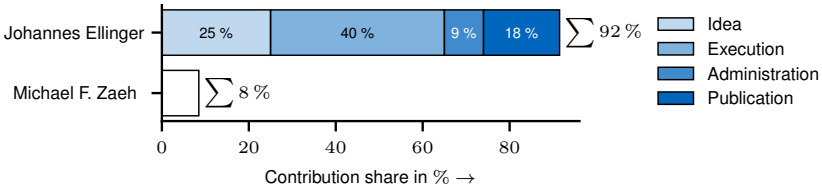

Figure 5.4: Author contributions to publication PUB3; detailed contributions are only labeled for the lead author and only if they are greater than or equal to 8 %.

5.3 Application of the Parameter Identification Methodology on a Real-World Machine Tool Structure (Publication PUB4)

In section 5.2, a theoretical methodology was presented for identifying the parameters of dynamic machine tool simulation models. This section and publication PUB4 aim to validate it by presenting the results of applying the proposed approaches to a real-world machine tool structure. Furthermore, the parameter identification methodology is benchmarked with an existing model updating method from the state of the art concerning its economic efficiency and its accuracy.

As a use case, a uniaxial system was chosen. It was approximated by supporting unnecessary machine tool components of a four-axis DMG DMC duo Block 55H machine tool (e.g., the other axes' feed drive motors, BSDs, and LGSs) by a crane and severing their connections to the remainder (i.e., the machine bed and the WPT) of the machine tool. For this structure, a model, which has been subjected to the dimensionality reduction approach presented in

publication PUB2 and section 5.2.1, already existed. FRF measurements were conducted at 17 nodes across the machine tool in all three coordinate directions for three different impulse hammer excitations at four WPT positions. With the help of the AutoEMA approach presented in publication PUB5 and section 5.2.2, 26 to 42 modes could be extracted per WPT position.

By using the dimensionality-reduced model and only a subset of the found modes to prevent mode tracking errors, updated model parameters were computed by means of the sensitivity-guided parameter identification method presented in publication PUB3 (see section 5.2.3). FRAC improvements of 15 percentage points could be reached. The remaining deviations between the simulated FRFs and their measured counterparts were mainly attributed to modeling errors but also errors in identifying the modal parameters and shortcomings of the parameter identification approach.

By using modal model evaluating criteria, a higher conformity could be reached with MAC values increased by up to 25 percentage points and some NDDs reduced to only a fraction of the original errors. Additionally, a state-of-the-art black-box model updating approach (SEMM et al. 2020a) was applied to the same data and model, which is fundamentally different from sensitivity-guided parameter identification.

Publication PUB4 found that there was no clear favorite in terms of the accuracy of the resulting simulation model. However, it was pointed out that modeling errors may have prevented a clear judgment. Additionally, the presented approaches were compared economically and also benchmarked against the method of sequential assembly. While the latter is unfeasible in many cases for fully assembled machine tools, it is also the least economical method because it involves many EMAs and identifications in different machine tool setups. The sensitivity-guided and black-box model updating approaches showed comparable efforts for first-time parameter identification runs. However, the parameter identification methodology presented in this thesis significantly outperforms the black-box approach for repeated runs, offering the opportunity to update dynamic machine tool models on standard hardware within minutes.

Figure 5.5 shows the individual contributions[8] of the authors of publication PUB4. The following key findings were elaborated by publication PUB4, leading to the

[8] see footnote 4 on page 74

achievement of research target RT4:

- The quality of the model and the reference data is crucial for the success of model updating.
- Black-box and sensitivity-guided parameter identification deliver similar results in terms of the resulting model accuracy.
- The presented parameter identification methodology economically outperforms other methods and offers the opportunity to rapidly update machine tool dynamic simulation models.

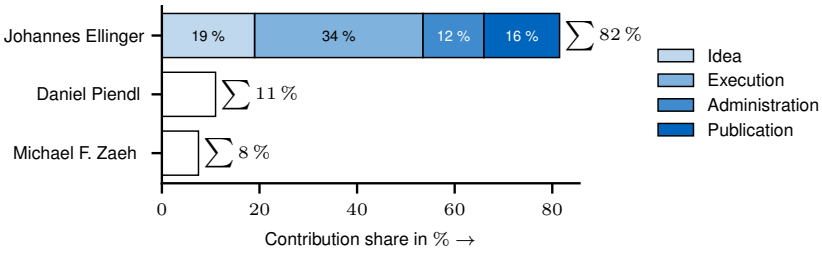

Figure 5.5: Author contributions to publication PUB4; detailed contributions are only labeled for the lead author and only if they are greater than or equal to 8 %.

Chapter 6

Discussion

This thesis presented a parameter identification methodology in section 5.2, which is to be discussed regarding its contribution to the state of the art. Furthermore, it is to be shown how the research targets (RTs) defined in section 4.1 have been achieved by the key findings of publications PUB1 to PUB5.

Figure 6.1 shows a classification of the model updating methodology's two main parts. On the one hand, figure 6.1a relates the automated modal parameter estimation approach presented in section 5.2.2 and publication PUB5 to existing works from the state of the art with regard to their automation level and their flexibility. It can be seen that there are three groups. First, there is the work of PEETERS et al. (2004), which introduced the PolyMAX algorithm. It is strongly based on user input but, in turn, provides high flexibility in terms of the selected modes and the extracted modal parameters. Second, the works of LAU et al. (2007), REYNDERS et al. (2012), and NEU et al. (2017) have replaced user interaction to various extents by algorithmic rules, increasing the automation level but also restricting the possible solution space for the estimated model parameters. This potentially leads to suboptimal solutions. Finally, there is publication PUB5, which has combined the work of PEETERS et al. (2004) with a Bayesian optimization algorithm and thus preserved its flexibility while fully automating the modal parameter identification process and exploring the entire solution space.

On the other hand, the presented parameter identification methodology includes a model dimensionality reduction and a parameterization method, which are classified with respect to similar works from the state of the art in figure 6.1b. It can be seen that methods and tools exist being able to handle model sizes from

small to high. However, all these approaches are based on expert knowledge, which needs to be provided by the user. The combination of the model updating strategy in publication PUB3 with the dimensionality reduction step presented in publication PUB2 enables parameter identification for very large models. Additionally, it is guided by global sensitivity analyses, which can replace the manual input of expert knowledge, providing a high level of automation. Furthermore, it can, in contrast to some works from the state of the art, also identify damping parameters.

Because of the high effort involved in creating and, more important, parameterizing them, high-fidelity dynamic machine tool models are used only for very specialized applications. Publication PUB1 has extended the state of the art by showing that condition monitoring is a use case that benefits from the existence of these types of models. Furthermore, publication PUB4 has benchmarked the presented parameter identification methodology against an existing method and extended the state of the art by an assessment with regard to the final model accuracy and the economic efficiency needed for the updating process.

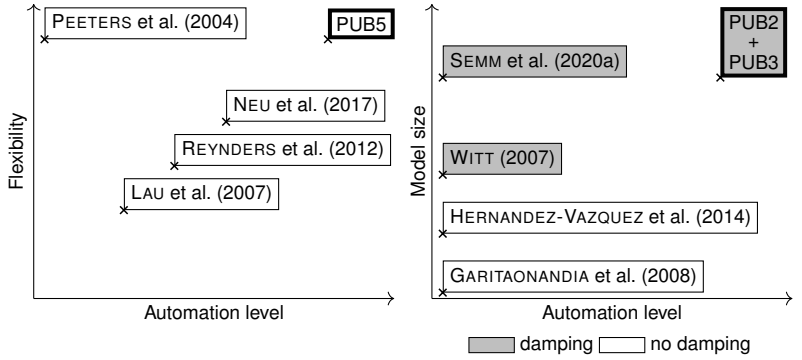

(a) Modal parameter estimation publication PUB5 **(b)** Parameter identification in publication PUB3

Figure 6.1: Classification of the publications of this thesis in comparison to exemplary works of the state of the art; the publications' reference point is indicated by a cross symbol.

In section 3.3, research gaps were identified, leading to the definition of RTs in section 4.1. Research gap RG1 stated a lack of widespread applications for parameterized, high-fidelity machine tool dynamic simulation models. In publication PUB1, it was shown how such models can enable and enhance the condition monitoring process of machine tool feed drives. Thus, research

target RT1, which defined the need for such an application, was achieved. Furthermore, it was stated that modal parameter estimation methods which have demonstrated their ability to accurately replicate the input measurement data and automatically yield accurate modal parameters are missing. The AutoEMA method, which was presented in publication PUB5, fulfills these requirements, thus meeting the demand of research target RT5 and closing research gap RG3. Finally, section 3.3 stated that there was no method for parameterizing high-fidelity machine tool models for a fully assembled machine tool system. This led to the formulation of research targets RT2 to RT4. In section 5.2, a parameter identification methodology was presented consisting of a method for reducing the dimensionality of complex models (see publication PUB2) and a sensitivity-guided approach for updating unknown model parameters of high-fidelity machine tool models. The approach was validated in publication PUB4. In this way, research targets RT2 to RT4 were completed, and research gap RG2 was closed. The described relations between the research gaps, the RTs, and the presented publications are visualized in figure 4.1 on page 69.

Chapter 7

Summary and Outlook

This chapter first summarizes the main results of this thesis in section 7.1 and, second, gives an outlook on further research possibilities in the field of parameterizing high-fidelity machine tool dynamic simulation models in section 7.2.

7.1 Summary

Even though its relative market volume in European economies may seem low, the machine tool sector is an important enabler for all other industry sectors. However, it constantly faces challenges such as the current transformation in the automotive industry and the increasing competition from Asian countries, driving machine tool builders to produce machines with higher flexibility, cost-efficiency, and productivity than before. A decisive factor for reaching these goals and consequently also to ensure the success in the market is given by the dynamic behavior of machine tools, as it governs their performance and can negatively affect the stability of production processes. Nowadays, virtual instead of physical prototypes are used in the design process of machine tools, resulting in a need for well-parameterized, high-fidelity dynamic machine tool models.

According to the review of the state of the art in chapter 3, however, parameterizing this type of model was a laborious and manual task before this thesis, such that high-fidelity dynamic machine tool models were only used in very specialized research projects. Thus, in chapter 4, a research approach was formulated

concerning how the objective of an automated parameter identification process of high-fidelity dynamic machine tool models could be reached.

Based on an already identified model, section 5.1 first presented another use case from the field of condition monitoring. By using the model, it was shown that preload loss due to (abrasive) wear of the feed drive components ball screw drive (BSD) and linear guiding system (LGS) affected different vibrational modes of the machine tool. This enabled not only the detection but also the localization of wear. Additionally, a test cycle was developed for reliably measuring frequency response functions and estimating the modal parameters of the system. Measurements with feed drive components in different wear states were conducted, validating the presented wear detection and localization approach.

Second, the parameter identification problem was solved in section 5.2. By using global sensitivity analyses, it was shown that the majority of the dynamic machine tool model parameters have little influence on the final model accuracy. Thus, they can be disregarded (i.e., chosen randomly) in the parameterization process, strongly reducing the dimensionality and the complexity of the optimization problem. As a next module, a new modal parameter estimation method has been developed, which serves as the basis for a method to find globally valid machine tool model parameters. The method combines the existing PolyMAX algorithm with Bayesian optimization, leading to a high level of automation and a high accuracy. This was validated by benchmarking it against a state-of-the-art algorithm from the numerical computation application MATLAB®. Finally, the parameter identification methodology from section 5.2 was successfully applied to a real-world machine tool structure in section 5.3, and its performance was benchmarked. It was shown that the approach presented in this thesis delivered similar results compared to a black-box parameter identification method from the state of the art in terms of the final model accuracy, but outperformed it with respect to the corresponding economic efficiency.

Chapter 6 recapitulated the previously defined research gaps, the research targets, and the key findings from the publications PUB1 to PUB5. It was shown that all research targets were completed and, as a consequence, all identified research gaps were closed. A method for automated parameter identification of high-fidelity dynamic machine tool simulation models now exists.

7.2 Outlook

With the results of this thesis, high-fidelity dynamic machine tool simulation models can be parameterized within minutes from modal parameter estimations of the corresponding machine tool structure. This offers the possibility of extending the condition monitoring approach presented in the work of IMIELA (2005) from a simple feed drive test bench to a real-world machine tool. To eliminate manual interactions, permanent sensors have to be installed for frequency response function measurements at the machine tool. As an excitation source, either the internal feed drive motors or external active vibration control devices (KLEINWORT 2021) can be used. In both cases, a measurement test cycle has to be developed and integrated into the computerized numerical control (CNC). The model has to be updated either in regular time intervals, based on the workload, or only when deviations between the model and the real-world machine tool are observed. In this way, the model parameters can be logged over time. It has already been shown (see section 5.1) that the feed drive stiffness parameters are sensitive to preload loss due to wear. Thus, these parameters are promising candidates for applying state-of-the-art condition monitoring and remaining useful life prediction approaches (BENKER 2023).

With the existence of high-fidelity dynamic machine tool simulation models and a method for updating these, an integrated simulation of the cutting process may gain new momentum. To ensure that both the machine tool and the cutting process model are up to date, the model updating module from this thesis has to be combined with an online cutting parameter identification module such as, for example, presented in the work of SCHMUCKER et al. (2021). Optionally, a workpiece model (WIMMER 2020) can also be included to increase the accuracy of the predictions. With all these modules in place and appropriate interface definitions, this approach offers the opportunity to improve and optimize cutting processes without the need for any manual tests. Possible design goals are the dynamic stability of the process or the geometric errors of the final part.

Finally, it was found in section 5.3 that the quality of the model and the reference data is crucial for the success of the model updating approach (see publication PUB4). Further research could deal with improving the robustness

of the presented approach. The research project called “The Next Step Towards Virtual Machine Tools: Simulation of Damping Effects Caused by Interaction between the Machine and the Process” funded by the German Research Foundation (project number 420581965, from 2019 to 2023) discovered that, for example, the machine tool’s load state, its axes positions, and its velocities affect the damping (and stiffness) behavior, and, as a result, established models for these effects. Incorporating these so-called process-induced damping models might increase both the robustness and the accuracy of the presented automated parameter identification method.

Bibliography

Note that references are sorted alphabetically by the last name of the lead author. The volume and article numbers of a journal are separated by the period symbol. For example, "In: *Applied Sciences* 9.2" means that the referenced article can be found in the second issue of the ninth volume of the *Applied Sciences* journal. Whereever no digital object identifier (DOI) is present, it either does not exist or is not available to the author of this thesis. The same is stated hereby for any other bibliographic data not provided in this list.

AHMADI, K. and ISMAIL, F. (2010). "Experimental Investigation of Process Damping Nonlinearity in Machining Chatter". In: *International Journal of Machine Tools and Manufacture* 50.11, pp. 1006–1014. DOI: 10.1016/j.ijmachtools.2010.07.002.

ALBERTZ, F. (1995). "Dynamikgerechter Entwurf von Werkzeugmaschinen-Gestellstrukturen (in English: Dynamically Appropriate Design of Machine Tool Frames)". PhD Thesis. Munich, Germany: Technical University of Munich.

ALLEMANG, R. and BROWN, D. (1982). "A Correlation Coefficient for Modal Vector Analysis". In: *Proceedings of the 1st International Modal Analysis Conference*, pp. 110–116.

ALTINTAS, Y. (2012). *Manufacturing Automation: Metal Cutting Mechanics, Machine Tool Vibrations, and CNC Design*. 2nd ed. Cambridge, United Kingdom: Cambridge University Press. ISBN: 9780511843723.

ALTINTAS, Y., BRECHER, C., WECK, M., and WITT, S. (2005). "Virtual Machine Tool". In: *CIRP Annals* 54.2, pp. 115–138. DOI: 10.1016/S0007-8506(07)60022-5.

APPRICH, S., WULLE, F., POTT, A., and VERL, A. (2016). "Online Parameter Identification for a Linear Parameter-Varying Model of Large-Scale Lightweight Machine Tool Structures with Pose-Dependent Dynamic Behavior". In: *IEEE International Conference on Advanced Intelligent Mechatronics (AIM)*. Piscataway, NJ, United States: IEEE, pp. 1558–1563. DOI: 10.1109/AIM.2016.7576992.

AVITABILE, P. (2017). *Modal Testing: A Practitioner's Guide*. 1st ed. Chichester, United Kingdom: John Wiley & Sons, Ltd. ISBN: 9781119222989.

BALASUBRAMANIAN, P. (2019). "Linear and Nonlinear Damping Identification in Vibrations of Thin-Walled Structures". PhD Thesis. Quebec, Canada: McGill University.

BENKER, M. (2023). "Condition Monitoring of Machine Tool Feed Drives and Methods for the Estimation of Remaining Useful Life". PhD Thesis. Munich, Germany: Technical University of Munich.

BENKER, M., JUNKER, S., ELLINGER, J., SEMM, T., and ZAEH, M. F. (2022). "Experimental Derivation of a Condition Monitoring Test Cycle for Machine Tool Feed Drives". In: *Production Engineering* 16.1, pp. 55–64. DOI: 10.1007/s11740-021-01085-9.

BESSELINK, B., TABAK, U., LUTOWSKA, A., VAN DE WOUW, N., NIJMEIJER, H., RIXEN, D. J., HOCHSTENBACH, M. E., and SCHILDERS, W. (2013). "A Comparison of Model Reduction Techniques from Structural Dynamics, Numerical Mathematics and Systems and Control". In: *Journal of Sound and Vibration* 332.19, pp. 4403–4422. DOI: 10.1016/j.jsv.2013.03.025.

BONIN, T. (2015). "Modern Model Order Reduction Methods for the Simulation of the Dynamical Behavior of Machine Tools". PhD Thesis. Munich, Germany: Technical University of Munich.

BRECHER, C., FEY, M., and BÄUMLER, S. (2013). "Damping Models for Machine Tool Components of Linear Axes". In: *CIRP Annals* 62.1, pp. 399–402. DOI: 10.1016/j.cirp.2013.03.142.

BRECHER, C. and WECK, M. (2006). *Werkzeugmaschinen 5 (in English: Machine Tools 5)*. 7th rev. ed. New York, United States: Springer Berlin Heidelberg. ISBN: 9783540329510.

BUSCH, M., SCHNOES, F., ELSHARKAWY, A., and ZAEH, M. F. (2022). "Methodology for Model-Based Uncertainty Quantification of the Vibrational Properties of Machining Robots". In: *Robotics and Computer-Integrated Manufacturing* 73, pp. 1–10. DOI: 10.1016/j.rcim.2021.102243.

BUSCH, M. and ZAEH, M. F. (2022). "Multi-Fidelity Information Fusion to Model the Position-Dependent Modal Properties of Milling Robots". In: *Robotics* 11.1, pp. 1–22. DOI: 10.3390/robotics11010017.

CANUDAS DE WIT, C., OLSSON, H., ASTROM, K. J., and LISCHINSKY, P. (1995). "A New Model for Control of Systems with Friction". In: *IEEE Transactions on Automatic Control* 40.3, pp. 419–425. DOI: 10.1109/9.376053.

CARVALHO, J., DATTA, B., GUPTA, A., and LAGADAPATI, M. (2007). "A Direct Method for Model Updating with Incomplete Measured Data and Without Spurious Modes". In: *Mechanical Systems and Signal Processing* 21.7, pp. 2715–2731. DOI: 10.1016/j.ymssp.2007.03.001.

CAUGHEY, T. (1960). "Classical Normal Modes in Damped Linear Dynamic Systems". In: *Journal of Applied Mechanics* 27.2, pp. 269–271. DOI: 10.1115/1.3643949.

CRAIG, R. and BAMPTON, M. (1968). "Coupling of Substructures for Dynamic Analyses". In: *AIAA Journal* 6.7, pp. 1313–1319. DOI: 10.2514/3.4741.

DIN 69651-1 (1981). *Werkzeugmaschinen für die Metallbearbeitung: Begriffe (in English: Machine Tools for Metalworking: Definitions)*. Berlin, Germany.

ELLINGER, J., BECK, L., BENKER, M., HARTL, R., and ZAEH, M. F. (2022a). "Automation of Experimental Modal Analysis Using Bayesian Optimization". In: *Applied Sciences* 13.2, pp. 1–16. DOI: 10.3390/app13020949.

ELLINGER, J., PIENDL, D., and ZAEH, M. F. (2023). "Comparison of Sensitivity-Guided and Black-Box Machine Tool Parameter Identification". In: *Journal of Manufacturing and Materials Processing* 7.4, pp. 1–16. DOI: 10.3390/jmmp7040120.

ELLINGER, J., SEMM, T., BENKER, M., KAPFINGER, P., KLEINWORT, R., and ZAEH, M. F. (2019). "Feed Drive Condition Monitoring Using Modal Parameters". In: *MM Science Journal*, pp. 3206–3213. DOI: 10.17973/MMSJ.2019_11_2019072.

ELLINGER, J., SEMM, T., and ZAEH, M. F. (2022b). "Dimensionality Reduction of High-Fidelity Machine Tool Models by Using Global Sensitivity Analysis". In: *Journal of Manufacturing Science and Engineering* 144.5, pp. 051010:1–051010:8. DOI: 10.1115/1.4052710.

ELLINGER, J. and ZAEH, M. F. (2022). "Automated Identification of Linear Machine Tool Model Parameters Using Global Sensitivity Analysis". In: *Machines* 10.7, pp. 1–18. DOI: 10.3390/machines10070535.

EWINS, D. (2000). *Modal Testing: Theory, Practice and Application*. 2nd ed. Vol. 10. Baldock, United Kingdom: Research Studies Press. ISBN: 0863802184.

FEY, M. (2014). "Identifikation geeigneter parametrierter Dämpfungsmodelle für Komponenten einer Linearachse (in English: Identification of Suitably Parameterized Damping Models for Components of Linear Axes)". PhD Thesis. Aachen, Germany: RWTH Aachen University.

FRISWELL, M., INMAN, D., and PILKEY, D. (1998). "Direct Updating of Damping and Stiffness Matrices". In: *AIAA Journal* 36.3, pp. 491–493. DOI: 10.2514/2.396.

FRISWELL, M. and MOTTERSHEAD, J. (1996). *Finite Element Model Updating in Structural Dynamics*. 1st ed. Vol. 38. Solid Mechanics and its Applications. Dordrecht, Netherlands: Kluwer. ISBN: 0792334310.

GARITAONANDIA, I., FERNANDES, M. H., and ALBIZURI, J. (2008). "Dynamic Model of a Centerless Grinding Machine Based on an Updated FE Model". In: *International Journal of Machine Tools and Manufacture* 48.7-8, pp. 832–840. DOI: 10.1016/j.ijmachtools.2007.12.001.

GARNETT, R. (2023). *Bayesian Optimization*. 1st ed. Cambridge, United Kingdom: Cambridge University Press. ISBN: 9781108348973.

GASCH, R., KNOTHE, K., and LIEBICH, R. (2021). *Strukturdynamik: Diskrete Systeme und Kontinua (in English: Structural Dynamics: Discrete Systems and Continua)*. 3rd ed. Berlin, Germany: Springer Vieweg. ISBN: 9783662617670.

GAWRONSKI, W. (2004). *Advanced Structural Dynamics and Active Control of Structures*. 1st ed. Mechanical Engineering Series. New York, United States: Springer New York. ISBN: 9780387721330.

GENTA, G. (2009). *Vibration Dynamics and Control*. 1st ed. Boston, United States: Springer US. ISBN: 9780387795805.

GROSSMANN, K., RUDOLPH, H., and WEISHART, H. (2012). "Verfahren zur Bestimmung modaler Dämpfungsmaße an Werkzeugmaschinen-Strukturen (in English: Procedures for Identifying Modal Damping Ratios for Machine Tool Frames)". In: *Zeitschrift für wirtschaftlichen Fabrikbetrieb (in English: Journal for Efficient Factory Operation)* 107.3, pp. 168–173. DOI: 10.3139/104.110730.

GUYAN, R. (1965). "Reduction of Stiffness and Mass Matrices". In: *AIAA Journal* 3.2, p. 380. DOI: 10.2514/3.2874.

HAAPANIEMI, H., LUUKKANEN, P., NURKKALA, P., ROSTEDT, J., and SAARENHEIMO, A. (2003). "Correlation Analysis of Modal Analysis Results from a Pipeline". In: *21st IMAC Conference and Exposition*, pp. 398–406.

HASSELMAN, T. (1976). "Modal Coupling in Lightly Damped Structures". In: *AIAA Journal* 14.11, pp. 1627–1628. DOI: 10.2514/3.7259.

HERNANDEZ-VAZQUEZ, J., GARITAONANDIA, I., FERNANDES, M. H., ALBIZURI, J., and MUNOA, J. (2014). "Comparison of Updating Strategies to Improve Finite Element Models of Multi-Axis Machine Tools". In: *Proceedings of the 9th International Conference on Structural Dynamics*, pp. 1–8.

HERNANDEZ-VAZQUEZ, J., GARITAONANDIA, I., FERNANDES, M. H., MUNOA, J., and LACALLE, L. N. (2018). "A Consistent Procedure Using Response Surface

Methodology to Identify Stiffness Properties of Connections in Machine Tools". In: *Materials* 11.7, pp. 1–21. DOI: 10.3390/ma11071220.

HEYLEN, W. and LAMMENS, S. (1996). "FRAC: A Consistent Way of Comparing Frequency Response Functions". In: *Identification in Engineering Systems*. Ed. by FRISWELL, M. and MOTTERSHEAD, J. Swansea, United Kingdom: Univ. of Wales, pp. 48–57.

IGLESIAS, A., TANER T., L., ÖZSAHIN, O., FRANCO, O., MUNOA, J., and BUDAK, E. (2022). "Alternative Experimental Methods for Machine Tool Dynamics Identification: A Review". In: *Mechanical Systems and Signal Processing* 170.108837, pp. 1–19. DOI: 10.1016/j.ymssp.2022.108837.

IMAMOVIC, N. (1998). "Validation of Large Structural Dynamics Models Using Modal Test Data". PhD Thesis. London, United Kingdom: Imperial College of Science, Technology & Medicine.

IMIELA, J. (2005). "Verfügbarkeitssicherung von Werkzeugmaschinenachsen mit Kugelgewindetrieb durch modellbasierte Verschleißüberwachung (in English: Securing the Availability of Machine Tools with Ball Screw Drive via Model-Based Condition Monitoring)". PhD Thesis. Hanover, Germany: Leibniz University Hannover.

ISERMANN, R. (1992). *Identifikation dynamischer Systeme 1 (in English: Identification of Dynamic Systems 1)*. 2nd ed. Berlin, Germany: Springer. ISBN: 9783642846809.

KEHNE, S., BERNERS, T., EPPLE, A., and BRECHER, C. (2018). "Automatic System Identification of Forward Feed Drives in Machine Tools". In: *Advances in Production Research*. Vol. 18. Springer, pp. 144–152. DOI: 10.1007/978-3-030-03451-1_15.

KLEINWORT, R. (2021). "Methodology for Enabling Active Vibration Control Systems of Machine Tools for Industrial Use". PhD Thesis. Munich, Germany: Technical University of Munich.

KLERK, D. de, RIXEN, D. J., and VOORMEEREN, S. N. (2008). "General Framework for Dynamic Substructuring: History, Review and Classification of Techniques". In: *AIAA Journal* 46.5, pp. 1169–1181. DOI: 10.2514/1.33274.

KRAFT, D. (1988). *A Software Package for Sequential Quadratic Programming*. Cologne, Germany.

LAU, J., LANSLOTS, J., PEETERS, B., and VAN DER AUWERAER, H. (2007). "Automatic Modal Analysis – Myth or Reality?" In: *25th International Modal Analysis Conference*, pp. 1–10.

LAW, M. (2013). "Position-Dependent Dynamics and Stability of Machine Tools". PhD Thesis. Vancouver, Canada: University of British Columbia.

LAW, M., PHANI, S., and ALTINTAS, Y. (2013). "Position-Dependent Multibody Dynamic Modeling of Machine Tools Based on Improved Reduced Order Models". In: *Journal of Manufacturing Science and Engineering* 135.2, pp. 021008:1–021008:11. DOI: 10.1115/1.4023453.

MAIA, N., ed. (1997). *Theoretical and Experimental Modal Analysis*. Vol. 9. Mechanical engineering research studies Engineering dynamics series. Taunton, England: Research Studies Press. ISBN: 0471970670.

MUGNAINI, V., ZANOTTI, L., and CIVERA, M. (2022). "A Machine Learning Approach for Automatic Operational Modal Analysis". In: *Mechanical Systems and Signal Processing* 170.108813, pp. 1–34. DOI: 10.1016/j.ymssp.2022.108813.

MUNOA, J., BEUDAERT, X., DOMBOVARI, Z., ALTINTAS, Y., BUDAK, E., BRECHER, C., and STEPAN, G. (2016). "Chatter Suppression Techniques in Metal Cutting". In: *CIRP Annals* 65.2, pp. 785–808. DOI: 10.1016/j.cirp.2016.06.004.

NATIONAL INFORMATION STANDARDS ORGANIZATION (2022). *ANSI/NISO Z39.104-2022: CRediT - Contributor Roles Taxonomy*. Baltimore, MD, United States.

NATKE, H. G. (1992). *Einführung in Theorie und Praxis der Zeitreihen- und Modalanalyse: Identifikation schwingungsfähiger elastomechanischer Systeme (in English: Introduction of Theory and Practice of Time-Domain and Modal Analysis: Identification of Vibrating Elastomechanical Systems)*. 3rd rev. ed. Wiesbaden, Germany: Vieweg+Teubner Verlag. ISBN: 9783322942661.

NEBELING, P. H. (1999). "Abgleich der dynamischen Eigenschaften numerischer Modelle mit realen mechanischen Strukturen (in English: Matching the

Dynamic Properties of Numerical Models with Real-World Mechanical Structures)". PhD Thesis. Aachen, Germany: RWTH Aachen University.

NELLES, O. (2020). *Nonlinear System Identification: From Classical Approaches to Neural Networks, Fuzzy Models, and Gaussian Processes*. 2nd ed. Cham, Germany: Springer International Publishing. ISBN: 9783030474393.

NEU, E., JANSER, F., KHATIBI, A., and ORIFICI, C. (2017). "Fully Automated Operational Modal Analysis Using Multi-Stage Clustering". In: *Mechanical Systems and Signal Processing* 84, pp. 308–323. DOI: 10.1016/j.ymssp.2016.07.031.

NIEHUES, K. (2015). "Identification of Linear Damping Models for Machine Tool Structures". PhD Thesis. Munich, Germany: Technical University of Munich.

NOCEDAL, J. and WRIGHT, S. (2006). *Numerical Optimization*. 2nd ed. New York, United States: Springer New York. ISBN: 9780387400655.

OBERKAMPF, L. and ROY, C. (2013). *Verification and Validation in Scientific Computing*. 1st ed. Cambridge, United Kingdom: Cambridge University Press. ISBN: 9780511760396.

OERTLI, T. (2008). "Structural Analysis and Control System Simulation of Machine Tools with Electromechanical Feed Drives". PhD Thesis. Munich, Germany: Technical University of Munich.

OKWUDIRE, C. and ALTINTAS, Y. (2009). "Hybrid Modeling of Ball Screw Drives With Coupled Axial, Torsional, and Lateral Dynamics". In: *Journal of Mechanical Design* 131.7, pp. 071002:1–071002:9. DOI: 10.1115/1.3125887.

OZDEMIR, A. and GUMUSSOY, S. (2017). "Transfer Function Estimation in System Identification Toolbox via Vector Fitting". In: *IFAC-PapersOnLine* 50.1, pp. 6232–6237. DOI: 10.1016/j.ifacol.2017.08.1026.

PEETERS, B., VAN DER AUWERAER, H., GUILLAUME, P., and LEURIDAN, J. (2004). "The PolyMAX Frequency-Domain Method: A New Standard for Modal Parameter Estimation?" In: *Shock and Vibration* 11.3-4, pp. 395–409. DOI: 10.1155/2004/523692.

POLI, R., KENNEDY, J., and BLACKWELL, T. (2007). "Particle Swarm Optimization". In: *Swarm Intelligence* 1.1, pp. 33–57. DOI: 10.1007/s11721-007-0002-0.

QUEINS, M. (2005). "Simulation des dynamischen Verhaltens von Werkzeugmaschinen mit Hilfe flexibler Mehrkörpermodelle (in English: Simulation of the Dynamic Behavior of Machine Tools via Flexible Multibody Models)". PhD Thesis. Aachen, Germany: RWTH Aachen University.

RAYLEIGH, J. (1945). *The Theory of Sound*. 2nd rev. ed. New York, United States: Dover Publications. ISBN: 9780486602929.

REBELEIN, C. (2019). "Predictive simulation of damping effects in mechatronic machine tool structures". PhD Thesis. Munich, Germany: Technical University of Munich.

REYNDERS, E. (2012). "System Identification Methods for (Operational) Modal Analysis: Review and Comparison". In: *Archives of Computational Methods in Engineering* 19.1, pp. 51–124. DOI: 10.1007/s11831-012-9069-x.

REYNDERS, E., HOUBRECHTS, J., and ROECK, G. de (2012). "Fully Automated (Operational) Modal Analysis". In: *Mechanical Systems and Signal Processing* 29, pp. 228–250. DOI: 10.1016/j.ymssp.2012.01.007.

RILL, G., SCHAEFFER, T., and BORCHSENIUS, F. (2020). *Grundlagen und computergerechte Methodik der Mehrkörpersimulation (in English: Basics and Computer-Friendly Methods of Multibody Simulation)*. 4th ed. Wiesbaden, Germany: Springer Vieweg. ISBN: 9783658289119.

RUDERMAN, R. (2012). "Zur Modellierung und Kompensation dynamischer Reibung in Aktuatorsystemen (in English: Modeling and Compensation of Friction in Actuator Systems)". PhD Thesis. Dortmund, Germany: Technische Universität Dortmund.

RUST, W. (2015). *Non-Linear Finite Element Analysis in Structural Mechanics*. Cham, Germany: Springer. ISBN: 9783319133805.

SALTELLI, A. (2004). *Sensitivity Analysis in Practice: A Guide to Assessing Scientific Models*. 1st ed. Hoboken, United States: John Wiley & Sons, Ltd. ISBN: 0470870931.

SALTELLI, A. and RATTO, M. (2008). *Global Sensitivity Analysis: The primer*. 1st ed. Chichester, United Kingdom: John Wiley & Sons, Ltd. ISBN: 9780470059975.

SATO, R. (2012). "Development of a Feed Drive Simulator". In: *Key Engineering Materials* 516, pp. 154–159. DOI: 10.4028/www.scientific.net/KEM.516.154.

SCHMUCKER, B., BUSCH, M., SEMM, T., and ZAEH, M. F. (2021). "Instantaneous Parameter Identifcation for Milling Force Models Using Bayesian Optimization". In: *MM Science Journal* 2021.5, pp. 4992–4999. DOI: 10.17973/MMSJ.2021_11_2021140.

SCHRÖDER, D. and BUSS, M. (2017). *Intelligente Verfahren (in English: Intelligent Procedures)*. 2nd ed. Berlin, Germany: Springer. ISBN: 9783662553268.

SCHULZ, B. (2014). *Mutter aller Maschinen, Vater der Produktion (in English: Mother of All Machines, Father of the Production)*. URL: https://www.maschinenmarkt.vogel.de/mutter-aller-maschinen-vater-der-produktion-a-439756/ (visited on 01/05/2024).

SCHWARZ, S. (2015). "Predictive Capability of Dynamic Simulations of Machine Tool Structures". PhD Thesis. Munich, Germany: Technical University of Munich.

SCHWERTASSEK, R. and WALLRAPP, O. (1999). *Dynamik flexibler Mehrkörpersysteme: Methoden der Mechanik zum rechnergestützten Entwurf und zur Analyse mechatronischer Systeme (in English: Dynamics of Flexible Multibody Systems: Mechanical Methods for Computer-Aided Design and Analysis of Mechatronic Systems)*. 1st ed. Braunschweig, Germany: Vieweg. ISBN: 9783322939760.

SCIONTI, M. and LANSLOTS, J. (2005). "Stabilisation Diagrams: Pole Identification Using Fuzzy Clustering Techniques". In: *Advances in Engineering Software* 36.11-12, pp. 768–779. DOI: 10.1016/j.advengsoft.2005.03.029.

SCIONTI, M., LANSLOTS, J., GOETHALS, I., VECCHIO, A., VAN DER AUWERAER, H., PEETERS, B., and MOOR, B. de (2003). "Tools to Improve Detection of Structural Changes from In-Flight Flutter Data". In: *8th International Conference on Recent Advances in Structural Dynamics*, pp. 1–12.

SEMM, T. (2020). "Position-Flexible Modeling Approach for an Efficient Optimization of the Machine Tool Dynamics Considering Local Damping Effects". PhD Thesis. Munich, Germany: Technical University of Munich.

SEMM, T., NIERLICH, M. B., and ZAEH, M. F. (2019a). "Substructure Coupling of a Machine Tool in Arbitrary Axis Positions Considering Local Linear Damping Models". In: *Journal of Manufacturing Science and Engineering* 141.7, pp. 071014:1–071014:8. DOI: 10.1115/1.4043767.

SEMM, T., REBELEIN, C., and ZAEH, M. F. (2019b). "Prediction of the Position Dependent Dynamic Behavior of a Machine Tool Considering Local Damping Effects". In: *CIRP Journal of Manufacturing Science and Technology* 27, pp. 68–77. DOI: 10.1016/j.cirpj.2019.08.001.

SEMM, T., SELLEMOND, M., REBELEIN, C., and ZAEH, M. F. (2020a). "Efficient Dynamic Parameter Identification Framework for Machine Tools". In: *Journal of Manufacturing Science and Engineering* 142.8, pp. 081003:1–081003:12. DOI: 10.1115/1.4046987.

SEMM, T., SPANNAGL, M. F., and ZAEH, M. F. (2018). "Dynamic Substructuring of Machine Tools Considering Local Damping Models". In: *Procedia CIRP* 77, pp. 670–674. DOI: 10.1016/j.procir.2018.08.180.

SEMM, T., SPESCHA, D., CERESA, N., ZAEH, M. F., and WEGENER, K. (2020b). "Efficient Dynamic Machine Tool Simulation with Included Damping and Linearized Friction Effects". In: *Procedia CIRP* 93, pp. 1442–1447. DOI: 10.1016/j.procir.2020.02.141.

SHAHRUZ, S. M. (1990). "Approximate Decoupling of the Equations of Motion of Damped Linear Systems". In: *Journal of Sound and Vibration* 136.1, pp. 51–64. DOI: 10.1016/0022-460X(90)90937-U.

SIEBERTZ, K., VAN BEBBER, D., and HOCHKIRCHEN, T. (2017). *Statistische Versuchsplanung (in English: Statistical Experimental Design)*. 2nd ed. Berlin, Germany: Springer. ISBN: 9783662557426.

SIEDL, D. (2008). "Simulation des dynamischen Verhaltens von Werkzeugmaschinen während Verfahrbewegungen (in English: Dynamic Simulation of Machine Tools During Traverse Movements)". PhD Thesis. Munich, Germany: Technical University of Munich.

SPESCHA, D. (2018). "Framework for Efficient and Accurate Simulation of the Dynamics of Machine Tools". PhD Thesis. Ilanz/Glion, Switzerland: Clausthal University of Technology. DOI: 10.21268/20181119-132644.

STARK, P. and PARKER, R. (1995). "Bounded-Variable Least-Squares: an Algorithm and Applications". In: *Computational Statistics* 10, pp. 1–13.

SWEVERS, J., AL-BENDER, F., GANSEMAN, C. G., and PROJOGO, T. (2000). "An Integrated Friction Model Structure with Improved Presliding Behavior for Accurate Friction compensation". In: *IEEE Transactions on Automatic Control* 45.4, pp. 675–686. DOI: 10.1109/9.847103.

TSENG, G. W. G., CHEN, C. Q. G., ERKORKMAZ, K., and ENGIN, S. (2019). "Digital Shadow Identification from Feed Drive Structures for Virtual Process Planning". In: *CIRP Journal of Manufacturing Science and Technology* 24, pp. 55–65. DOI: 10.1016/j.cirpj.2018.11.002.

VACHER, P., JACQUIER, B., and BUCHARLES, A. (2010). "Extensions of the MAC Criterion to Complex Modes". In: *24th International Conference on Noise and Vibration Engineering*. Proceedings of ISMA2010 Including USD2010, pp. 2713–2726.

VAN DER AUWERAER, H. and PEETERS, B. (2004). "Discriminating Physical Poles from Mathematical Poles in High Order Systems: Use and Automation of the Stabilization Diagram". In: *21st IEEE Instrumentation and Measurement Technology Conference*. IEEE, pp. 2193–2198. DOI: 10.1109/IMTC.2004.1351525.

VAN OVERSCHEE, P. and MOOR, B. de (1996). *Subspace Identification for Linear Systems*. 1st ed. Boston, United States: Springer US. ISBN: 9781461380610.

VDI (2004). *VDI 3830 Part 1: Damping of materials and members: Classification and survey*. Ed. by VEREIN DEUTSCHER INGENIEURE (IN ENGLISH: THE ASSOCIATION OF GERMAN ENGINEERS). Berlin, Germany.

VDW (2022). *Marktbericht 2022: Die deutsche Werkzeugmaschinenindustrie und ihre Stellung im Weltmarkt (in English: Market Report 2022: German Machine Tools and Their Position in the Global Market)*. Ed. by VEREIN DEUTSCHER WERKZEUGMASCHINENFABRIKEN E. V. (IN ENGLISH: GERMAN MACHINE TOOL BUILDERS' ASSOCIATION). Frankfurt, Germany.

VERBOVEN, P. (2019). "Frequency-Domain System Identification for Modal Analysis". PhD Thesis. Brussels, Belgium: Free University of Brussels.

WANG, C., ERKORKMAZ, K., MCPHEE, J., and ENGIN, S. (2020). "In-Process Digital Twin Estimation for High-Performance Machine Tools with Coupled Multibody Dynamics". In: *CIRP Annals*, pp. 1–4. DOI: 10.1016/j.cirp.2020.04.047.

WANG, X., HILL, T., NEILD, S., SHAW, A., HADDAD KHODAPARAST, H., and FRISWELL, M. (2018). "Model Updating Strategy for Structures with Localised Nonlinearities Using Frequency Response Measurements". In: *Mechanical Systems and Signal Processing* 100, pp. 940–961. DOI: 10.1016/j.ymssp.2017.08.004.

WECK, M. (2002). *Werkzeugmaschinen-Fertigungssysteme 2: Konstruktion und Berechnung (in English: Machine Tool Production Systems 2: Design and Calculation)*. 7th rev. ed. Berlin, Germany: Springer Berlin Heidelberg. ISBN: 9783662109205.

WIMMER, S. (2020). "Prediction and Compensation of Form Deviations During Milling of Thin-Walled Structures". PhD Thesis. Munich, Germany: Technical University of Munich.

WITT, S. T. (2007). "Integrierte Simulation von Maschine, Werkstück und spanendem Fertigungsprozess (in English: Integrated Simulation of Machine Tool, Workpiece, and Cutting Process)". PhD Thesis. Aachen, Germany: RWTH Aachen University.

WONG, W. and ERKORKMAZ, K. (2010). "Constrained Identification of Virtual CNC Drives Using a Genetic Algorithm". In: *The International Journal of Advanced Manufacturing Technology* 50, pp. 275–288. DOI: 10.1007/s00170-009-2496-7.

ZIENKIEWICZ, O., TAYLOR, R., and ZHU, J. (2005). *The Finite Element Method: Its Basis and Fundamentals*. 6th ed. Vol. 1. Amsterdam, Netherlands: Elsevier Butterworth-Heinemann. ISBN: 9780750663205.

Appendix A

Embedded Publications

The following publications (PUBs) were embedded in this publication-based thesis[9]:

PUB1 ELLINGER, J., SEMM, T., BENKER, M., KAPFINGER, P., KLEINWORT, R., and ZAEH, M. F. (2019). "Feed Drive Condition Monitoring Using Modal Parameters". In: *MM Science Journal*, pp. 3206–3213. DOI: 10.17973/MMSJ.2019_11_2019072

PUB2 ELLINGER, J., SEMM, T., and ZAEH, M. F. (2022b). "Dimensionality Reduction of High-Fidelity Machine Tool Models by Using Global Sensitivity Analysis". In: *Journal of Manufacturing Science and Engineering* 144.5, pp. 051010:1–051010:8. DOI: 10.1115/1.4052710

PUB3 ELLINGER, J. and ZAEH, M. F. (2022). "Automated Identification of Linear Machine Tool Model Parameters Using Global Sensitivity Analysis". In: *Machines* 10.7, pp. 1–18. DOI: 10.3390/machines10070535

PUB4 ELLINGER, J., PIENDL, D., and ZAEH, M. F. (2023). "Comparison of Sensitivity-Guided and Black-Box Machine Tool Parameter Identification". In: *Journal of Manufacturing and Materials Processing* 7.4, pp. 1–16. DOI: 10.3390/jmmp7040120

PUB5 ELLINGER, J., BECK, L., BENKER, M., HARTL, R., and ZAEH, M. F. (2022a). "Automation of Experimental Modal Analysis Using Bayesian Optimization". In: *Applied Sciences* 13.2, pp. 1–16. DOI: 10.3390/app13020949

[9] see footnote 3 on page 69

Appendix B

Supervised Student Theses

In the context of the research performed for this thesis at the Institute for Machine Tools and Industrial Management (in German: Institut für Werkzeugmaschinen und Betriebswissenschaften) of Technical University of Munich (*iwb*) of the Technical University of Munich (in German: Technische Universität München) (TUM) (in German: Institut für Werkzeugmaschinen und Betriebswissenschaften der Technischen Universtität München) in the years from 2018 to 2023, the author has supervised several student theses (see table B.1) concerning the methodology, the problem statements, the objectives, the research approach, and the interpretation and documentation of all results, and he has provided essential scientific, technical, and content-related guidance. Some of these theses have dealt with automated parameter identification of high-fidelity structural dynamic machine tool models and have contributed to the publications PUB1 to PUB5. The author would like to thank all supervised students for their contributions and their dedication.

Table B.1: Supervised Bachelor's theses (BTs), Semester's theses (STs), Master's theses (MTs), and interdisciplinary projects (IDPs)

Student name	Type	Year	Title of the thesis
Tobias Petry	BT	2018	Analyse und Bewertung bestehender Predictive-Maintenance-Ansätze im Bereich Werkzeugmaschinen (in English: Analysis and Evaluation of Existing Machine Tool Predictive Maintenance Approaches)

Table B.1: (continued)

Student name	Type	Year	Title of the thesis
Philipp Kapfinger	MT	2019	Condition Monitoring an Vorschubantrieben unter Verwendung eines Inertialaktors (in English: Feed Drive Condition Monitoring via an Inertial Actuator)
Moritz Fundel	BT	2019	Erweiterung eines Vorschubantriebsversuchsstandes um ein Tool zur automatischen Vermessung der Dynamik (in English: Upgrade of a Feed Drive Test Bench with a Tool for Dynamic Measurements)
Son-Pham Khanh	BT	2020	Feed Drive Modeling and Parameter Identification
Hannes Dechant	BT	2020	Aufbau von Simulationsmodellen für Werkzeugmaschinen mithilfe der Finite-Elemente-Methode (in English: Creation of Machine Tool Simulation Models via Finite Element Analysis)
Peter Lingauer	MT	2020	Systemidentifikation an der Werkzeugmaschine mit einer Rapid-Identification-Methode (in English: Machine Tool System Identification Using a Rapid Identification Approach)
Martin Zeschg	ST	2020	Parametrierung achsflexibler nichtlinearer Werkzeugmaschinenmodelle mit lokaler Dämpfungsmodellierung (in English: Parameterization of Position-Flexible Nonlinear Machine Tool Models with Local Damping Modeling)
Martin Zeitz	BT	2021	Durchführung einer experimentellen Modalanalyse einer Werkzeugmaschine unter Verwendung verschiedener Software-Lösungen (in English: Conduction of an Experimental Modal Analysis on a Machine Tool Using Various Software Tools)
Martin Zeschg	MT	2021	Parametrierung achsflexibler linearer Werkzeugmaschinenmodelle mit lokaler Dämpfungsmodellierung (in English: Parameterization of Position-Flexible Nonlinear Machine Tool Models with Local Damping Modeling)
Konrad Streich	BT	2021	Modellierung einer Werkzeugmaschine mittels Mehrkörpersimulation und Finite-Elemente-Methode (in English: Machine Tool Modeling Using Multibody Simulation and Finite Element Analysis)
Stefan Nikić	ST	2022	Identifikation und Bewertung KI-basierter Reibmodelle (in English: Identification and Evaluation of AI-based friction models)

Table B.1: (continued)

Student name	Type	Year	Title of the thesis
Moritz Fundel	ST	2022	Integration und Weiterentwicklung eines quelloffenen Modalanalysetools (in English: Integration and Further Development of an Open-Source Modal Analysis Tool)
Johannes Glas	MT	2022	Aufbau eines flexiblen Mehrkörpersimulationsmodells einer 5-Achs-Werkzeugmaschine (in English: Creation of a Flexible Multibody Simulation Model of a Five-Axis Machine Tool)
Severin Kölbl	BT	2022	Kinematikidentifikation von Drehschwenkeinheiten an fünfachsigen Hochpräzisionsfräsmaschinen (in English: Kinematics Identification of Turn-Swivel Units of Five-Axis High-Precision Machine Tools)
Jan Auchter	MT	2022	Modellierung einer Werkzeugmaschine mittels Finite-Elemente-Methode (in English: Machine Tool Modeling via Finite Element Analysis)
Luis Olenscki	ST	2022	Development of an IoT Demonstrator for a Machine Tool
Leopold Beck	ST	2022	Automatisierung der experimentellen Modalanalyse für Werkzeugmaschinen (in English: Automation of Experimental Modal Analysis of Machine Tools)
Felix Christ	IDP	2022	Entwicklung eines IoT-Demonstrators für eine industrielle Werkzeugmaschine (in English: Development of an IoT Demonstrator for Industrial Machine Tools)
Sebastian Warter	IDP	2023	Entwicklung einer erweiterbaren Software-Infrastruktur für die Anregung von und Messungen an Bosch-Rexroth-Antrieben für Verschleißbeobachtungen (in English: Development of an Extensible Software Infrastructure for Exciting and Measuring Bosch Rexroth Drives for Wear Monitoring)